ORNL/MSP/1.7-82/2

U.S. Department of Energy

Nuclear Energy

LMFBR Materials and Structures Program

ADVANCED-ALLOY TECHNOLOGY PROGRAM

SEMIANNUAL PROGRESS REPORT

FOR PERIOD ENDING SEPTEMBER 30, 1982

Oak Ridge National Laboratory

Combustion Engineering, Inc.

Westinghouse Electric Corporation

Date Published: January 1983

Compiled by:

Materials and Structures
Technology Management Center

OAK RIDGE NATIONAL LABORATORY
Oak Ridge, Tennessee 37830
operated by
UNION CARBIDE CORPORATION
for the
DEPARTMENT OF ENERGY

Contract No. W-7405-eng-26

DISCLAIMER

PREVIOUS PEPORTS IN THIS SERIES

Report No.	Period Ending
ORNL/BRP-79/2	April-September 30, 1978
ORNL/BRP-79/4	October-March 31, 1979
ORNL/BRP-80/1	April-September 30, 1979
ORNL/MSP-1.7-80/1	October-March 31, 1980
ORNL/MSP-1.7-80/2	September 1980
ORNL/MSP-1.7-80/3	March-September 30, 1980
ORNL/MSP-1.7-81/1	October-March 31, 1981
ORNL/MSP-1.7-81/3	March-September 30, 1981
ORNL/MSP-1.7-82/1	October-March 31, 1982

CONTENTS

FOREWORD

This is the ninth in a series of semiannual progress reports on the development of a modified 9 Cr-1 Mo steel for advanced breeder reactor structural applications. The work described is being carried out under the Advanced Alloy Technology work element (MSP-1.7) of the DOE-LMFBR Materials and Structures Program. During this report period, work was carried out at Combustion Engineering, Inc., Oak Ridge National Laboratory, and Westinghouse Electric Corporation. Continued emphasis has been placed on fabrication of samples for commercial power plant evaluation, determination of mechanical properties for *ASME Boiler and Pressure Vessel Code* packages, and weldability studies.

This report was compiled by the ORO-ORNL Materials and Structures Technology Management Center from camera-ready copy submitted by the participating organizations. Distribution is limited to LMFBR participants and to selected organizations in related projects.

The next report in this series will cover the period October 1982 to March 31, 1983. Contributions to this report are due to the MSTMC by April 30, 1983.

J. R. DiStefano
Materials and Structures Technology
Management Center

SUMMARY

1. Oak Ridge National Laboratory

Modified 9 Cr-1 Mo steel tubes supplied to the Central Electric Generating Board (U.K.) were installed in its Agecroft Power Station during April 1982.

Charpy impact, tensile, and creep properties and the optical microstructure of tubes fabricated from a 2-ton Sumitomo heat are reported along with chemical analysis and Charpy impact properties of a 50-ton Sumitomo heat. Properties of the 2- and 50-ton heats are compared.

Charpy impact, tensile, and creep properties of the 5-ton NKK heat are described. The optical microstructures of tubes fabricated from this heat are also shown.

The status of operating experience of modified 9 Cr-1 Mo tubes in various power plants is summarized.

Modified 9 Cr-1 Mo steel is recommended for use in the normalized and tempered condition. The nominal normalizing temperature is 1038°C and the tempering temperature is 760°C. A study of the effect of varying the normalizing temperature from 927 to 1121°C for times of 10 to 480 min. on the grain growth, microhardness, tensile, Charpy impact, and creep properties of modified 9 Cr-1 Mo steel has been carried out. The grain size of the modified alloy remained unchanged after a 1 h normalizing treatment at temperatures from 927 to 1121°C. When the hold time was increased to 8 h, the grain size increased at temperatures higher than 1093°C. Room-temperature yield strength, ultimate tensile strength, and microhardness increased with increasing normalizing temperature and time. A similar effect was observed for tensile properties at 593°C. Creep strength increased with increasing normalizing temperature and time and reached a maximum for normalizing temperatures of 1038°C and higher. A recommendation is made for an upper limit on normalizing temperature and time.

Tensile properties of forged slabs and billets from three commercial heats of modified 9 Cr-1 Mo steel are presented. Data are compared with the minimum property curves based on the minimum specified values for tube, plate, and bar.

Results are given from a number of strain-controlled fatigue tests conducted in air at 538 and 593°C. All test data of this type currently available are summarized. Interim conclusions concerning the behavior of modified 9 Cr-1 Mo steel under cyclic loading conditions and tentative plans for future test activity are presented.

The Charpy-V impact (C_V) properties of electroslag remelt (ESR) and argon-oxygen-deoxidized (AOD) heats of modified 9 Cr-1 Mo steel were determined after aging for 10,000 and 1,200 h, respectively, at a minimum of four test temperatures (482, 538, 593, and 649°C). The C_V properties of 51-mm-thick plate originally melted by the AOD process and remelted by the ESR process (AOD/ESR) were determined at two depth locations and in two orientations.

The welding development program for modified 9 Cr-1 Mo steel has been examining three processes: gas tungsten arc, shielded metal arc, and submerged arc. The weldments and weld metal properties have been evaluated by tensile, creep, and Charpy V-notch toughness testing. Results are presented for welds made by all three processes; however, most of the data are from GTA weld deposits. Preliminary data from SMA and SA processes are presented.

Analytical predictions from an inelastic structural analysis appear to show good agreement with experimental results from a deformation-controlled beam test. A topical report is being prepared.

2. Combustion Engineering, Inc.

Technical consultation was provided for the production of modified 9 Cr-1 Mo boiler tubing at T. I. Stainless Tubes Ltd. (UK). Boiler tubes were later installed at the Agecroft Power Plant of the Central Electricity Generating Board (Ref. 1).

Technical consultation was also provided relative to production of various dimensionally modified 9 Cr-1 Mo alloy steel tubing from two small (2, 5.1 Mg) vacuum induction melted (VIM) and one commercial scale (50.8 Mg) electric furnace/vacuum oxygen decarburized (EF/VOD) heats. Selected samples of tubing were examined, checked by chemical analyses, and tested for mechanical properties.

Tube sections (safe ends) were joined to modified 9 Cr-1 Mo alloy steel tubes by Combustion Engineering, Metallurgical and Materials Laboratory, (C-E MML) and the samples were shipped to Ontario Hydro Lambton TGS for future installation and field testing. Fabrication of additional modified 9 Cr-1 Mo alloy steel tubes with safe ends for Ontario Hydro Nanticoke TGS was 90% complete and shipment is scheduled for October 1982.

3. Westinghouse Electric Corporation Advanced Reactors Division

Creep-rupture testing of prototypic commercial heats of modified 9 Cr-1 Mo continued. Data are reported for one test on CarTech heat 30182 at 593°C and a stress of 131 MPa. The rupture time recorded, 18,505.6 h, was in line with predictions based on extrapolation of data from tests at higher stress levels. Thus, it maintained the trend in which the rupture strength of this heat of material becomes progressively greater than that of the ASME Code Case N47 minimum for type 304 stainless steel at 593°C as the stress level is reduced. Metallography and microhardness measurements on the specimen indicated a generally stable microstructure over the nearly 20,000 h aging period at 593°C.

The status of tests on Cartech heats 30394E and 30176, which have been in progress for times from 11,200 to 15,400 h at 593 and 677°C, is reported. All of these tests are expected to last in excess of 16,000 h.

1. OAK RIDGE NATIONAL LABORATORY

V. K. Sikka

1.1 Introduction

A modified 9 Cr-1 Mo steel development program is in progress at ORNL. Parts of the work on this program are subcontracted to Combustion Engineering, Inc. (CE), Westinghouse Advanced Reactor Division (W-ARD), and Battelle Memorial Institute (BMI). The contribution from the BMI subcontract is included in the results presented here by ORNL. However, the CE and W-ARD contributions are reported in separate chapters.

Work on modified 9 Cr-1 Mo steel continued at ORNL in the following areas during the last six months:

1. material procurement and processing,
2. weldability,
3. tensile and creep testing of base and weld metal,
4. Charpy impact testing of base and weld metal,
5. thermal aging, and
6. corrosion.

Status and progress made in most of these areas are described in the following sections.

1.2 Material Procurement and Processing

V. K. Sikka, G. C. Bodine*, and W. J. Stelzman

The task deals with the procurement of commercial heats, their fabrication into various product forms, fabrication of tubes for installation in utility boilers, and fabrication of filler wire for welding.

---

*Combustion Engineering, Inc., Chattanooga, Tenn.

1.2.1 Fabrication of Tubes for Installation in the Agecroft Power Station of the Central Electric Generating Board (U.K.)

Six tubes 54 mm OD by 9.5 mm wall by 1830 mm long of modified 9 Cr-1 Mo steel were installed in the Agecroft Power Station of the Central Electric Generating Board (U.K.) during April 1982. The fabrication details of these tubes were reported in the last semiannual report.[1] The modified 9 Cr-1 Mo steel tubes replaced 2 1/4 Cr-1 Mo tubes — the current material in use at that power plant. The installed modified 9 Cr-1 Mo tubes in Agecroft are shown in Fig. 1.1. The modified 9 Cr-1 Mo tubes are thermocoupled, so we expect to obtain a complete thermal operating history. We expect these tubes to operate for several months.

1.2.2 Melting of Modified 9 Cr-1 Mo Steel in Japan

Three heats of modified 9 Cr-1 Mo steel have been melted and fabricated by two Japanese steel companies since the last reporting period. Two of the heats were melted by Sumitomo and one by Nippon Kokan KK (NKK). The melting, fabrication, and testing of Japanese heats are described here.

1.2.2.1 Sumitomo heats

Sumitomo initially melted a 2-ton heat of modified 9 Cr-1 Mo steel by the vacuum induction melting (VIM) process. The composition of this heat was reported in the last semiannual report.[1] A test report on this heat was supplied by Sumitomo. The 2-ton heat was fabricated into 76-mm-OD by 12.7-mm-wall and 51-mm-OD by 6.35-mm-wall tubes. All tubes

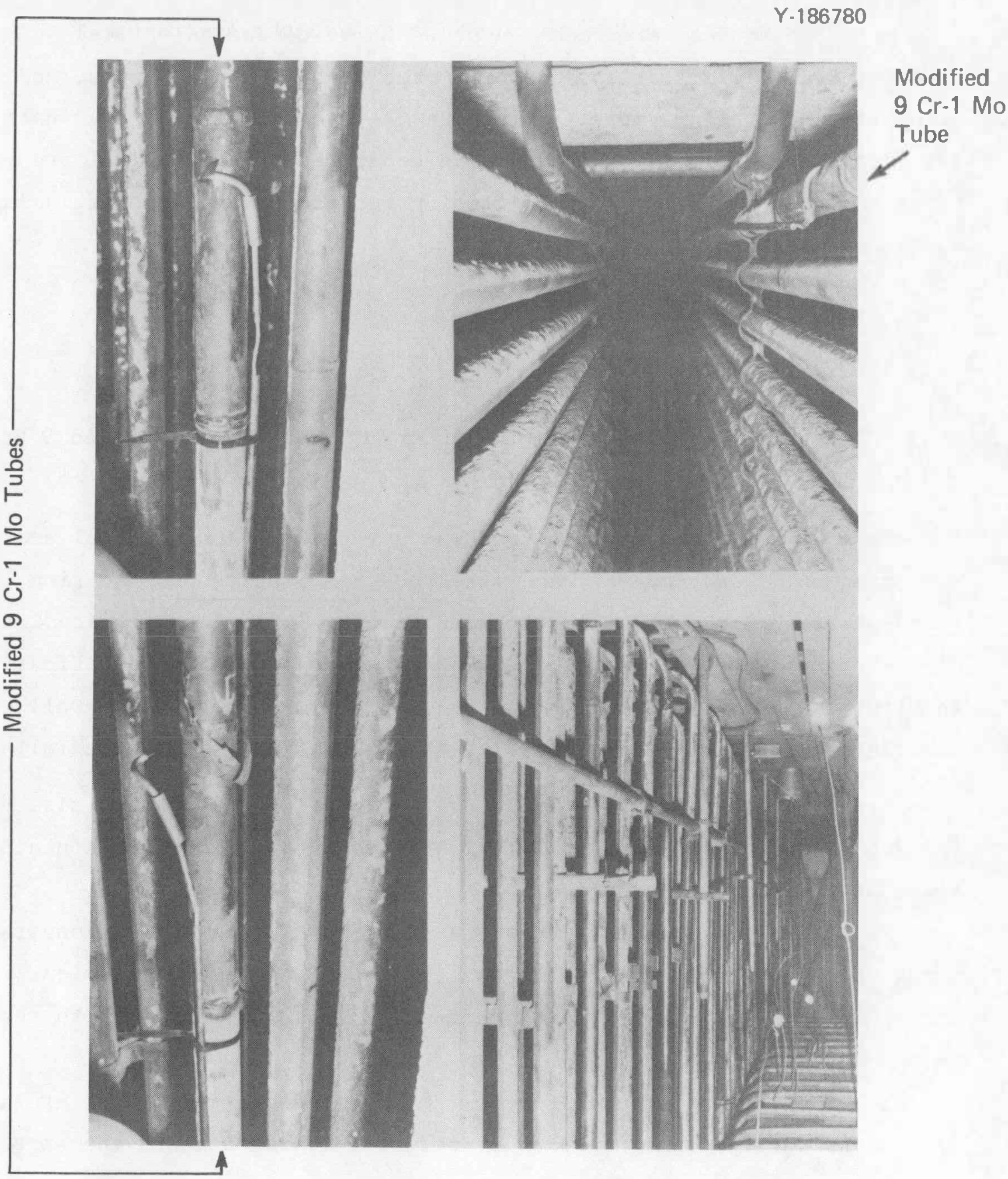

Fig. 1.1. Modified 9 Cr-1 Mo steel tubes installed in Agecroft power plant United Kingdom.

were supplied to ORNL in the final heat-treated condition. It should be noted, however, that Sumitomo decided to temper at 780°C rather than at our nominal tempering temperature of 760°C. This heat was melted and fabricated at no cost to ORNL.

After the tubes were received at ORNL, we conducted optical microstructural examination, Charpy impact tests, tensile tests, and creep tests on this material. Although the microstructural examination was carried out on both size tubes, we conducted all mechanical property tests on 76-mm-OD by 12.7-mm-wall tubing because of the ease of making specimens from the larger tubing.

1.2.2.2 Microstructure and properties of 2-ton Sumitomo heat

We examined the optical microstructure of both longitudinal and circumferential sections of each size tube. A longitudinal section of a 76-mm-OD by 12.7-mm-wall tube is shown in Fig. 1.2. Both longitudinal and circumferential sections of this tube are shown at higher magnifications in Figs. 1.3 and 1.4. Similar sections of 51-mm-OD by 6.35-mm-wall tubes are shown in Figs. 1.5 through 1.7. All these figures show the following.

1. Both sizes of tubes are very fine grained (ASTM grain size 9–10). The 7.6-mm-OD tube appears to be slightly coarser grained and contains somewhat of a mixed grain size.

2. All microstructures show the presence of inclusions elongated along the tubes from this heat. Sumitomo indicated that inclusions generally show up in small heats because of some slag mixing with the molten metal during pouring.

3. The microstructure of both the longitudinal and circumferential directions was the same for both size tubes. This suggests the absence of any directionality in the properties of tubing.

Microhardness was measured on both the longitudinal and circumferential sections of both size tubes. Values observed (and standard deviations) were 212 ± 4 and 214 ± 3 dph for the longitudinal and circumferential sections of the 76-mm-OD by 12.7-mm tube and 219 ± 5 and 214 ± 7 dph for the 51-mm-OD by 6.35-mm-wall tube.

Y-185063

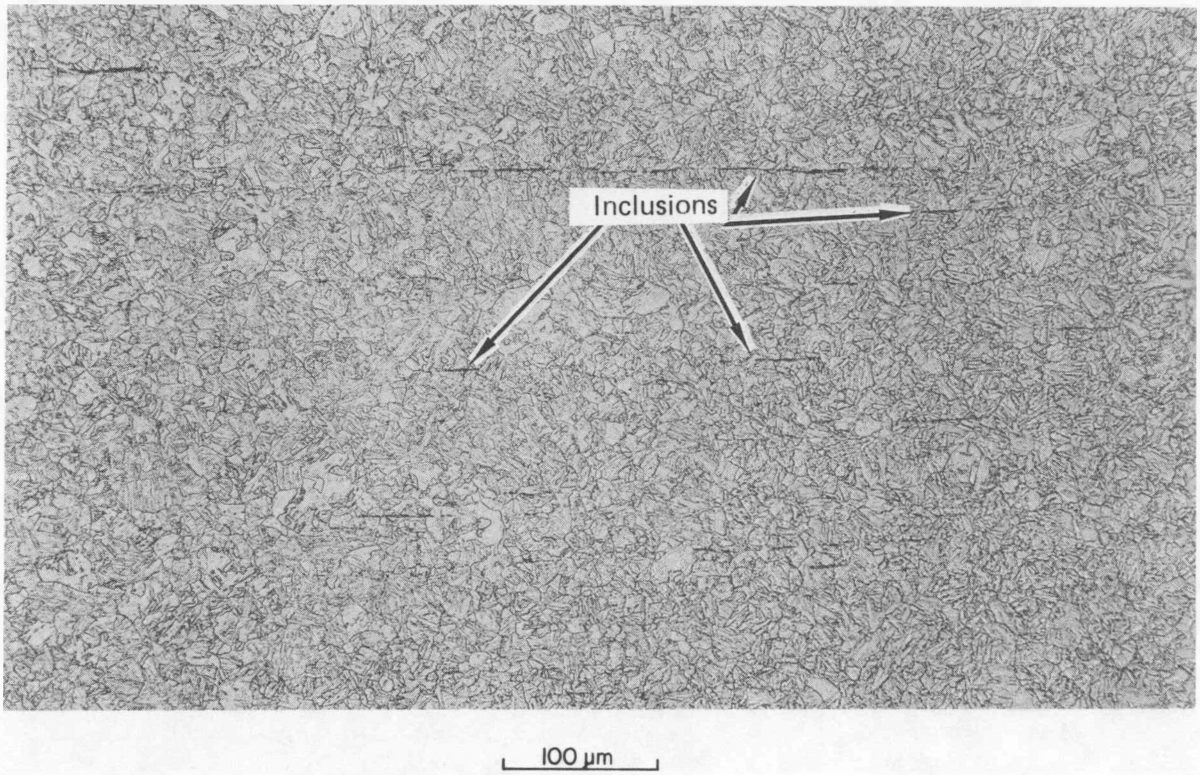

Fig. 1.2. Longitudinal section of 76-mm-OD by 12.7-mm-wall tube made by Sumitomo from a 2-ton heat.

Charpy impact testing was conducted on specimens machined from 76-mm-OD by 12.7-mm-wall tubing. The Charpy V-notch was broached in both the AC and AT orientations. In the AC orientation the notch faces the circumferential direction, whereas in the AT orientation the notch faces the radial direction or thickness of the tube. Figure 1.8 shows a schematic of AC and AT specimen orientations. The Charpy impact energy for the two orientations is plotted against temperature in Fig. 1.9. The transition temperature and upper-shelf energy values from these plots are listed in Table 1.1. Curves in Fig. 1.9 show that the Charpy impact behavior of the Sumitomo tube is nearly the same in both the AC and AT orientations. The 68-J (50-ft-lb) ductile-brittle transition temperature

Y-185066

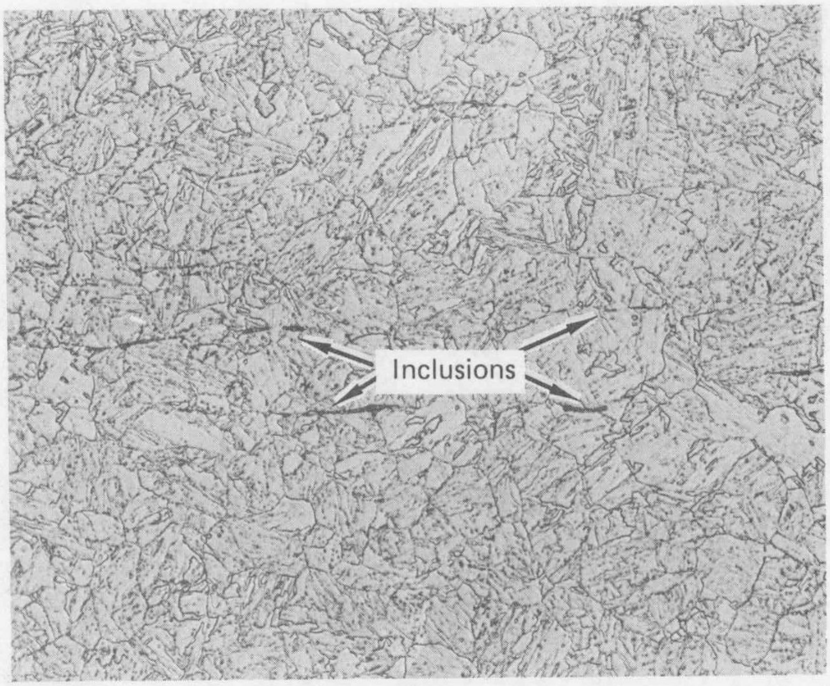

(a)

40 μm

Y-185065

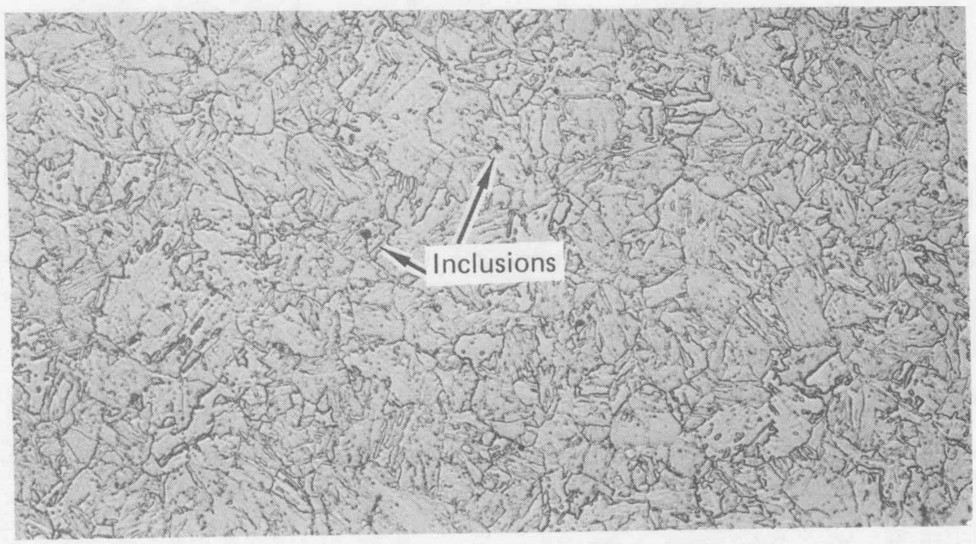

(b)

Fig. 1.3. Microstructure of (*a*) longitudinal and (*b*) circumferential sections of 76-mm-OD by 12.7-mm-wall tube made by Sumitomo from a 2-ton heat.

Y-185070

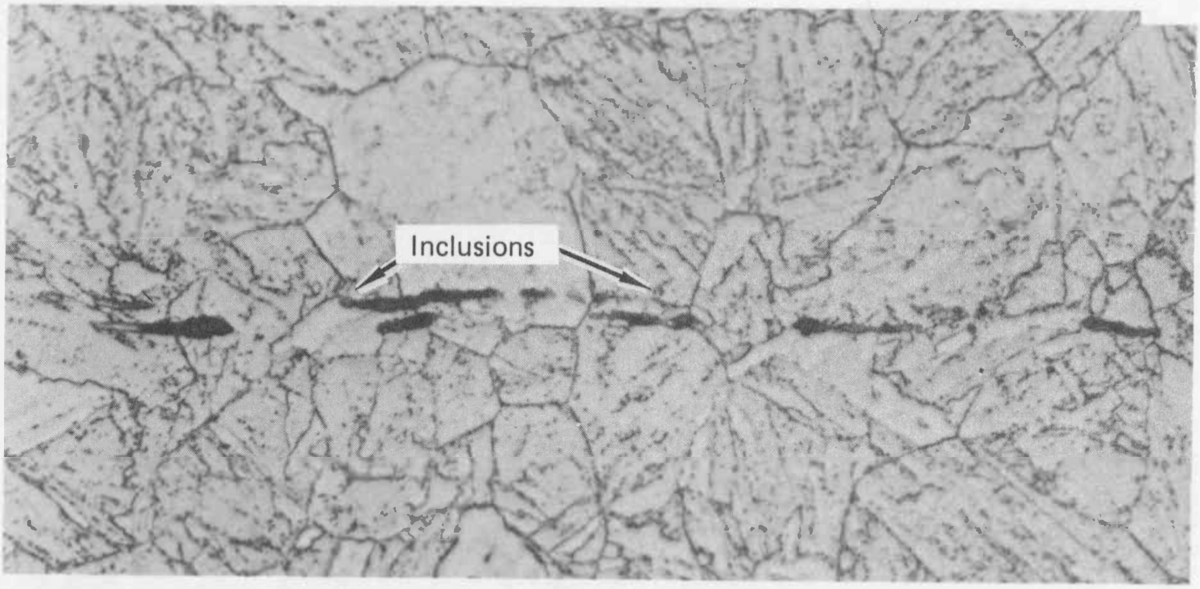

(a)

13.4 μm

Y-185069

(b)

Fig. 1.4. High-magnification microstructure of (*a*) longitudinal and (*b*) circumferential sections of 76-mm-OD by 12.7-mm-wall tube made by Sumitomo from a 2-ton heat.

Y-185064

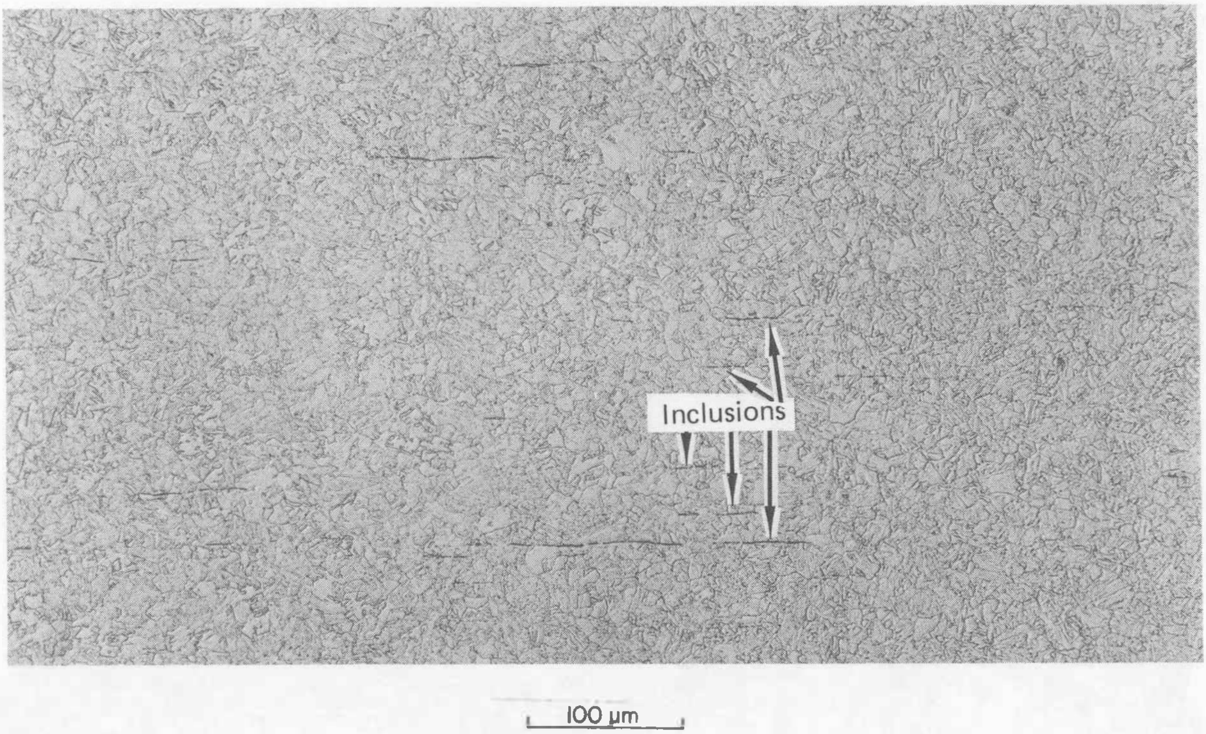

Fig. 1.5. Longitudinal section of 51-mm-OD by 6.35-mm-wall tube made by Sumitomo from a 2-ton heat.

is about −68°C (−90°F), and the upper-shelf energy is above 240 J (180 ft-lb). Irrespective of the inclusions in this material, the Charpy impact values for the Sumitomo tubing are exceptionally good. One reason why the inclusions have little effect on the impact properties might be the notch orientations possible in this study. If a notch were possible along the tube, poor impact properties might be expected because of the notch being parallel to the inclusions. However, from the service point of view, the important notch direction for the tubing is the AT orientation. In this orientation, Sumitomo tubing showed exceptionally good impact properties.

Tensile tests were conducted on the longitudinal specimens machined from a 76-mm-OD by 12.7-mm-wall tube. These specimens were tested at room temperature, 93, 204, 316, 427, and 649°C. All tests were conducted at a nominal strain rate of 0.004/min. Test data on these specimens are summarized in Table 1.2.

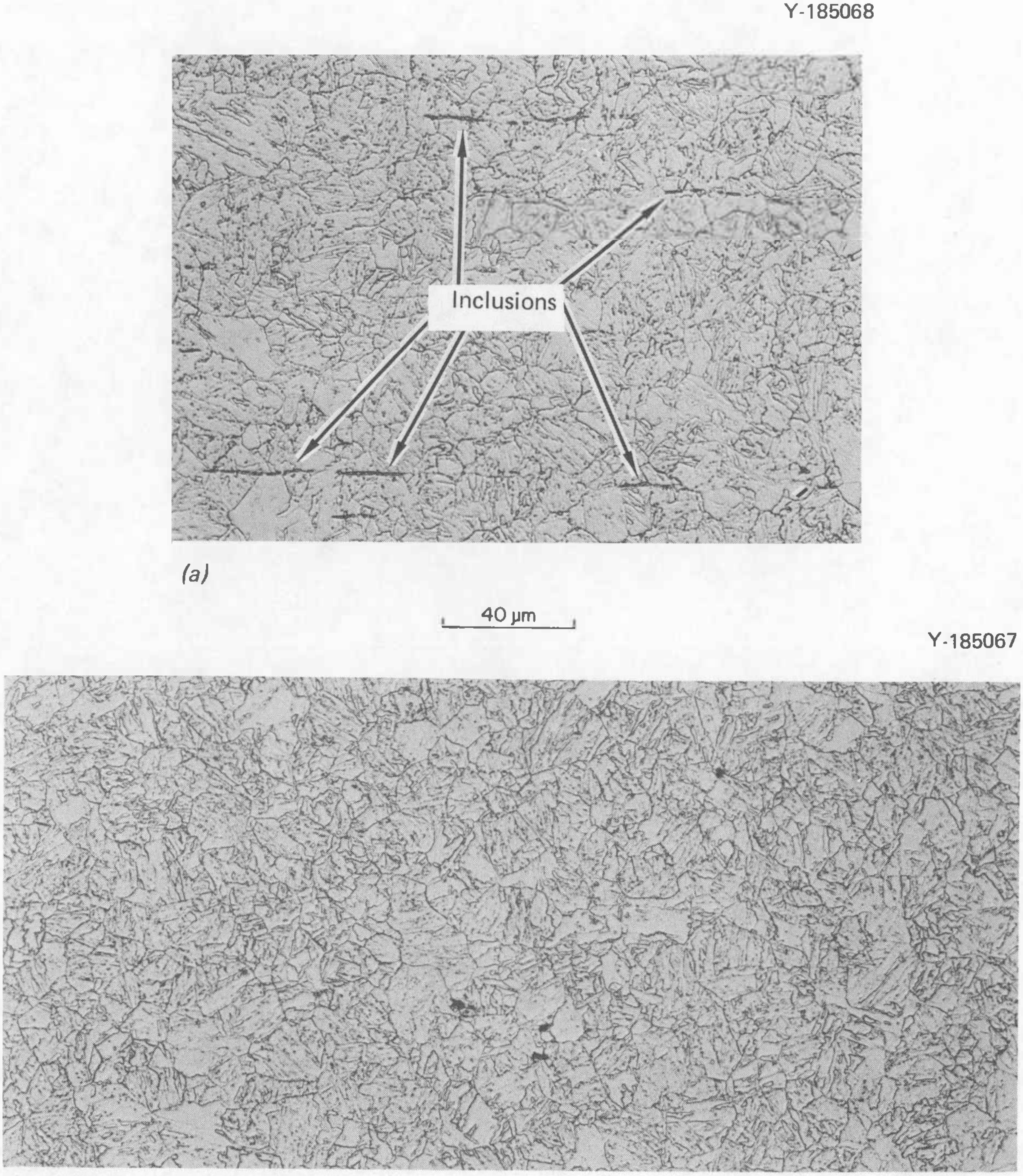

Fig. 1.6. Microstructure of (*a*) longitudinal and (*b*) circumferential sections of 51-mm-OD by 6.35-mm-wall tube made by Sumitomo from a 2-ton heat.

Y-185072

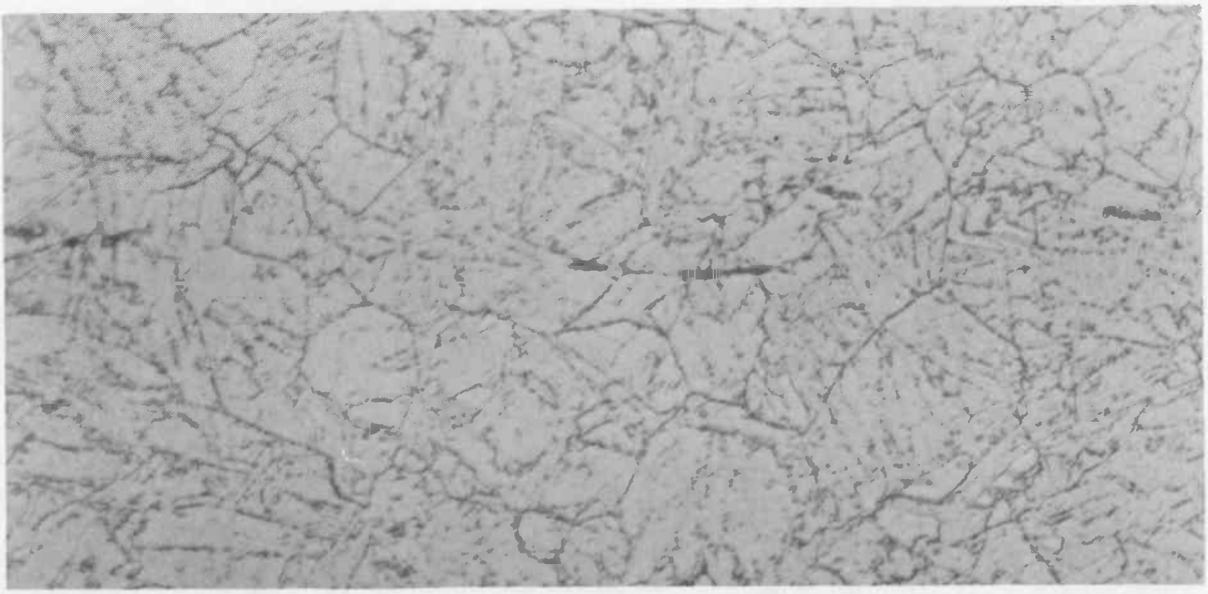

(a)

13.4 μm

Y-185071

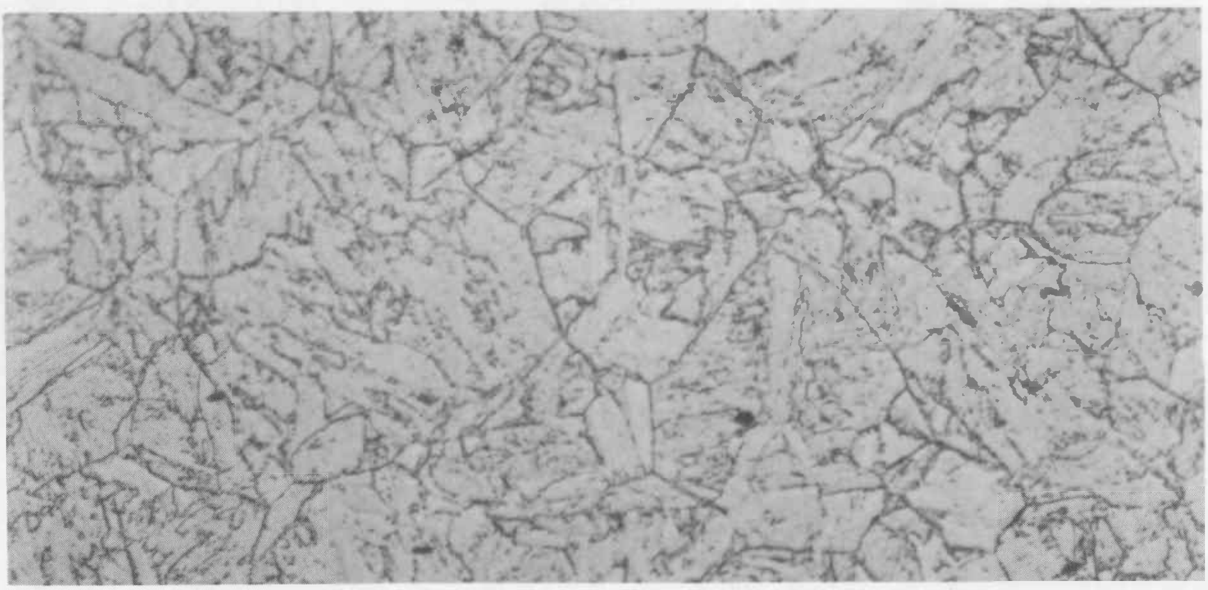

(b)

Fig. 1.7. High-magnification microstructure of (*a*) longitudinal and (*b*) circumferential sections of 51-mm-OD by 6.35-mm-wall tube made by Sumitomo from a 2-ton heat.

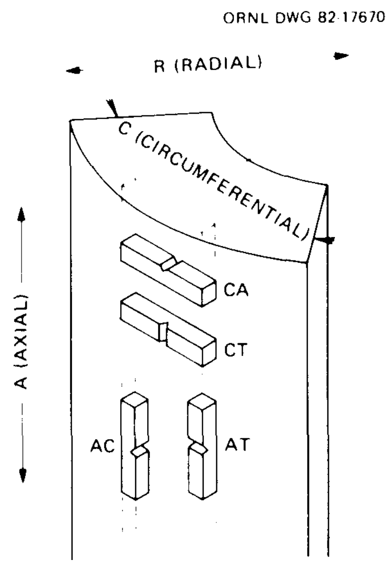

Fig. 1.8. Charpy-V orientation notation for cylindrical product forms.

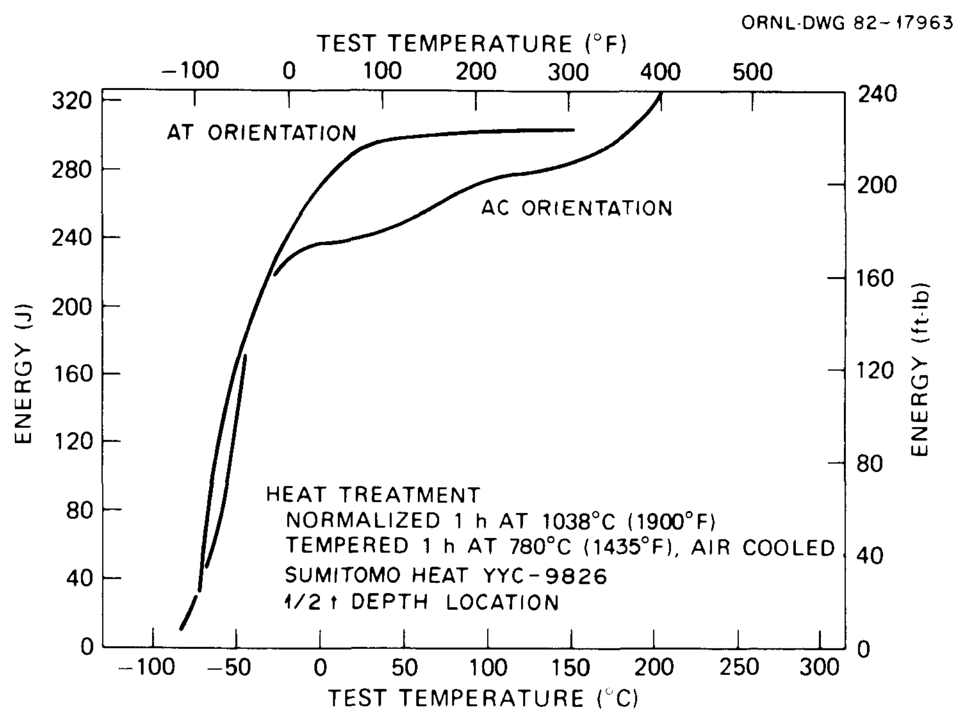

Fig. 1.9. Effect of specimen orientation on the Charpy-V impact energy of 76-mm-OD by 12.7-mm-wall tubing of modified 9 Cr-1 Mo steel. Sumitomo heat YYC 9826.

Table 1.1 Summary of Charpy-V toughness data of various commercial heats of modified 9 Cr-1 Mo steel melted in Japan

Specimen[a] orientation	Temperature [°C (°F)]				Energy [J (ft-lb)]	
	68-J (50-ft-lb) energy	0.89-mm (35-mil) Lateral expansion	50% Shear	100%[b] Shear	24°C (75°F)	Upper shelf at 149°C (300°F)
76-mm-OD by 48-mm-ID tubing[c]						
AC	−65 (−85)	−62 (−80)	−57 (−70)	−34 (−30)	245 (180)	284 (209)[d]
AT	−68 (−90)	−71 (−95)	−48 (−55)	−18 (0)	295 (218)	310 (228)
44-mm-OD by 19-mm-ID tubing[e]						
AC	<−73 (−100)	<−73 (−100)	−54 (−65)	−18 (0)	256 (188)	
27-mm-thick plate[f]						
RW	−65 (−85)	−65 (−85)	−51 (−60)	10 (50)	269 (198)	284 (209)[g]
WR	−29 (−20)	−32 (−25)	−9 (15)	27 (80)	150 (110)	163 (120)
76-mm-OD by 49-mm-ID tubing[f]						
AC	−82 (−115)	−79 (−110)	−54 (−65)	−18 (0)	235 (173)	272 (200)[d]
AT	−73 (−100)	−76 (−105)	−48 (−55)	−12 (10)	253 (186)	291 (214)[d]

[a]AC — specimen axis parallel to tube axis (A); fracture perpendicular to radius (C).
AT — specimen axis parallel to A; fracture parallel to radius (T).
RW — specimen axis parallel to major rolling direction; fracture transverse to R.
WR — specimen axis transverse to R; fracture parallel to R.

[b]Estimated temperature.

[c]1.8-Mg (2-t) Sumitomo heat YYC-9826.

[d]Exceeded machine capacity (326 J) near 204°C (400°F).

[e]45-Mg (50-t) Sumitomo heat A-231001.

[f]4.5-Mg (5-t) Nippon Kokan KK heat 59020.

[g]Exceeded machine capacity (326 J) near 177°C (350°F).

Table 1.2. Tensile data for 76-mm-OD by 12.7-mm-wall tube made from the 2-ton heat (9826) vacuum induction melted by Sumitomo, Japan. Tubes were normalized and tempered (1038°C for 1 h; 780°C for 1 h) at Sumitomo. All tests were conducted at a nominal strain rate of 0.004/min.

Test	Specimen	Temperature (°C)	Modulus (GPa)	Strength (MPa)					Elongation (%)		Reduction of area (%)
				Proportional limit	0.02% Offset	0.2% Offset	0.5% Offset	Ultimate tensile	Uniform	Total	
23140	1L	RT	212	231	357	493	536	676	8.38	28.65	74.66
23141	2L	93	212	274	358	474	514	625	7.59	26.95	75.44
23142	3L	204	190	281	362	464	496	597	6.47	26.20	76.44
23143	4L	316	193	273	367	459	491	581	5.86	23.65	74.15
23144	5L	427	192	252	336	437	469	535	6.72	28.40	78.56
23145	6L	538	152	172	268	370	395	402	2.54	33.60	88.26
23146	7L	649	90	79	130	198	219	222	1.61	45.85	93.90

Tensile data on specimens from the Sumitomo tube are compared with the average and average − 1.65 standard error of estimate (SEE) curves for the U.S.-melted heats of modified 9 Cr-1 Mo steel in Figs. 1.10 through 1.13. These figures are for 0.2% yield, ultimate tensile strength, total elongation, and reduction of area and show the following.

1. The yield strength of the Sumitomo tube is below the average for the U.S. commercial heats. We believe that the reason for this lower yield strength is the higher tempering temperature of 780°C used by Sumitomo as compared with 760°C used by ORNL in testing the U.S. commercial heats.

2. The ultimate tensile strength of the Sumitomo heat also falls below the average for the U.S. commercial heats for the same reasons as for the yield strength.

3. Total elongation and reduction of area for the Sumitomo heat are slightly above the average curve for the U.S. commercial heats. This behavior is consistent with the slightly lower yield and ultimate tensile strength values.

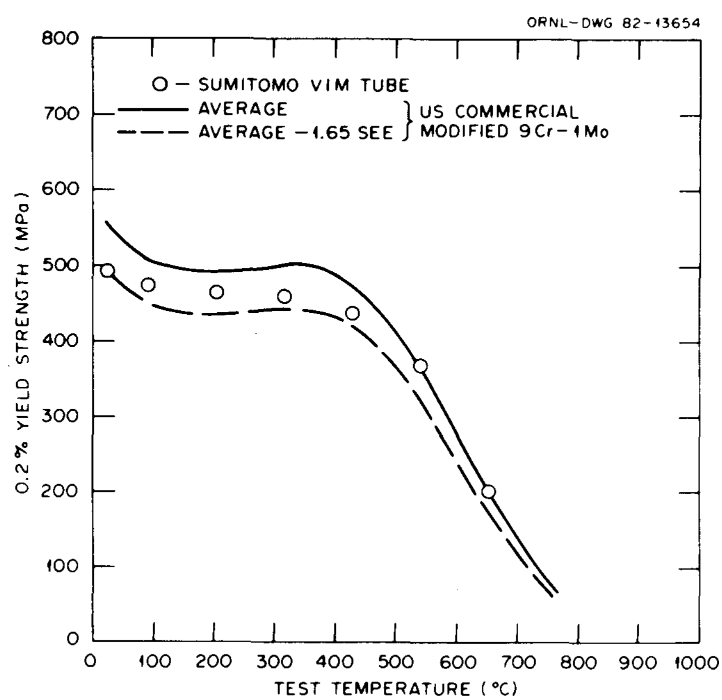

Fig. 1.10. Comparison of 0.2% yield strength data for 76-mm-OD by 12.7-mm-wall tube of the Sumitomo heat with the average and average — 1.65 SEE curves for the U.S. commercial heats of modified 9 Cr-1 Mo steel.

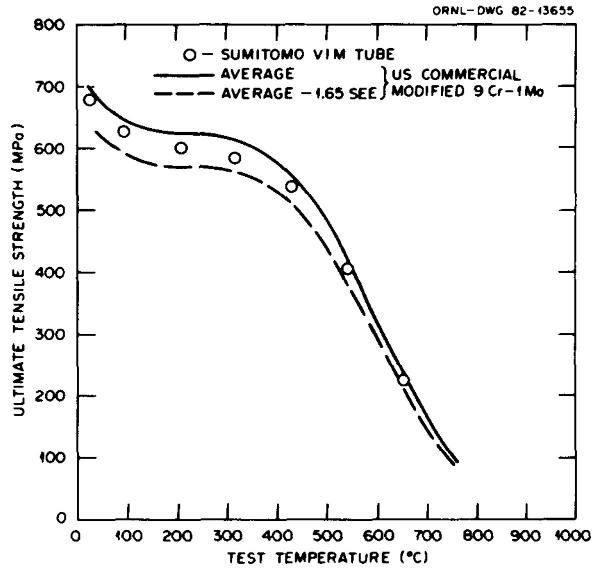

Fig. 1.11. Comparison of ultimate tensile strength data for 76-mm-OD by 12.7-mm-wall tube of the Sumitomo heat with the average and average – 1.65 SEE curves for the U.S. commercial heats of modified 9 Cr-1 Mo steel.

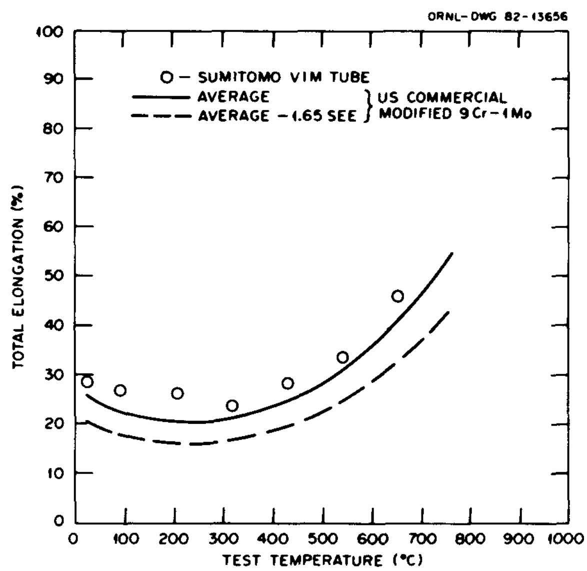

Fig. 1.12. Comparison of total elongation data for 76-mm-OD by 12.7-mm-wall tube of the Sumitomo heat with the average and average – 1.65 SEE curves for the U.S. commercial heats of modified 9 Cr-1 Mo steel.

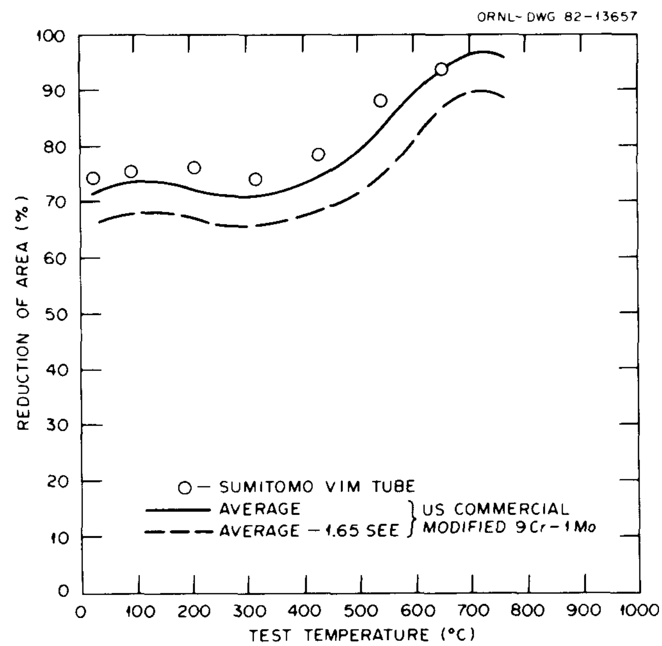

Fig. 1.13. Comparison of reduction of area data for 76-mm-OD by 12.7-mm-wall tube of the Sumitomo heat with the average and average — 1.65 SEE curves for the U.S. commercial heats of modified 9 Cr-1 Mo steel.

A limited number of creep tests have either ruptured or are in progress on specimens of the 76-mm-OD by 12.7-mm-wall tube of the Sumitomo heat (Table 1.3). Test data available are compared with the average curves for the U.S.-melted material in Fig. 1.14. This figure shows that the creep-rupture strength of the Japanese-melted heat is nearly the same as that observed for the U.S.-melted commercial heats. Tests in progress suggest that some values might even exceed the average observed for the U.S.-melted material.

1.2.2.3 Sumitomo 50-ton heat

Besides the 2-ton VIM heat, Sumitomo has also melted a 50-ton heat of the modified 9 Cr-1 Mo steel. This is the first heat melted of such a size. This heat was processed by using vacuum oxygen deoxidation (VOD).

Table 1.3. Creep data for 76-mm-OD by 12.7-mm-wall tube made from the 2-ton heat (9826) melted by Sumitomo, Japan. The heat was made by the vacuum induction process. The tubes were normalized and tempered (1038°C for 1 h; 780°C for 1 h) at Sumitomo

Test	Specimen	Stress (MPa)	Strain (%)						Time (h)				Minimum creep rate, $\dot{e}_m$ (%/h)	Reduction of area (%)	Stable creep strain $t_r \cdot \dot{e}_m$ (%)
			Loading e_l	Transient e_{pc}	Primary e_1	Secondary e_2	0.2% Offset e_s	Fracture e_f	Primary t_1	Secondary t_2	0.2% Offset t_s	Rupture t_r			
								593°C							
23153	9L	193	0.24	0.50	0.55	3.75	4.375	30.11	3.0	98.0	109.0	175.3	3.38 E-2	86.23	5.92
23147	8L	172	0.18	0.70	0.80	4.25	4.75	32.05	20.0	640.0	690.0	931.2	5.55 E-3	90.34	5.17
23163	13L	145	0.18									>2670.3			
								649°C							
23158	10L	117	0.20	0.75	1.00	2.75	3.25	29.86	20.0	160.0	187.5	325.8	1.25 E-2	88.78	4.07
23157	11L	90	0.12									>2718.5			
23160	12L	90	0.14									>2669.8			

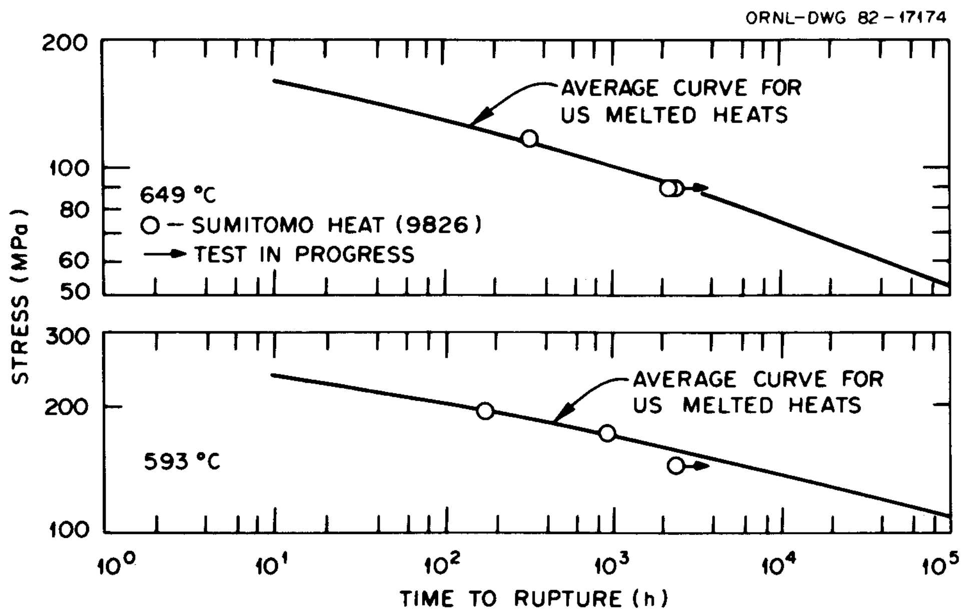

Fig. 1.14. Comparison of creep rupture data for 76-mm-OD by 12.7-mm-wall tube of Sumitomo heat with the average curves observed for the U.S.-melted commercial heats of modified 9 Cr-1 Mo steel.

It was fabricated into several different tube sizes. The chemical analysis of this heat is given in Table 1.4. Note that it is well within the specifications. Tubes from this heat were provided to CE for installation in the Consolidated Edison power plant. Tubes from this heat were also supplied (at no cost to ORNL) to ORNL and CE for installation in the two power plants of Ontario Hydro, Canada. A 44-mm OD by 12.7-mm-wall tube from this heat is being used for examining the microstructural, Charpy impact, tensile, and creep properties. Since this material became available, we have completed only the Charpy impact tests. The Charpy impact data in the AC orientation on the 44-mm-OD by 12.7-mm-wall tubing of the 50-ton heat are compared with the data on the tubing for the 2-ton heat in Fig. 1.15. This figure shows no difference in the Charpy impact behavior of the two heats.

Other properties of this heat are being determined and will be reported later.

Table 1.4. Analysis of Japanese 50-ton heat (A231001) of modified 9 Cr-1 Mo steel made by vacuum oxygen deoxidation process

Element	Content (wt %)		
	Specified range	Ladle	Check
C	0.08–0.12	0.10	0.097
Mn	0.30–0.50	0.38	0.38
Si	0.2–0.5	0.38	0.40
P	0.02 max	0.013	0.015
S	0.01 max	0.005	0.005
Cr	8–9.5	8.39	8.46
Ni	0.4 max	0.10	0.11
Mo	0.85–1.05	0.94	0.96
Cu	0.1 max	0.02	0.02
V	0.18–0.25	0.21	0.23
Nb	0.06–0.10	0.077	0.076
N	0.03–0.07	0.0375	0.0390
Al (soluble)	0.04 max	0.002	0.005

1.2.2.4 NKK 5-ton heat

A 5-ton heat of modified 9 Cr-1 Mo steel was melted by NKK, Japan, by the VIM process. It was fabricated into a 25-mm-thick plate and into 76-mm-OD by 12.7-mm-wall and 51-mm-OD by 6.35-mm-wall tubes. This heat was melted, fabricated, and shipped at no cost to ORNL. Since the arrival of various products of the NKK heat at ORNL, we have completed microstructure, hardness, Charpy impact, tensile, and creep tests. These data are described below.

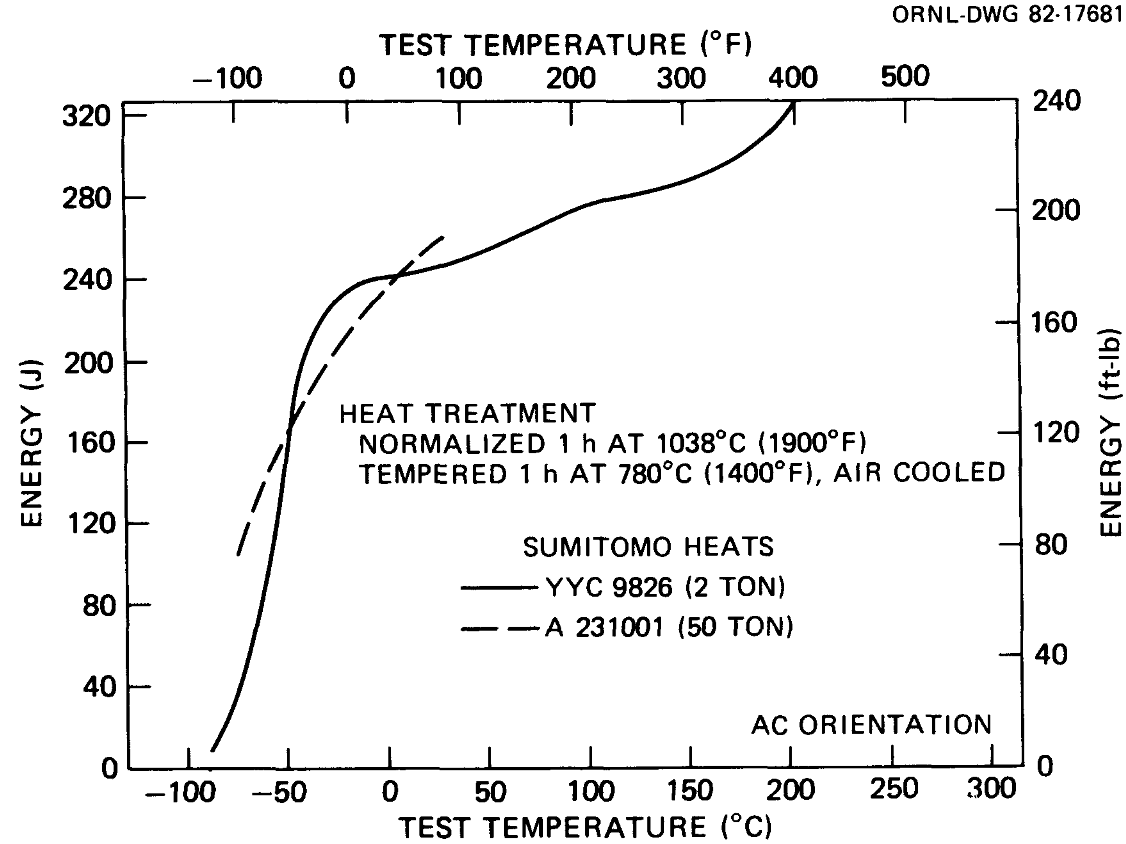

Fig. 1.15. Comparison of the Charpy impact curves for the Sumitomo 50- and 2-ton heats. For the 50-ton heat, we tested the 76-mm-OD by 12.7-mm-wall tubing, and for the 2-ton heat, we tested 44-mm-OD by 12.7-mm-wall tubing.

The optical microstructures of longitudinal and circumferential sections from 76-mm-OD by 12.7-mm-wall and 51-mm-OD by 6.35-mm-wall tubes are compared in Figs. 1.16 and 1.17. These photomicrographs also show the presence of inclusions. However, the inclusions are round and much fewer than those observed in the 2-ton Sumitomo heat. The greater size of the NKK heat might be responsible for the lower inclusion content. As pointed out previously, the smaller the heat, the more difficult it is to prevent the mixing of slag with the molten metal during pouring. The grain size of both size tubes is very fine (ASTM grain size numbers 8–9)

Y-185743

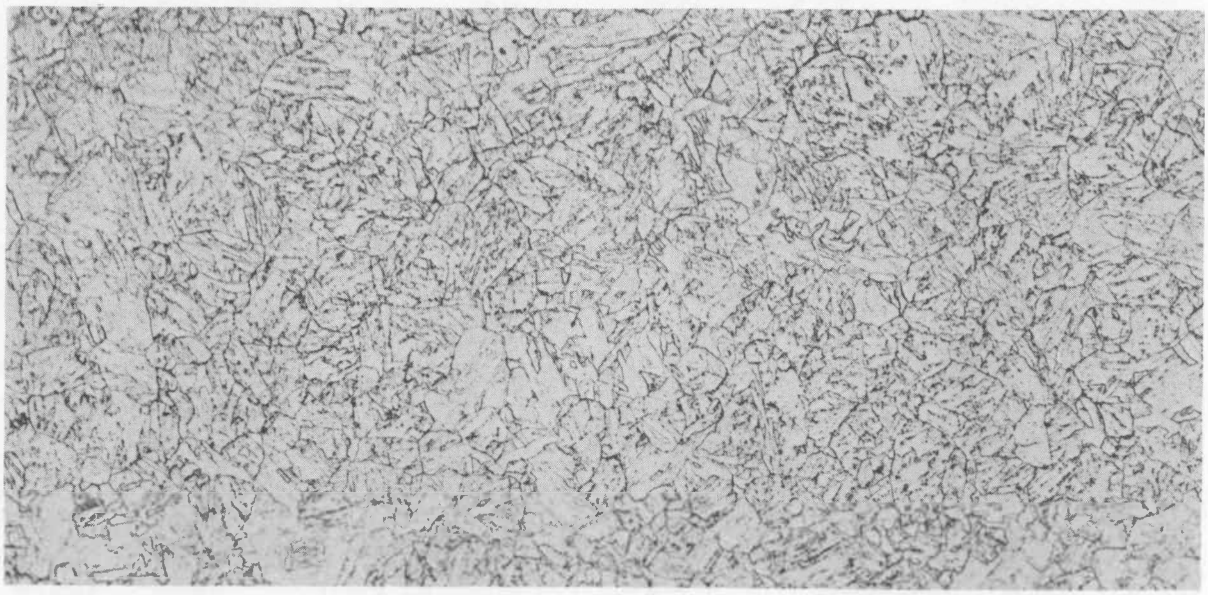

(a)

40 μm

Y-185744

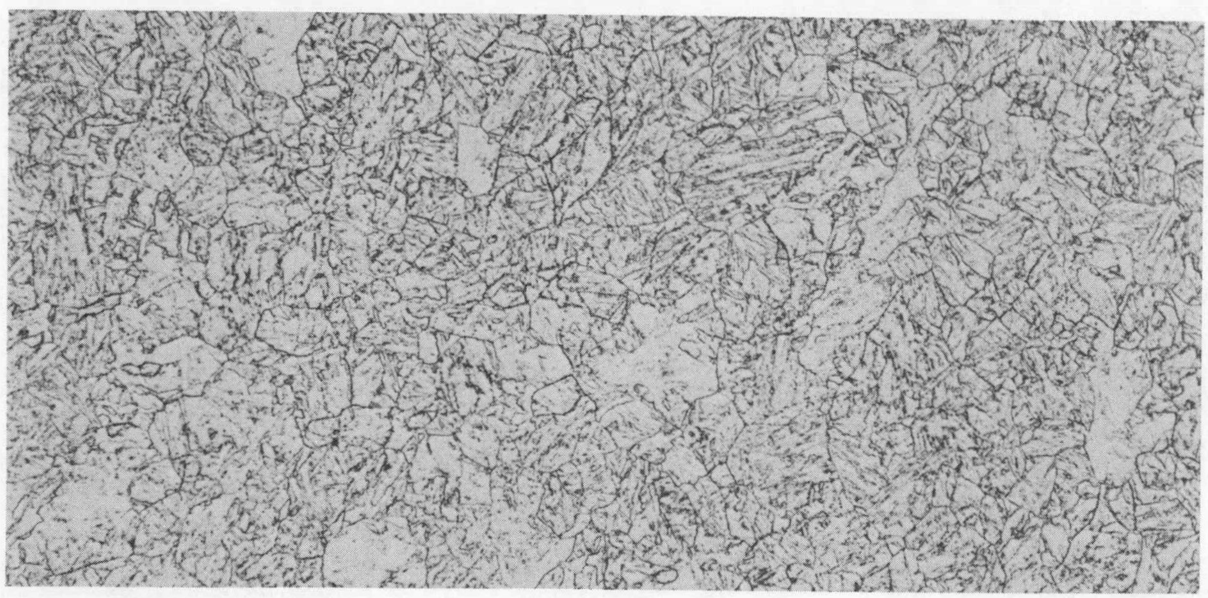

(b)

Fig. 1.16. Microstructure of (*a*) longitudinal and (*b*) circumferential sections of 76-mm-OD by 12.7-mm-wall tube made by NKK from a 5-ton heat.

Y-185741

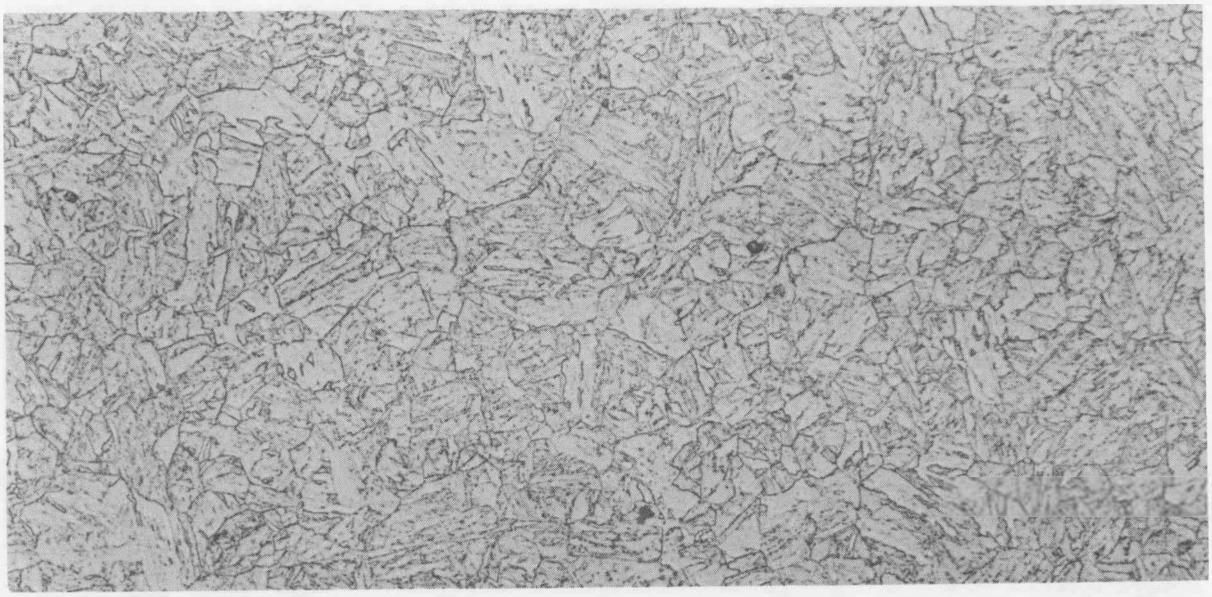

(a)

40 μm

Y-185742

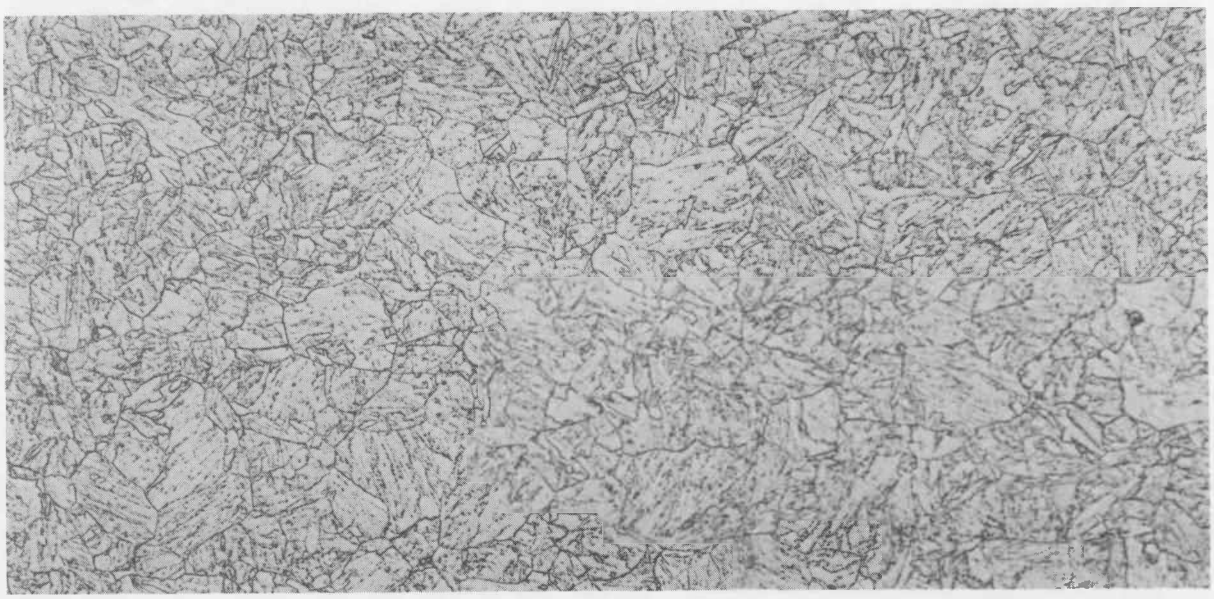

(b)

Fig. 1.17. Microstructure of (*a*) longitudinal and (*b*) circumferential sections of 51-mm-OD by 6.35-mm-wall tube made by NKK from a 5-ton heat.

and is nearly the same for both orientations. The microhardness values (and standard deviations) for the longitudinal and circumferential sections of 76-mm-OD by 12.7-mm-wall tubes were 218 ± 3 and 219 ± 3 dph. Microhardness values of 51-mm-OD by 6.35-mm-wall tubes were 219 ± 4 and 215 ± 4 dph, respectively, for the two specimen orientations.

The Charpy impact energy curves for WR and RW specimen orientations of the 25-mm plate are shown in Fig. 1.18. The V-notch is parallel to the rolling direction in the WR orientation and perpendicular in the RW orientation. The difference in the Charpy impact curves for the two orientations is consistent with the results expected when the plate is not extensively cross-rolled. The slightly worse Charpy impact properties of the WR orientation is a result of low resistance to crack propagation along the inclusion-matrix interface. The ductile-brittle transition temperature and upper-shelf energy data for the plate are listed in Table 1.1.

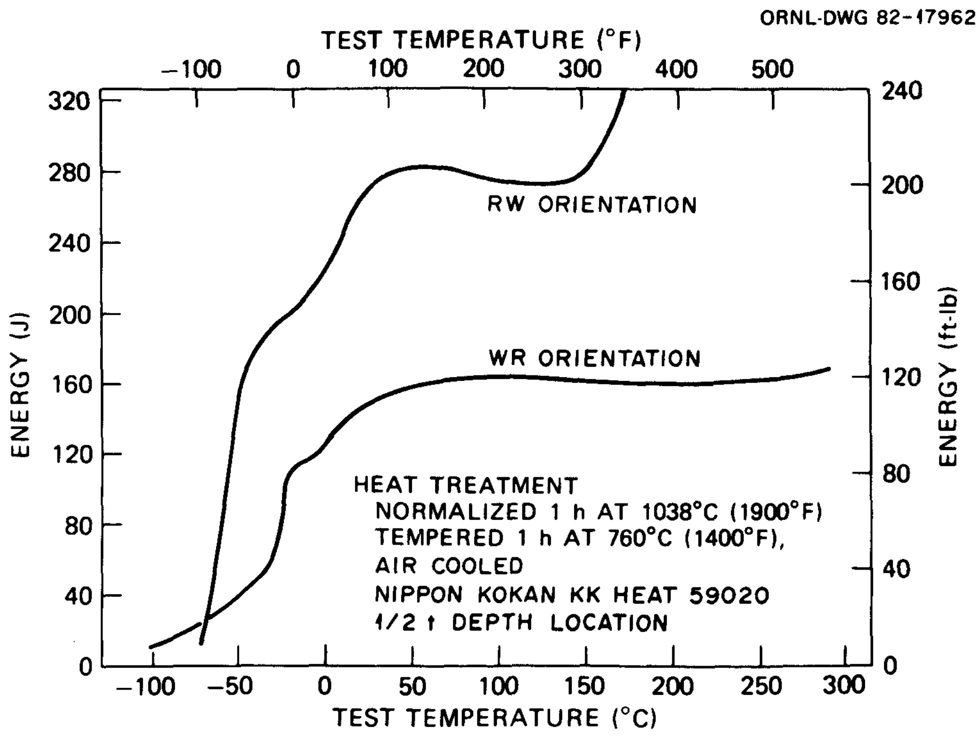

Fig. 1.18. Effect of specimen orientation on the Charpy-V impact energy from 25-mm-thick modified 9 Cr-1 Mo steel plate of NKK heat 59020.

The Charpy impact energy curves for the AC and AT orientations of the 76-mm-OD by 12.7-mm-wall tube are plotted in Fig. 1.19. Data from this figure are also listed in Table 1.1. Figure 1.19 shows no difference in Charpy impact energy curves for the two orientations. This result is similar to that observed for the Sumitomo tubing, as shown in Fig. 1.9.

Tensile tests were conducted on specimens from both the 25-mm-thick plate and 76-mm-OD by 12.7-mm-wall tubing of the NKK heat. For the plate, we used transverse specimens 12.83 mm in diameter. For the tubing, we used longitudinal specimens 6.35 mm in diameter. Data on both products are summarized in Table 1.5. Various tensile properties of the 25 mm plate and the 76-mm-OD by 12.7-mm-wall tubes of the NKK heat are compared with the average and average — 1.65 standard error of estimate curves for the U.S. commercial heats of modified 9 Cr-1 Mo steel in Figs. 1.20 through 1.23. These figures show the following.

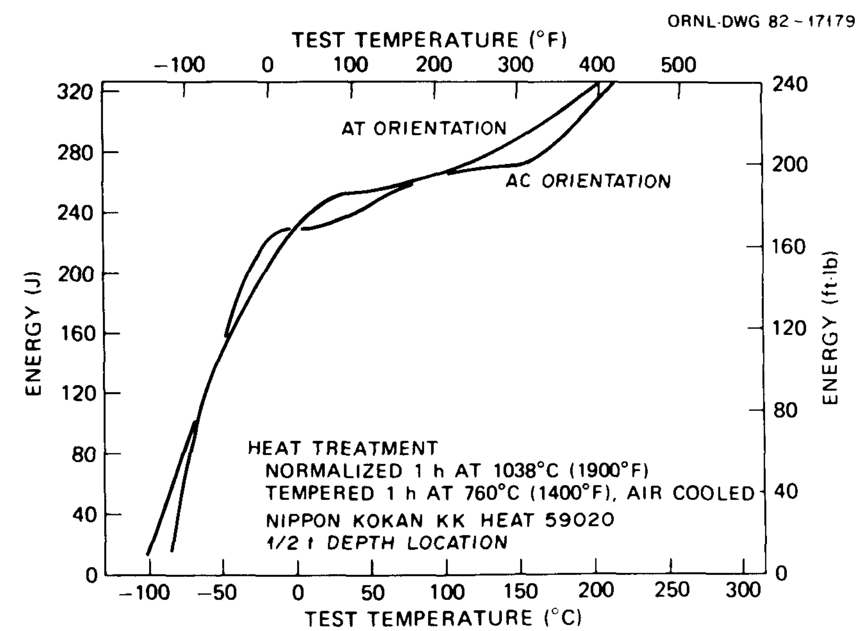

Fig. 1.19. Effect of specimen orientation on the Charpy-V impact energy of 76-mm-OD by 12.7-mm-wall modified 9 Cr-1 Mo steel tubing of NKK heat 59020.

Table 1.5. Tensile data for 25-mm-OD by 12.7-mm-wall tube made from the 5-ton heat (59020) melted by NKK, Japan. Both the plate and tube were normalized and tempered (1038°C for 1 h; 760°C for 1 h) at NKK. All tests were conducted at a nominal strain rate of 0.004/min.

Test	Specimen	Temperature		Modulus (GPa)	Strength (MPa)				Elongation (%)		Reduction of area (%)
		(°C)	(°F)		Proportional limit	0.02% Offset	0.2% Offset	Ultimate tensile	Uniform	Total	
					25-mm-Thick plate (12.83-mm-diam specimen)						
23166	1T	25	77	213	380	475	544	683	8.01	24.58	67.92
23167	2T	204	400	207	278	405	472	598	6.21	24.52	68.26
23168	3T	427	800	185	351	388	443	527	5.21	25.73	70.79
23169	4T	649	1200	90	81	127	185	216	2.69	46.05	93.10
					76-mm-OD by 12.7-mm-wall tube						
23201	4L	25	77	205	325	421	512	686	11.43	29.15	71.26
23202	5L	93	200	212	285	402	497	664	7.29	26.15	73.76
23203	6L	204	400	207	302	383	471	625	6.42	24.05	76.15
23204	7L	316	600	391	387	423	499	594	6.17	24.60	72.75
23205	8L	427	800	196	169	289	416	530	5.96	30.85	78.90
23237	12L	538	1000	154	152	251	356	397	1.71	38.32	88.27
23206	9L	538	1000					394	2.19	38.25	89.4
23207	10L	649	1200	79	68	115	185	221	2.14	45.01	92.17

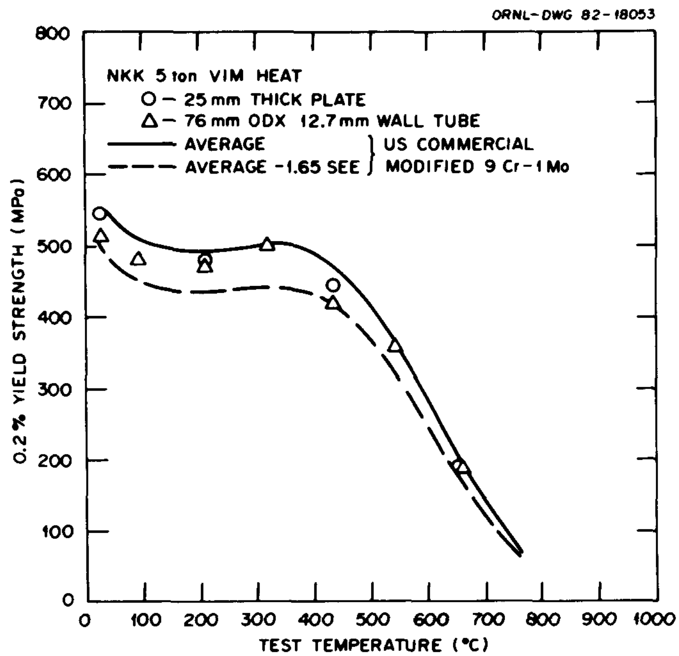

Fig. 1.20. Comparison of 0.2% yield strength data for 25-mm-thick plate and 76-mm-OD by 12.7-mm-wall tube of the NKK heat with the average and average — 1.65 SEE curves for the U.S. commercial heats of modified 9 Cr-1 Mo steel.

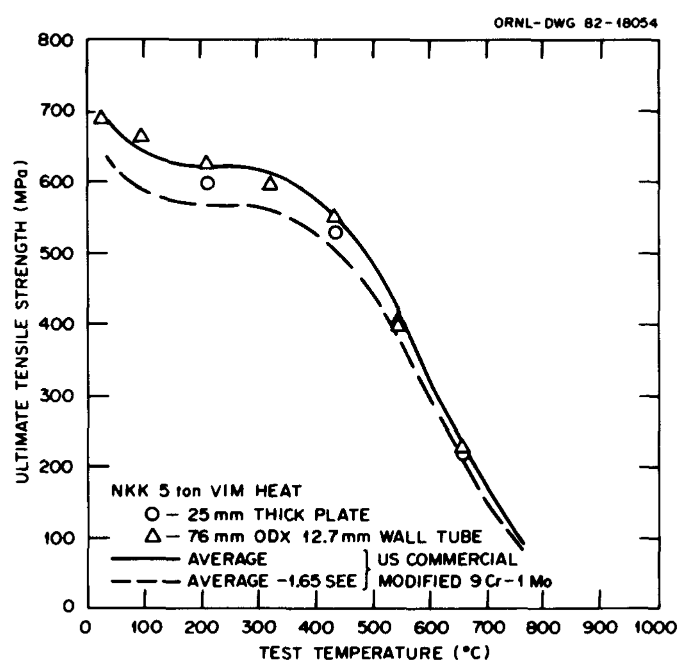

Fig. 1.21. Comparison of the ultimate tensile strength data for 25-mm-thick plate and 76-mm-OD by 12.7-mm-wall tube of the NKK heat with the average and average — 1.65 SEE curves for the U.S. commercial heats of modified 9 Cr-1 Mo steel.

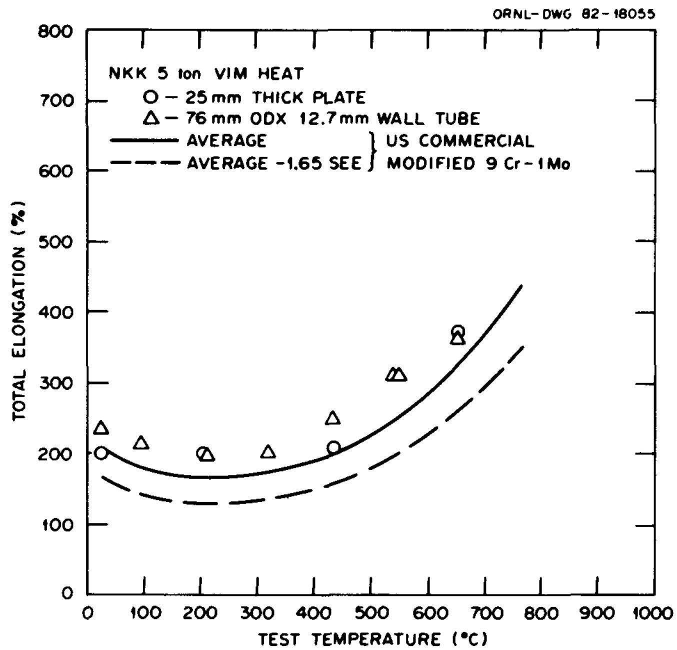

Fig. 1.22. Comparison of total elongation data for 25-mm-thick plate and 76-mm-OD by 12.7-mm-wall tube of the NKK heat with the average and average — 1.65 SEE curves for the U.S. commercial heats of modified 9 Cr-1 Mo steel.

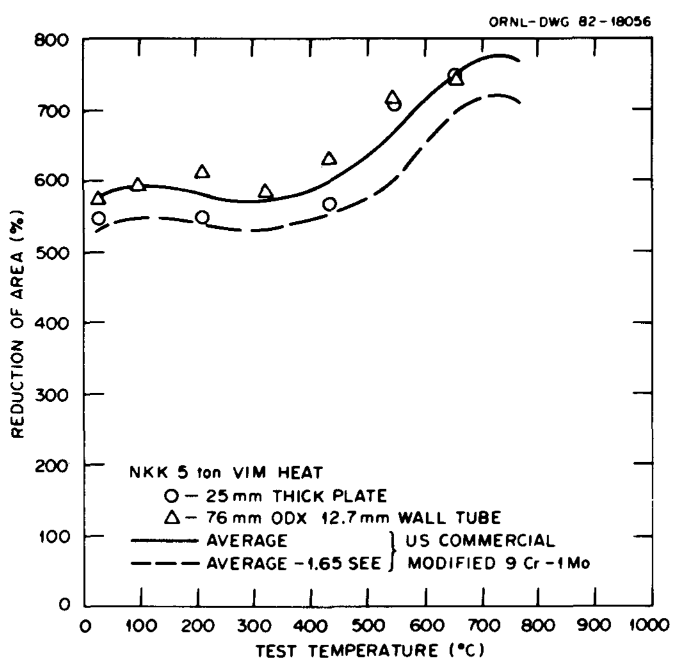

Fig. 1.23. Comparison of reduction of area data for 25-mm-thick plate and 76-mm-OD by 12.7-mm-wall tube of the NKK heat with the average and average — 1.65 SEE curves for the U.S. commercial heats of modified 9 Cr-1 Mo steel.

1. The 0.2% yield strength of the NKK tube and plate are nearly the same. However the values are slightly below the average curve for the U.S.-melted material. We believe that the difference is probably due to slight heat treatment differences. The NKK products were heat-treated at the NKK fabrication shop, whereas the U.S. commercial heats were heat-treated at ORNL. The latter might provide slightly better controlled heat treatment.

2. The ultimate tensile strength of the NKK tube and plate are nearly the same but are slightly below the average curve for the U.S.-melted commercial heats for the same reasons.

3. The total elongation values of the NKK tube and plate are above the average value curve for the U.S.-melted commercial heats.

4. The reduction of area values of the NKK tube were equal to or slightly above the average curve observed for the U.S.-melted commercial heats. However, the values for the plate are slightly below the average curve for the U.S.-melted commercial heats.

A limited number of creep tests conducted on 76-mm-OD by 12.7-mm-wall tubing of the NKK heat are summarized in Table 1.6. These data are compared with the average curve for the U.S.-melted material in Fig. 1.24. This figure shows that the rupture time of tests failed have either matched or exceeded the average values observed for the U.S.-melted material. The only test in progress is expected to fail after about 9000 h.

1.2.3 Operating Experience on Modified 9 Cr-1 Mo Steel Tubes

Tubes of modified 9 Cr-1 Mo steel have been either operating or getting ready to be installed in various power plants. The current status of installation of modified 9 Cr-1 Mo steel in various power plants is summarized in Table 1.7. This table indicates that the range of utilities involved is international: United States, United Kingdom, and Canada.

Table 1.6. Creep data for 76-mm-OD by 12.7-mm-wall tube made from 5-ton heat (59020) vacuum induction melted by Nippon Kokan KK, Japan. Tubes were normalized and tempered (1038°C for 1 h; 760°C for 1 h) at NKK

Test	Specimen	Stress (MPa)	Strain (%)						Time (h)				Minimum creep rate, $\dot{e}_m$ (%/h)	Reduction of area (%)	Stable creep strain $t_r \cdot \dot{e}_m$ (%)
			Loading e_l	Transient e_{pc}	Primary e_1	Secondary e_2	0.2% Offset e_s	Fracture e_f	Primary t_1	Secondary t_2	0.2% Offset t_s	Rupture t_r			
								593°C							
23189	1L	193	0.25	0.75	1.00	5.75	6.25	31.42	6.0	126.0	133.0	186.3	3.875 E-2	88.74	7.22
23191	3L	172	0.27	1.00	1.25	4.75	5.50	29.49	25.0	365.0	405.0	602.8	1.025 E-2	85.64	6.18
								649°C							
23190	2L	117	0.20	0.75	0.85	3.25	4.00	32.96	10.0	160.0	185.0	298.9	1.6 E-2	90.92	4.78
23211	11L	76	0.09									>1948.8			

Table 1.7. Current status of testing of modified 9 Cr-1 Mo steel tubes in U.S. and foreign steam power plants

Utility	Plant	Tube location	Operating temperature (°C)	Tubes being replaced	Number of tubes	Date installed	Status
Tennessee Valley Authority	Kingston Steam Plant, Unit 5	Superheater	593	Type 321	8	May 1980	Operating
American Electric Power	Tanners Creek Unit 3	Secondary superheater	593	Type 304	10	April 1981	Operating
Detroit Edison	St. Clair Unit 2	Reheater	538	Type 347	2	February 1981	Operating
Central Electric Generating Board (U.K.)	Agecroft Power Station	Superheater	590–620	2 1/4 Cr-1 Mo	6	April 1982	Operating
Ontario Hydro (Canada)	Lambton TGS	Reheater Reheater	538 538	Tye 304H Std 9 Cr-1 Mo	9 9	September 1982	Planned
Ontario Hydro (Canada)	Nanticoke TGS	Secondary superheater	538	2 1/4 Cr-1 Mo	11	September 1982	Planned

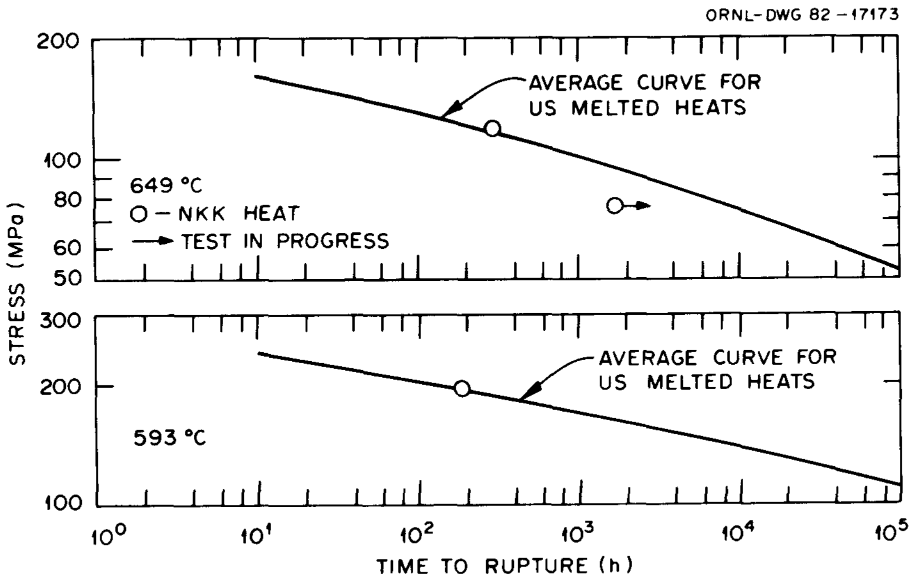

Fig. 1.24. Comparison of creep rupture data for 76-mm-OD by 12.7-mm-wall tube of the NKK heat with the average curves observed for the U.S. commercial heats of modified 9 Cr-1 Mo steel.

And, in fact, alloy produced in Japan will be used in the Canadian installation. In most cases, the tubes being replaced are stainless steel. The longest operating time has been reached for tubes installed at the Kingston Steam Plant. Tubes in the Agecroft Power Station were installed during April 1982. Tubes in the Lambton and Nanticoke plants are expected to be installed during September and October 1982. This operating experience will be very useful for obtaining approval of this alloy in the ASME code.

1.3 Effect of Normalizing Temperature on Mechanical Properties of Modified 9 Cr-1 Mo Steel (Grade 91)

V. K. Sikka

A modified 9 Cr-1 Mo steel (see Table 1.8 for specifications) with properties significantly improved over the standard 9 Cr-1 Mo and 2 1/4 Cr-1 Mo steel has been developed[2] jointly by ORNL and CE, Chattanooga. The alloy obtains its improved strength through the optimum additions of strong carbide formers, such as niobium and vanadium. The modified alloy is designated as grade 91 by ASTM. The presence of niobium and vanadium carbides in the alloy requires a higher austenitizing (normalizing) temperature than that of the standard alloy, where only chromium carbides need to dissolve. The purpose of this report is to study the effect of normalizing temperature on the mechanical properties of modified 9 Cr-1 Mo steel. This report also examines the conditions under which grain coarsening might occur in this alloy.

1.3.1 Material and Test Procedure

This study was conducted primarily on heat 30394. However, the Charpy impact testing was conducted on another heat, 10148. Chemical analysis of both these heats is included in Table 1.8. Blocks from heat 30394 were normalized at eight different temperatures: 927, 954, 982, 1010, 1038, 1065, 1093, and 1121°C. The normalizing times varied from 10 to 480 min. Blocks in various normalizing conditions were machined into tensile, creep, and Charpy impact specimens. Coupons from each block were mounted for metallography and microhardness measurements. Grain size was measured for each of the normalizing conditions.

Tensile tests were conducted at room temperature and 593°C at a strain rate of 0.004/min. Creep tests were conducted at 649°C with only one test at 593°C. Charpy impact tests were conducted at room temperature.

1.3.2 Tensile Data

Tensile properties at room temperature and 593°C after various normalizing conditions are listed in Table 1.9. Room-temperature tensile

Table 1.8. Chemical specifications for modified 9 Cr-1 Mo steel and the analyses of two heats used in this study

Element	Content (wt %)		
	Specified range	Heat 30394	Heat 10148
C	0.08–0.12	0.084	0.091
Mn	0.30–0.60	0.46	0.49
P	⩽0.020	0.010	0.018
S	⩽0.010	0.003	0.007
Si	0.20–0.50	0.40	0.35
Ni	⩽0.40	0.09	0.16
Cr	8.00–9.50	8.57	9.34
Mo	0.85–1.05	1.02	0.99
V	0.18–0.25	0.198	0.21
Nb	0.06–0.10	0.073	0.061
Ti		0.005	0.004
Co		0.055	0.025
Cu		0.04	0.007
Al	⩽0.04	0.014	0.001
B		<0.001	<0.001
W		0.05	0.01
As		<0.001	0.002
Sn		<0.001	0.003
Zr		<0.001	0.001
N	0.030–0.070	0.053	0.037
O			0.006

properties are plotted as a function of a time-temperature parameter [Holloman-Jaffee (HJ)] in Figs. 1.25 and 1.26. Figure 1.25 shows that both yield and ultimate tensile strengths continue to increase with increasing normalizing temperature and time; the ultimate tensile strength increases less than does the yield strength. Ductility values, especially uniform and total elongation, show some decrease after normalizing above 1093°C for times exceeding 1 h. Note, however, that the total elongation values are still above the room-temperature specified value of 18% for this alloy. Reduction of area values did not show any significant change, even after normalizing at 1121°C for 8 h.

Tensile properties at 593°C are plotted as a function of HJ parameter in Figs. 1.27 and 1.28. These figures show that the effect of normalizing temperature on the tensile properties at 593°C is similar to that observed at room temperature.

Table 1.9. Effect of normalizing temperature and time on tensile properties of modified 9 Cr-1 Mo steel (heat 30394). All specimens were tempered at 760°C for 1 h before testing

Normalizing conditions		Strength (MPa)		Elongation (%)	Reduction of area (%)
Temperature (°C)	Time (min)	Yield	Ultimate		
		Room-temperature data			
927	60	469	648	32.20	70.91
954	60	505	665	28.25	70.73
982	120	519	673	29.16	70.04
1010	60	538	686	28.95	70.27
1038	30	552	700	27.15	69.32
1038	60	578	715	26.00	69.05
1065	15	556	698	29.05	70.72
1065	30	559	701	30.99	70.16
1093	10	576	713	27.80	69.79
1093	20	593	728	27.20	70.29
1093	120	623	750	24.35	69.26
1093	480	603	724	25.15	74.33
1121	60	637	756	23.65	71.21
1121	120	688	790	21.85	70.75
1121	240	625	746	24.55	70.84
1121	480	658	771	22.90	71.45
		593°C Data			
927	60	259	310	48.98	90.81
954	60	283	318	36.80	88.86
982	120	287	310	43.21	90.13
1010	60	305	330	43.20	89.28
1038	30	302	337	42.00	89.30
1038	60	312	346	37.75	88.44
1065	15	293	321	47.80	89.63
1065	30	323	348	40.98	89.01
1093	10	318	350	41.95	88.63
1093	20	322	349	40.22	88.57

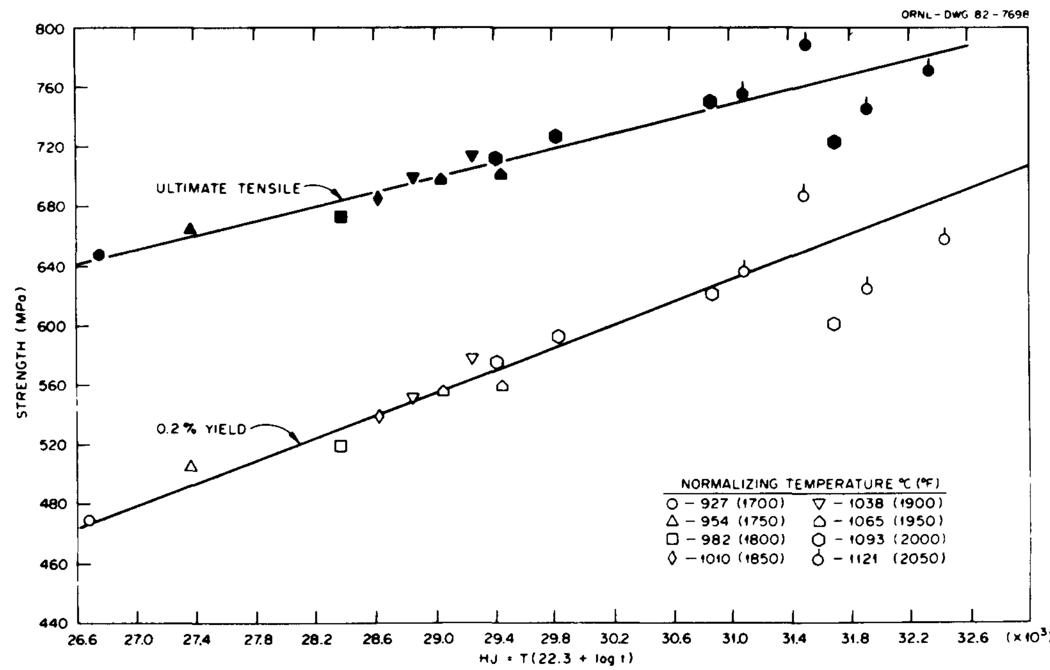

Fig. 1.25. Room-temperature yield and ultimate tensile strengths as functions of Holloman-Jaffee parameter for various normalizing temperature and time combinations.

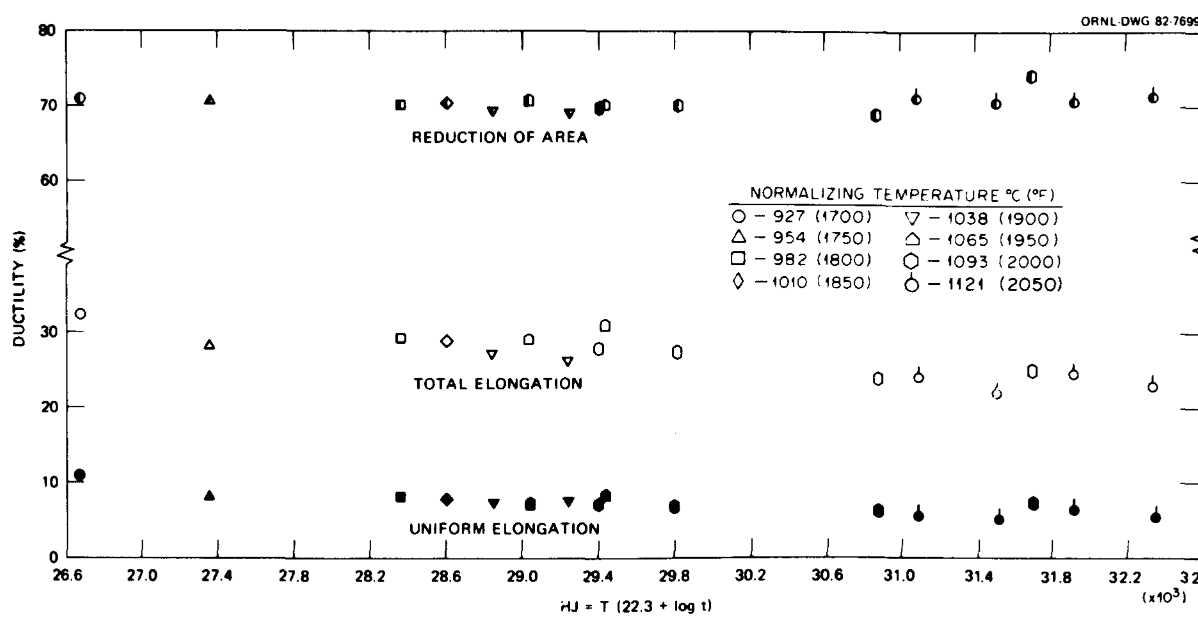

Fig. 1.26. Room-temperature ductility quantities as functions of Holloman-Jaffee parameter for various normalizing temperature and time combinations.

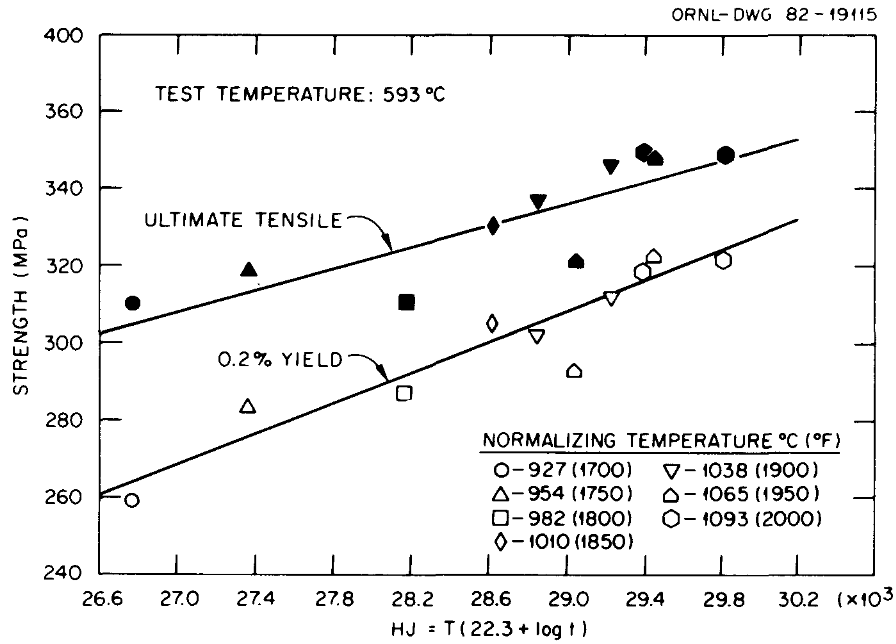

Fig. 1.27. Yield and ultimate tensile strengths at 593°C as functions of Holloman-Jaffee parameter for various normalizing temperature and time combinations.

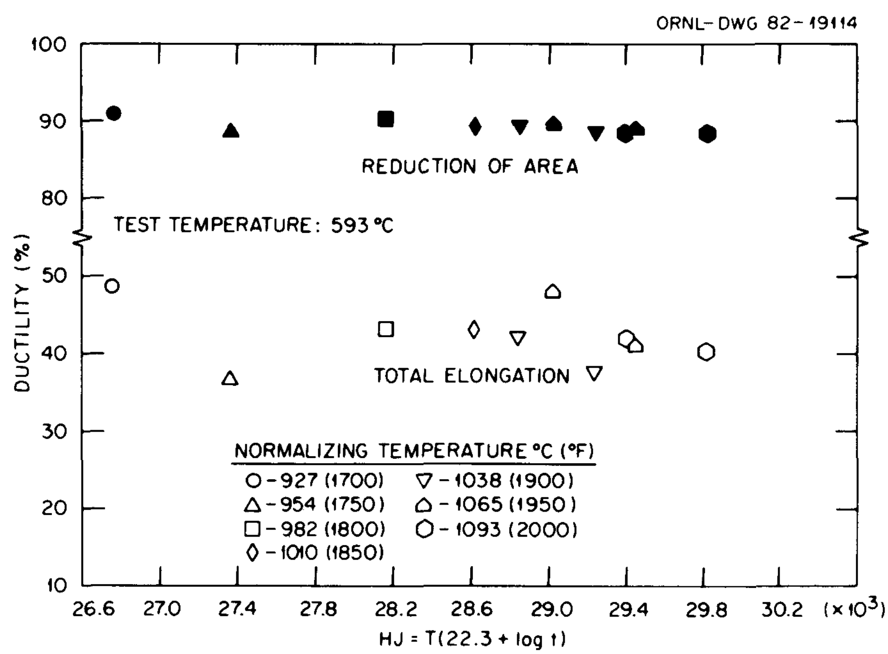

Fig. 1.28. Ductility quantities at 593°C as functions of Holloman-Jaffee parameter for various normalizing temperature and time combinations.

1.3.3 Hardness Data

Microhardness data on specimens after various normalizing temperatures and a fixed tempering temperature of 760°C for 1 h are plotted as a function of HJ parameter in Fig. 1.29. The hardness values show a trend similar to that observed for ultimate tensile strength — namely, the increase in the values with increasing normalizing temperature and time.

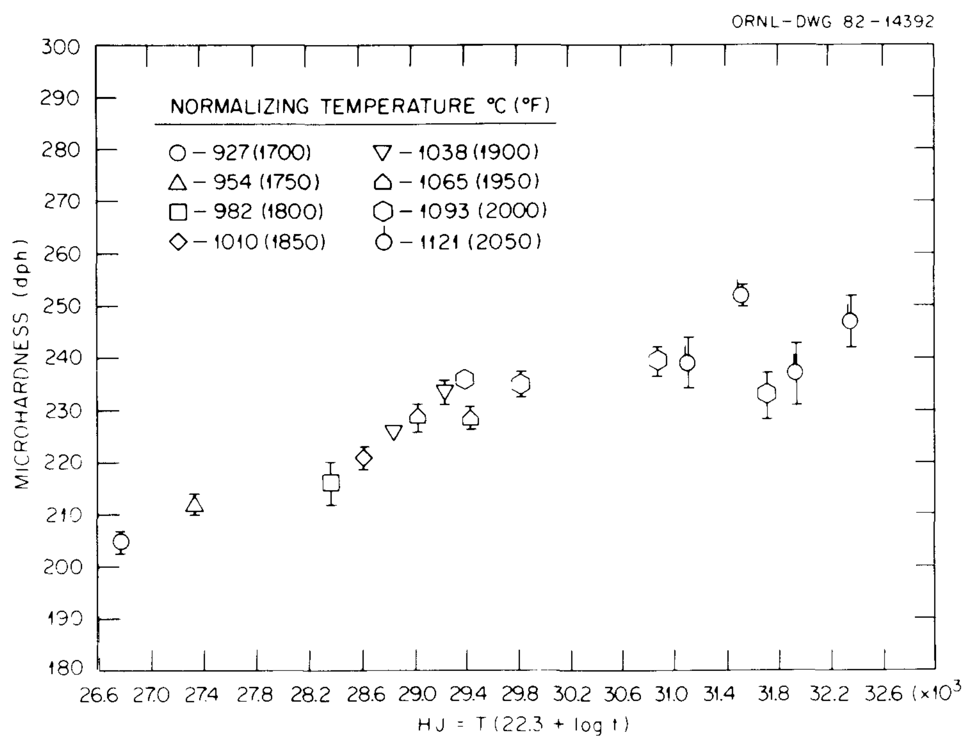

Fig. 1.29. Microhardness data as a function of Holloman-Jaffee parameter for various normalizing temperature and time combinations.

1.3.4 Creep Data

Creep data obtained after various normalizing temperatures and times are listed in Table 1.10. Time-to-rupture data from these tests are plotted as a function of HJ parameter in Fig. 1.30. These data show an

Table 1.10. Effect of normalizing temperature and time on the creep properties of modified 9 Cr-1 Mo steel (heat 30394). Normalizing temperature and time were varied in this study; however, the tempering temperature was kept at 760°C for all specimens

Test	Specimen	Normalizing		Strain (%)						Time (h)				Minimum creep rate, $\dot{e}_m$ (%/h)	Reduction of area (%)
		Temperature (°C)	Time (min)	Loading e_l	Transient e_{pc}	Primary e_1	Secondary e_2	0.2% Offset e_s	Fracture e_f	Primary t_1	Secondary t_2	0.2% Offset t_s	Rupture t_r		
							649°C at 103 MPa (15 ksi)								
23036	411T	927	60	0.18	0.50	0.625	3.00	3.50	33.34	4.0	91.0	100.0	144.4	3.01 E-2	88.43
23038	355T	982	120	0.15	0.725	0.775	3.00	3.75	31.78	20.0	275.0	325.0	531.5	8.525 E-3	87.38
23039	371T	1038	30	0.13	0.30	0.375	2.75	3.50	35.43	10.0	465.0	545.0	777.2	5.2 E-3	85.69
23047	379T	1065	15	0.18	0.375	0.4125	1.875	2.625	24.50	15.0	415.0	550.0	861.9	3.625 E-3	88.45
23050	387T	1065	30	0.14	0.20	0.25	2.00	2.50	25.16	10.0	500.0	595.0	962.6	3.3 E-3	82.75
23052	395T	1093	10	0.13	0.00	0.00	1.75	2.25	32.35	0.0	740.0	850.0	1383.0	2.25 E-3	86.20
23051	403T	1093	20	0.18	0.20	0.25	1.75	2.50	27.94	10.0	560.0	740.0	1117.8	2.71 E-3	86.03
							649°C at 90 MPa (13 ksi)								
23046	412T	927	60	0.12	0.675	0.75	2.75	3.25	34.87	22.5	272.5	300.0	410.8	7.65 E-3	90.26
23117	349T	954	60	0.12	0.50	0.75	2.50	3.00	32.87	30.0	385.0	430.0	789.5	5.25 E-3	84.93
23105	356T	982	120	0.14	0.325	0.50	2.75	3.25	26.78	40.0	800.0	950.0	1324.1	3.09 E-3	84.72
23106	364T	1010	60	0.16	0.25	0.3125	3.125	4.00	22.61	50.0	1675.0	2050.0	2668.8	1.7 E-3	76.10
23111	372T	1038	30	0.17	0.00	0.00	2.75	3.50	26.24	0.0	1575.0	1825.0	2785.1	1.7 E-3	78.07
23200	404T	1093	20	0.14									>2830.5		
							593°C at 159 MPa (23 ksi)								
23008	363T	1010	60	0.22	0.90	1.30	2.50	3.0	19.98	350.0	1350.0	1512.5	2306.9	12.E-3	79.71

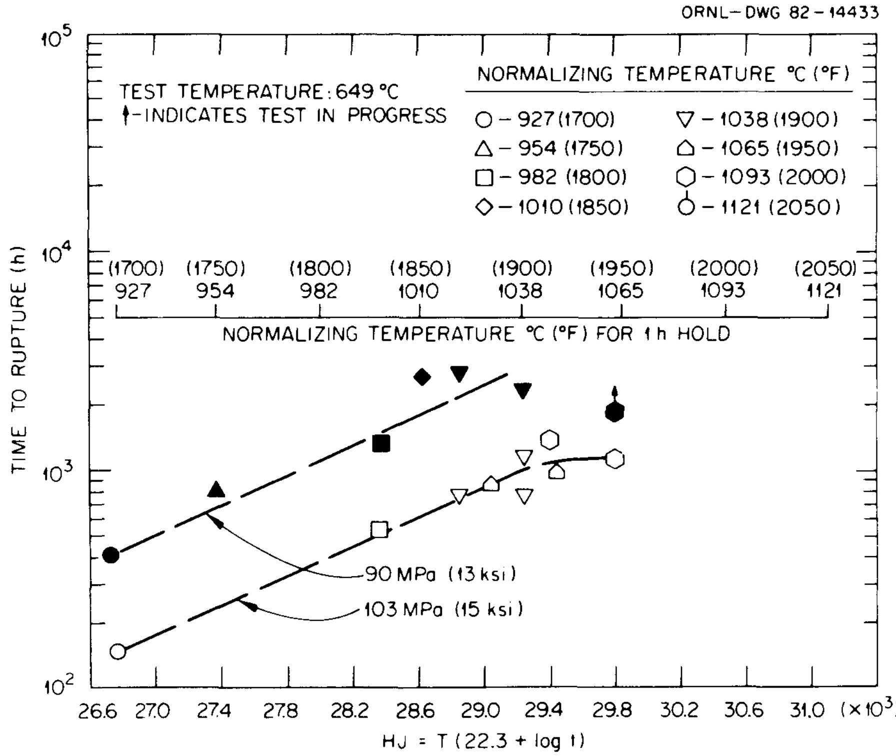

Fig. 1.30. Time-to-rupture data at 649°C as a function of Holloman-Jaffee parameter for various normalizing temperature and time combinations.

increase in time to rupture with increasing normalizing temperature and time. This figure also shows that the rupture time may level off at a normalizing temperature of 1038°C and a tempering temperature of 760°C. These normalizing and tempering conditions are those recommended to obtain the optimum strength properties from this alloy. The creep ductility was not affected by increasing the normalizing temperature or time.

1.3.5 Optical Microstructure and Grain Size Measurements

The optical microstructure of specimens normalized at 1093°C for 2 and 8 h is shown in Figs. 1.31 and 1.32 at 500 and 1500×, respectively. Figures 1.33 and 1.34 show the 500 and 1500× photomicrographs, respectively, of specimens normalized at 1121°C for 1, 2, 4, and 8 h. The

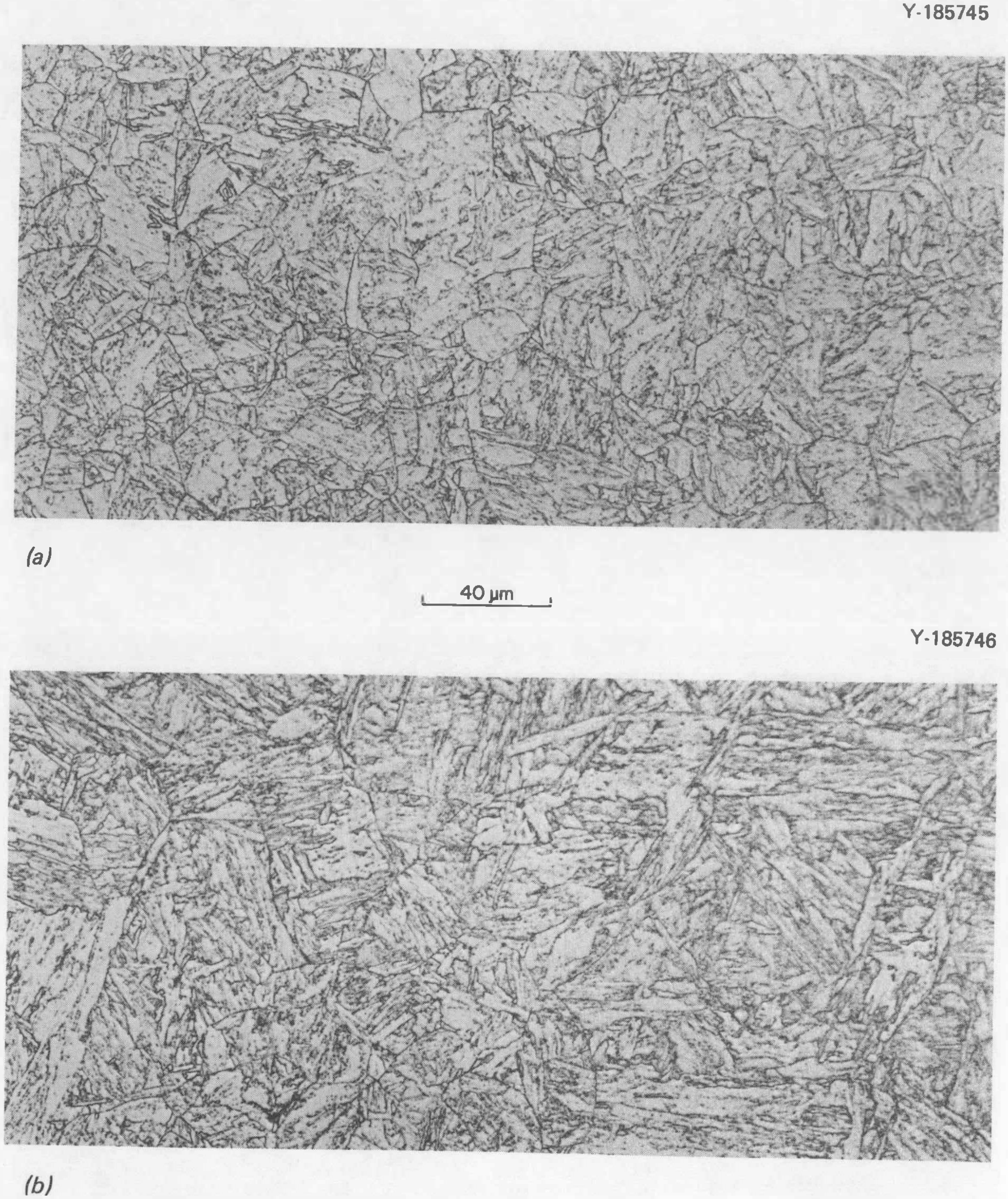

Fig. 1.31. Microstructure of specimens normalized at 1093°C for (*a*) 2 h and (*b*) 8 h.

Y-185755

(a)

13.4 μm

Y-185756

(b)

Fig. 1.32. Higher magnification optical micrographs of specimens normalized at 1093°C for (*a*) 2 h and (*b*) 8 h.

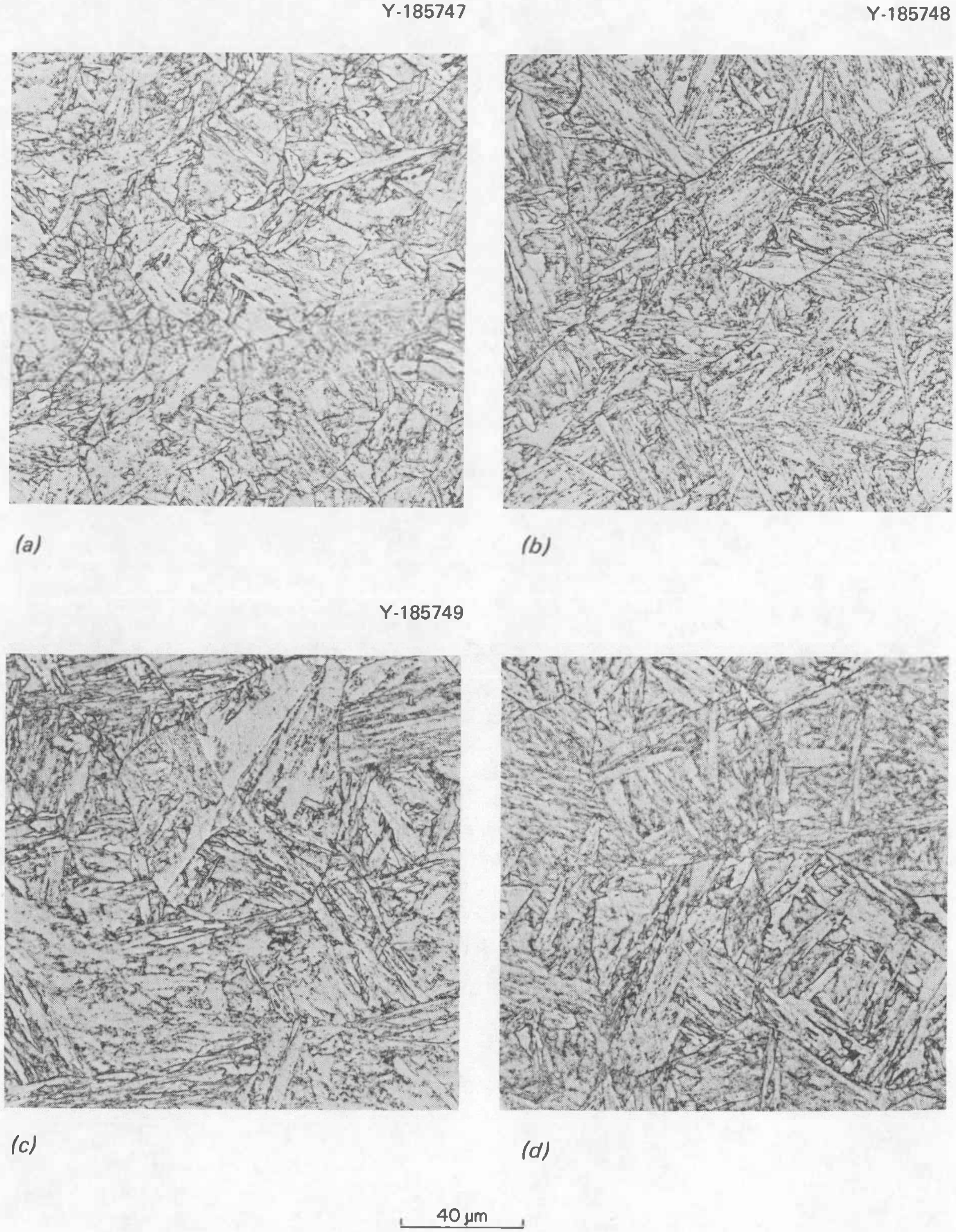

Fig. 1.33. Microstructure of specimens normalized at 1121°C for (*a*) 1 h, (*b*) 2 h, (*c*) 4 h, and (*d*) 8 h.

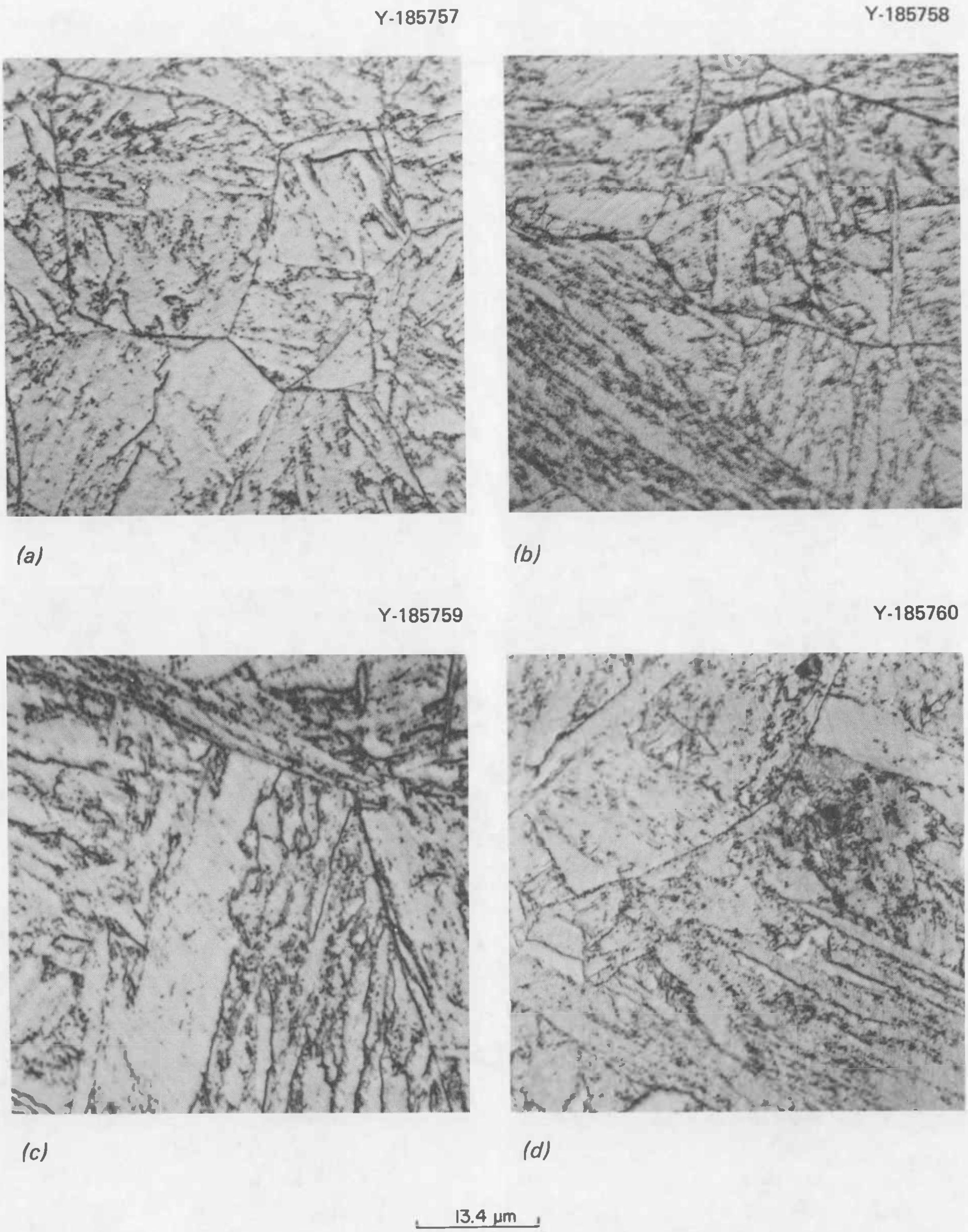

Fig. 1.34. Higher magnification optical micrographs of specimens normalized at 1121°C for (*a*) 1 h, (*b*) 2 h, (*c*) 4 h, and (*d*) 8 h.

500× photomicrographs were used to measure the grain size after various normalizing treatments. The measured grain size is plotted as a function of HJ parameter in Fig. 1.35. Temperature scales for holding periods of 1 and 8 h are also shown in Fig. 1.35. This figure shows that the grain size of the modified alloy remains essentially the same for 1-h normalizing treatment at temperatures up to 1121°C. When the hold time is increased to 8 h, the grain size increases at temperatures higher than 1065°C. It should be noted, however, that the grain size increases only to about ASTM 5 after an 8-h hold period at 1121°C.

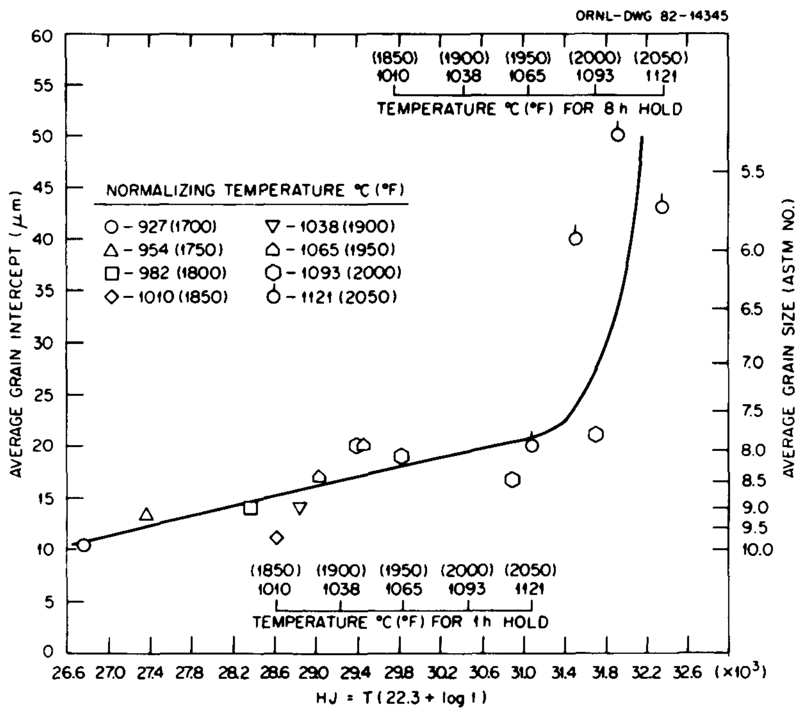

Fig. 1.35. Grain size as a function of Holloman-Jaffee parameter for various normalizing temperature and time combinations.

1.3.6 Charpy Impact Data

Charpy impact specimens from heat 10148 were given the grain coarsening treatment at 1121°C for 1 and 8 h and tested at room temperature. Results of these tests are listed in Table 1.11. This table shows

Table 1.11. Effect of normalizing temperature on room-temperature Charpy impact energy of heat 10148. All specimens were tempered at 760°C for 1 h before testing

Normalizing conditions		Room-temperature Charpy energy (J)
Temperature (°C)	Time (h)	
1038	1	249
1121	1	177
1121	8	175

that the room-temperature energy drops somewhat in going from a normalizing temperature of 1038 to 1121°C. However, increasing the time to 8 h at 1121°C does not produce any additional change in energy. The room-temperature energy of 175 J after a normalizing treatment at 1121°C for 8 h is considered very high.

1.3.7 Discussion

Results of the data presented here show that the grain size of the modified alloy will coarsen when it is normalized at 1093°C for periods exceeding 8 h. At 1121°C, the grain coarsening can occur after a hold period of 1 h. Note, however, that even after normalizing at 1121°C for 8 h, the grain size increases only to ASTM 5.

Data presented here show that, even when the grain size is coarsened, the tensile elongation still remains above 20%. This observation is contrary to the expectation that ductility will be severely reduced in the coarse-grained material.

We believe that in the normalized and tempered 9 Cr-1 Mo steel, the substructure controls the mechanical properties rather than the grain size. The higher normalization temperature makes possible a complete dissolution of niobium and vanadium carbides. This results in a higher degree of supersaturation of austenite and thus results in a finer distribution of carbides during the tempering process. The finer distribution of niobium carbides provides more nucleating sites for $M_{23}C_6$ and thus makes it finer. These fine carbides result in higher yield and ultimate tensile strengths, hardness, and creep strength.

Our data have shown that the grain size has only a minimal effect on the mechanical properties of modified 9 Cr-1 Mo steel. However, if an upper limit on the normalizing temperature is required to prevent any grain growth, we recommend it to be 1093°C (2000°F) for periods not to exceed 8 h.

1.3.8 Summary and Conclusions

The modified 9 Cr-1 Mo steel developed jointly by ORNL and CE is recommended for use in the normalized and tempered condition. The nominal normalizing temperature is 1038°C and the tempering temperature is 760°C. However, there was some concern about the grain growth response and the resultant mechanical properties in the event of using higher normalizing temperature. This report deals with the effect of normalizing temperature on the grain size, microhardness, Charpy impact, tensile, and creep properties. We used normalization temperatures of 927, 954, 982, 1010, 1038, 1065, 1093, and 1121°C and times ranging from 10 to 480 min. In all our studies, we used a single tempering temperature of 760°C. The following conclusions were reached from this study.

1. The grain size of modified 9 Cr-1 Mo steel remains essentially unchanged for a 1-h normalizing treatment at temperatures from 927 to

1121°C. When the hold time is increased to 8 h, the grain size increases at temperatures higher than 1093°C. The grain size increases only to ASTM 5 even after an 8-h hold period at 1121°C.

2. Room-temperature yield strength, ultimate tensile strength, and microhardness increased with increasing normalizing temperature and time. Associated with the increased strength is a small decrease in total elongation. However, it still remained above a recommended minimum value of 18% for this alloy.

3. Yield and ultimate tensile strengths at 593°C also increase with increasing normalizing temperature and time. Total elongation is slightly lowered and reduction of area is not affected.

4. Creep strength at 649°C increases with increasing normalizing temperature and time. It appears to reach a maximum at and above the normalizing temperature of 1038°C. The creep ductility is not affected by the increased normalization temperature.

5. Charpy impact energy is somewhat lowered by increasing the normalization temperature from 1038 to 1121°C. However, it showed no change when the hold period at 1121°C was increased from 1 to 8 h.

6. We believe that grain size has only a minimal effect on the mechanical properties of modified 9 Cr-1 Mo steel. However, if an upper limit on the normalizing temperature is desired to prevent any grain growth, we recommend it to be 1093°C for periods not to exceed 8 h.

1.4 Tensile Properties of Forgings of Modified 9 Cr-1 Mo Steel

V. K. Sikka

Tensile tests were completed on forged slabs and billets from three commercial heats (30182, 30394, and 10148) of modified 9 Cr-1 Mo steel. We tested a slab of 203-mm thickness from heat 30182, 232-mm-diam rounds from heats 30182 and 30394, and a 197-mm octagon and 229-mm-diam billets from heat 10148. In each case we austenitized the forging at 1038°C and then air cooled to room temperature and tempered at 760°C. The austenitizing and tempering treatment times were selected as 1 h for the first 25-mm thickness and 30 min for each additional 25-mm thickness.

The 203-mm-thick slab was tested at the surface, quarter thickness, and midthickness. All specimens were transverse to the long direction of the slab. The octagon and 229-mm round from heat 10148 were tested only at the midthickness. The 232-mm-diam rounds of heats 30182 and 30394 were tested by taking specimens along the diameter. All tensile tests were conducted at a nominal strain rate of 0.004/min.

Data on various forgings are summarized in Tables 1.12 through 1.14. Tensile data for various forgings are plotted as functions of test temperature in Figs. 1.36 through 1.39. The minimum curves based on room-temperature specified values of various properties are also included. These figures show the following.

1. The tensile properties at the surface, quarter thickness, and midthickness levels of the 203-mm-thick slab were identical. This fact implies that air cooling from the austenitizing temperature produces a uniform hardening across the entire thickness up to 203 mm.

2. The properties of various forgings differ some. However, both the strength and ductility properties for forgings exceed the minimum property curves for the plate, bar, and tube.

The creep testing of various forgings is currently in progress.

Table 1.12. Tensile properties of 203-mm-thick forged slab of heat 30182 of modified 9 Cr-1 Mo steel. The slab was normalized for 4.5 h at 1038°C and tempered for 4.5 h at 760°C. Tensile tests were conducted at a nominal strain rate of 0.004/min

Test	Specimen	Test temperature		Modulus (GPa)	Strength (MPa)					Elongation (%)		Reduction of area (%)
		(°C)	(°F)		Proportional limit	0.02% Offset	0.2% Offset	0.5% Offset	Ultimate tensile	Uniform	Total	
					Surface							
22921	2T	25	77	189	287	371	441	462	598	9.21	30.22	75.24
22922	3T	93	200	171	308	357	414	435	552	7.21	28.17	77.49
22923	4T	204	400	272	226	325	405	430	527	7.08	25.90	77.88
22924	5T	316	600	145	237	266	308	325	392	6.13	25.52	75.28
22925	6T	427	800	179	224	280	363	391	463	7.03	27.60	75.44
22926	7T	538	1000	154	184	252	332	354	366	1.97	37.95	87.73
22927	8T	649	1200	90	73	102	175	202	208	1.27	39.90	94.68
22928	9T	760	1400	56	21	34	59	69	80	3.11	54.95	96.68
					Quarter thickness							
22892	34T	25	77	215	315	402	462	483	611	8.49	30.92	73.81
22893	35T	93	200	201	302	372	435	457	569	7.32	26.93	76.38
22894	36T	204	400	215	261	344	411	435	547	6.29	25.25	76.27
22895	37T	316	600	88	267	309	410	444	513	5.20	24.50	75.58
22977	43T	316	600	212	238	332	399	423	525	6.16	24.15	75.58
22896	38T	427	800	173	238	294	377	405	474	6.20	26.58	76.30
22897	39T	538	1000	158	174	247	328	354	368	1.92	36.85	88.85
22898	40T	649	1200	126	76	106	189	206	211	1.50	42.10	94.48
22899	41T	760	1400	38	17	31	55	66	80	3.21	56.62	97.93
					Midthickness							
22900	60T	25	77	243	310	384	455	479	610	8.87	31.10	74.90
22901	61T	93	200	222	352	386	428	449	561	7.90	28.15	76.15
22902	62T	204	400	206	266	337	402	428	533	5.92	26.50	77.87
22903	63T	316	600	162	302	341	394	416	504	6.53	25.68	74.52
22904	64T	427	800	185	249	303	372	400	470	6.91	28.35	76.68
22905	65T	538	1000	151	161	247	335	358	377	2.74	34.30	87.64
22906	66T	649	1200	111	105	139	195	211	215	1.52	43.33	95.27
22907	67T	760	1400	47	20	32	58	68	87	3.72	68.50	98.03

Table 1.13. Tensile properties of 232-mm-diam forged rounds of heats 30182 and 30394 of modified 9 Cr-1 Mo steel. 25-mm-thick slices of these rounds were normalized at 1038°C for 1 h and tempered at 760°C for 1 h. Tests were conducted at a nominal strain rate of 0.004/min

Test	Specimen	Test temperature		Modulus (GPa)	Strength (MPa)					Elongation (%)		Reduction of area (%)
		(°C)	(°F)		Proportional limit	0.02% Offset	0.2% Offset	0.5% Offset	Ultimate tensile	Uniform	Total	
					Heat 30182							
21987	1T	25	77	219	315	420	494	518	637	7.51	27.28	72.90
21988	6T	93	200	216	291	402	471	495	594	6.20	24.55	74.04
21989	7T	204	400	203	262	386	448	472	554	5.53	23.98	75.96
21990	8T	316	600	213	305	371	437	462	537	4.45	21.28	72.97
21991	9T	427	800	187	159	319	417	418	506	5.24	24.55	72.29
21992	10T	538	1000	151	114	267	353	448	385	1.92	32.90	85.43
21993	11T	649	1200	78	12	142	194	209	218	2.00	44.83	93.09
21994	12T	760	1400	64		28	67	80	94	3.14	67.63	96.32
					Heat 30394							
21979	1T	25	77	211	307	457	523	544	674	7.48	27.50	70.58
21980	6T	93	200	214	389	460	511	528	642	6.61	23.64	61.27
21981	7T	204	400	204	332	426	485	505	616	5.69	22.05	70.40
21982	8T	316	600	253	201	340	452	479	587	5.90	22.20	69.17
21983	9T	427	800	192	249	339	434	465	540	6.25	26.95	72.46
21984	10T	538	1000	167	132	257	368	396	403	2.13	37.25	85.71
21985	11T	649	1200	73	109	141	190	207	219	2.15	49.15	94.24
22008	14T	760	1400	39	20	39	66	76	91	3.91	53.32	93.55

Table 1.14. Tensile properties of 197-mm-forged octagon and 229-mm-diam forged round of heat 10148 of modified 9 Cr-1 Mo steel. Both were tested in the normalized and tempered condition at a nominal strain rate of 0.004/min

Test	Specimen	Test temperature (°C)	Modulus (GPa)	Strength (MPa)				Elongation (%)		Reduction of area (%)
				Proportional limit	0.02% Offset	0.2% Offset	Ultimate tensile	Uniform	Total	
197-mm Octagon normalized at 1038°C for 4.5 h and tempered at 760°C for 4.5 h										
23130	1T	RT	215	384	451	492	647	10.56	26.90	68.86
23131	2T	204	191	356	409	449	582	7.86	34.18	72.79
23132	3T	427	179	213	329	409	517	7.67	24.03	72.88
23134	5T	649	109	79	120	177	204	2.21	44.30	97.29
229-mm-diam Round normalized at 1038°C for 5 h and tempered at 760°C for 5 h										
23135	2T	RT	210	379	449	492	646	9.72	28.25	71.87
23136	3T	204	198	253	394	439	577	8.51	24.58	72.47
23137	4T	427	168	228	330	395	513	7.12	21.68	55.07
23138	5T	649	93	69	114	180	212	2.18	47.88	96.94

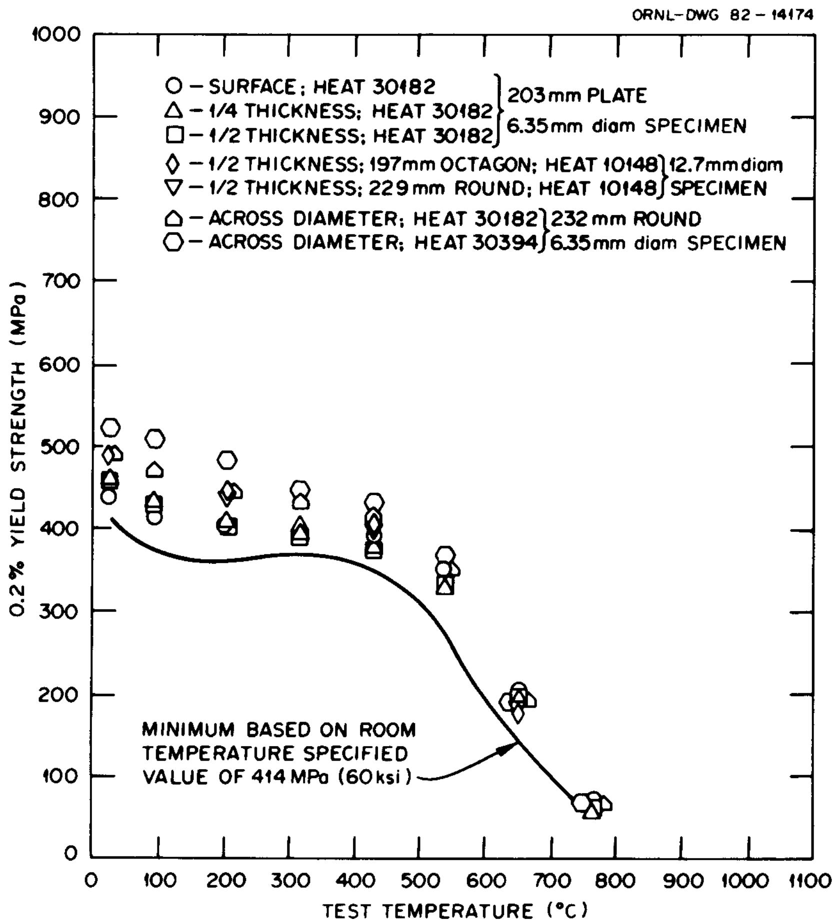

Fig. 1.36. Yield strength as a function of test temperature for forgings of three commercial heats of modified 9 Cr-1 Mo steel.

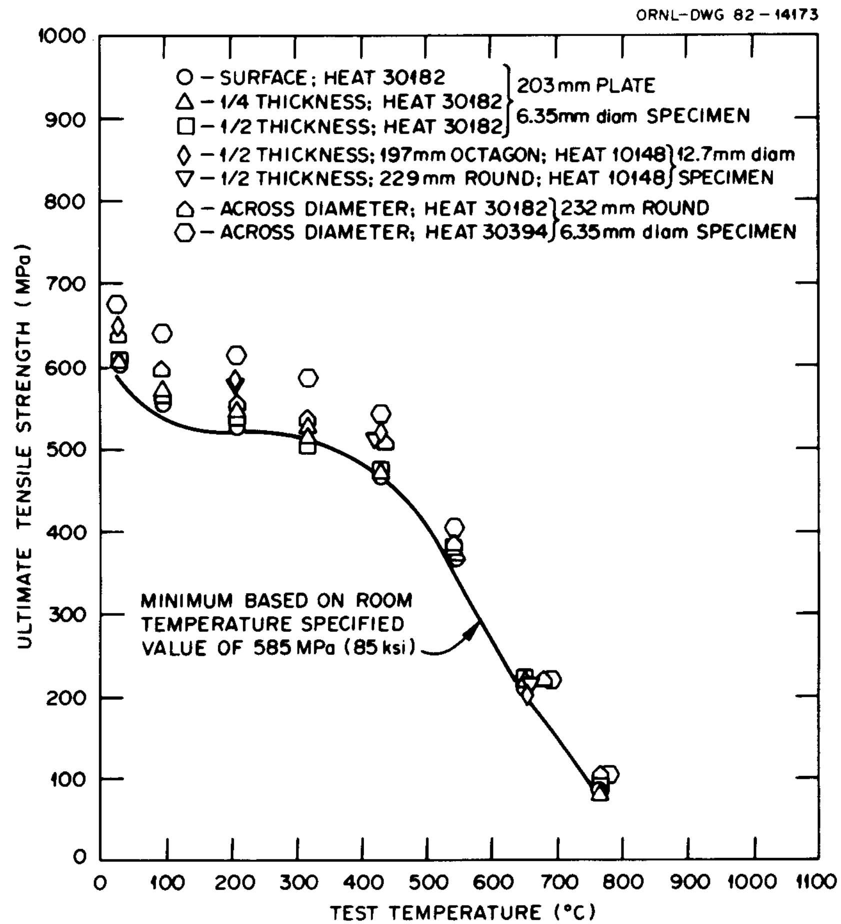

Fig. 1.37. Ultimate tensile strength as a function of test temperature for forgings of three commercial heats of modified 9 Cr-1 Mo steel.

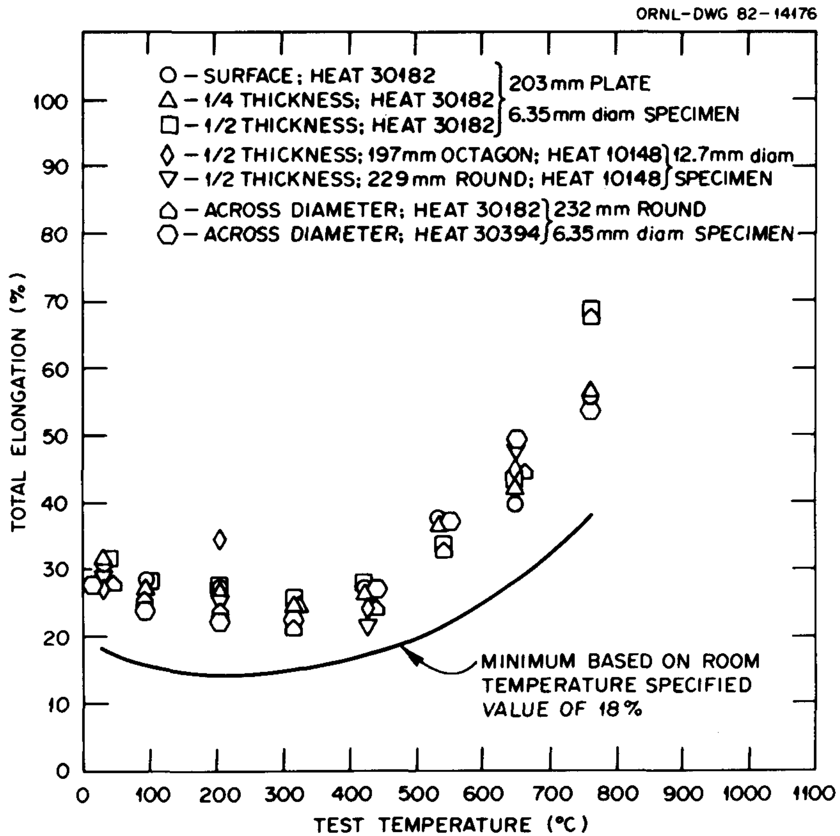

Fig. 1.38. Total elongation as a function of test temperature for forgings of three commercial heats of modified 9 Cr-1 Mo steel.

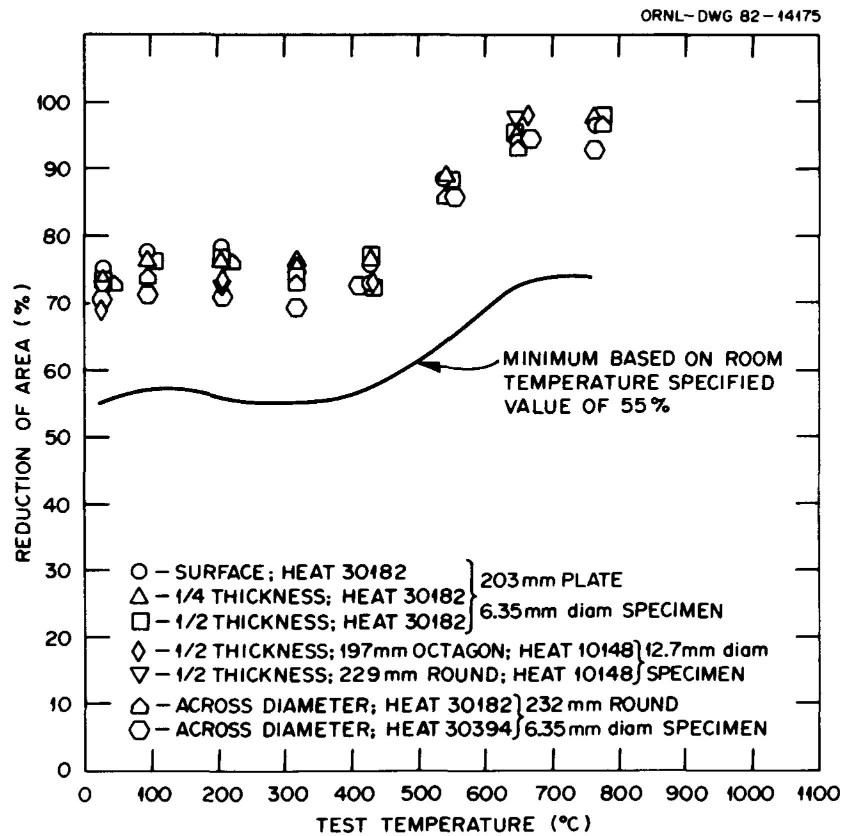

Fig. 1.39. Reduction of area as a function of test temperature for forgings of three commercial heats of modified 9 Cr-1 Mo steel.

1.5 Creep Testing of Base Metal

V. K. Sikka, R. H. Baldwin, and E. B. Patton

The creep testing of modified 9 Cr-1 Mo steel continued on several different heats at various laboratories as follows:

1. AOD Quaker heat F5349 at ORNL;
2. AOD and AOD-ESR CarTech 15-ton heats 30383, 30394, and 30176 at ORNL, W-ARD, and BMI;
3. AOD and AOD-ESR Electralloy 15-ton heat 10148 at ORNL and BMI; and
4. cenrifugally cast and cold-pilgered tube heats XA3602 and XA3618 at ORNL.

All heats are being tested in the normalized and tempered condition. This treatment consists of holding for 1 h at 1040°C, air cooling to room temperature, holding at 760°C for 1 h, and again air cooling to room temperature. In all cases, a 6.35-mm-diam by 31.75-mm-gage-length round bar was used for creep testing.

The status of creep tests on heats F5349, 30182, 30176, 30394, 30383, 10148, XA3602, and XA3618 is presented in Tables 1.15 through 1.23. All these data are being collected in support of ASME code data needs. The tables show the following on individual heats.

Quaker Heat F5349 — One creep test is still continuing with a test time of 28,534 h. Except for the longest term test in progress, creep testing of the Quaker heat is considered completed.

CarTech Heats 30182 and 30176 — These two heat numbers represent the same heat because CarTech numbers each ingot by a heat number. The last long-term creep test on heat 30182 ruptured after 18,505.6 h. One long-term test on heat 30176 ruptured after 14,732 h. Seven additional long-term creep tests are still in progress on this heat. Most of these tests have accumulated at least 13,000 h.

Table 1.15. Summary of creep data on 16-mm-thick plate of Quaker heat F5349 of modified 9 Cr-1 Mo steel (Heat melted by AOD process. Plate normalized at 1040°C for 1 h and tempered at 760°C for 1 h)

ORNL test[a]	Stress (MPa)	Strain (%)						Time (h)				Minimum creep rate, $\dot{e}_m$ (%/h)	Reduction of area (%)	Stable creep strain $t_r \cdot \dot{e}_m$ (%)
		Loading e_l	Transient e_{pc}	Primary e_1	Secondary e_2	0.2% Offset e_s	Fracture e_f	Primary t_1	Secondary t_2	0.2% Offset t_s	Rupture t_r			
							482° C							
	414[b]						20.24				26.8	1.10 E-1	75.97	
	379[b]						22.58				151.2	2.25 E-2	77.00	
	345[b]						21.69				1,708.3	9.0 E-4	78.9	
							538° C							
20592	317	0.34	0.00	0.00	3.25	3.50	26.99	0.0	6.15	6.3	9.2	5.25 E-1	77.20	4.83
20636	262	0.23	0.32	0.50	4.00	4.75	29.33	4.0	90.0	100.0	149.9	4.025 E-2	82.97	6.03
20680	248	0.20	0.50	1.12	4.00	4.92	35.03	21.2	117.5	137.5	209.5	3.0 E-2	84.87	6.285
20682	234	0.18	0.75	1.50	4.25	5.12	27.07	85.0	450.0	540.0	802.2	7.75 E-3	80.40	6.22
20824	207	0.13	1.875	2.50	4.75	5.50	25.14	2500.0	10,400.0	11,800.0	14,648.2	2.81 E-5	84.06	4.12
21413	207	0.18	1.00	2.125	6.00	6.625	23.30	280.0	1,200.0	1,290.0	>1,525.3	4.156 E-3	56.81	*c*
20842	179										>28,534.0			*d*
							593° C							
	221						34.38				11.8	5.65 E-1	84.1	
21442	205[b]	0.43	0.75	1.25	5.25	5.75	38.22	2.0	19.75	21.0	33.2	2.23 E-1	86.35	7.40
21288	193[b]	0.34	1.25	2.00	4.50	5.00	26.70	14.0	62.0	70.0	106.3	5.3 E-2	86.71	5.61
21531	179[b]	0.23	1.25	1.75	4.50	5.50	34.44	25.0	165.0	210.0	303.2	1.95 E-2	86.48	5.91
	166[b]	0.31					26.57				1,697.1	2.4 E-3	85.00	
21449	152[b]	0.30	1.125	1.50	4.00	4.50	29.73	162.5	1,562.5	1,712.5	2,341.1	1.9 E-3	88.68	4.45
	145[b]	0.26					37.38				4,265.9	7.0 E-4	87.9	
	138[b]	0.16					27.52				8,342.2	3.0 E-4	85.4	2.50
	131	0.20					26.40				10,288.4	1.91 E-4	85.9	

Table 1.15. (Continued)

ORNL test[a]	Stress (MPa)	Strain (%) Loading e_l	Strain (%) Transient e_{pc}	Strain (%) Primary e_1	Strain (%) Secondary e_2	Strain (%) 0.2% Offset e_s	Strain (%) Fracture e_f	Time (h) Primary t_1	Time (h) Secondary t_2	Time (h) 0.2% Offset t_s	Time (h) Rupture t_r	Minimum creep rate, $\dot{e}_m$ (%/h)	Reduction of area (%)	Stable creep strain $t_r \cdot \dot{e}_m$ (%)
							649°C							
20486	131	0.16	0.62	0.75	4.75	5.25	32.68	1.0	25.25	27.0	>44.1	1.625 E-1	43.82	[c]
20491	131	0.19	0.75	0.85	4.50	5.25	35.17	1.2	24.5	26.25	42.0	1.6 E-1	88.69	6.72
20490	117	0.16	0.75	1.00	3.38	4.00	35.85	5.0	56.0	65.0	116.3	4.56 E-2	88.70	5.31
20567	103	0.13	0.62	0.75	2.75	3.50	32.77	12.5	175.0	207.5	356.3	1.23 E-2	86.50	4.36
20850	103	0.16	0.375	0.50	1.75	2.25	41.89	15.0	265.0	315.0	576.2	5.125 E-3	91.58	2.95
20566	97	0.14	0.50	0.62	2.25	2.75	27.37	15.0	305.0	370.0	630.7	5.75 E-3	86.50	3.63
20593	83	0.11	0.38	0.50	2.00	2.25	29.10	40.0	610.0	710.0	1,301.4	1.375 E-3	87.86	1.79
20624	69	0.08	0.12	0.12	1.50	2.25	29.50	0.0	2,300.0	2,775.0	4,768.2	6.25 E-4	84.55	2.98
21010	69	0.12	0.25	0.25	1.25	1.75	29.24	0.0	3,250.0	4,100.0	6,859.2	3.0 E-4	88.59	2.06
21404	62	0.07	0.24	2.50	1.75	2.25	21.47	400.0	10,500.0	12,000.0	17,953.8	1.506 E-4	83.65	2.70
							704°C							
21518	97[b]	0.30	0.25	0.375	3.00	3.625	42.74	0.1	5.45	6.3	11.5	0.475	93.42	5.46
21517	83[b]	0.20	0.20	0.25	2.25	2.50	35.14	0.5	12.25	13.75	28.5	0.1535	95.11	4.37
20597	69	0.10	0.25	0.25	2.00	2.50	45.95	1.0	42.0	49.0	104.4	1.81 E-2	94.99	1.89
	69[b]	0.21					35.38				78.05	3.72 E-2	95.20	
	55[b]						35.31				214.4	1.5 E-2	95.50	
	41[b]						57.26				882.4	5.5 E-3	96.20	

[a]Tests conducted at ORNL except as noted.

[b]Test conducted at W-ARD.

[c]Test discontinued.

[d]Test in progress.

Table 1.16. Creep data on 16-mm plate made by hot forging and hot rolling from ESR ingot 30182 of heat 1 of two 15-ton heats procured from CarTech. The plate was normalized at 1040°C for 1 h and tempered at 760°C for 1 h

ORNL test	Specimen	Stress (MPa)	Strain (%)						Time (h)				Minimum creep rate, $\dot{e}_m$ (%/h)	Reduction of area (%)	Stable creep strain $t_r \cdot \dot{e}_m$ (%)
			Loading e_l	Transient e_{pc}	Primary e_1	Secondary e_2	0.2% Offset e_s	Fracture e_f	Primary t_1	Secondary t_2	0.2% Offset t_s	Rupture t_r			
								482°C							
		365[a]	0.42					20.90				1,614.9	1.26 E-3	79.9	
								538°C							
21670	9T	276	0.30	0.50	0.75	2.75	3.25	29.53	14.0	113.0	127.0	199.0	2.00 E-2	83.38	3.98
21672	8T	234	0.18	0.62	1.00	3.75	4.125	24.16	400.0	3200.0	3375.0	4,387.1	9.5 E-4	84.42	4.17
								593°C							
		207[a]	0.56					30.28				38.1	1.36 E-1	88.6	
		193[a]	0.36					27.23				131.5	3.78 E-2	88.0	
		172[a]	0.29					34.40				367.9	1.39 E-2	89.1	
		159[a]	0.15					28.02				1,332	3.25 E-3	91.1	
		145[a]	0.15					30.08				6,369.2	5.76 E-4	89.1	
		131[a]	0.15					23.77				18,505.6	1.10 E-4	84.3	
								649°C							
21659	6T	131	0.18	0.55	0.625	3.25	4.0	39.26	1.0	35.5	40.0	64.1	7.95 E-2	92.46	5.10
21669	7T	103	−0.05	0.0	0.0	2.0	2.5	41.91	0.0	305.0	340.0	566.5	6.25 E-3	92.27	3.54
21671	10T	90	0.13	0.50	0.55	2.25	2.75	27.22	30.0	850.0	950.0	1,555.4	2.1 E-3	86.44	3.27
								677°C							
21953	13T	90	0.13	0.50	0.75	2.875	3.375	39.41	12.5	117.5	137.5	222.3	2.0 E-2	92.71	4.45
								704°C							
21977	14T	90	0.22	0.60	0.75	3.625	4.00	41.72	0.6	11.1	11.6	21.0	2.76 E-1	95.09	5.80

[a]Tests conducted at W-ARD. All other tests were conducted at ORNL.

Table 1.17. Creep data on 25-mm plate made by hot forging and hot rolling from ESR ingot 30176 of heat 1 of two 15-ton heats procured from CarTech. The plate was normalized at 1040°C for 1 h and tempered at 760°C for 1 h

ORNL test	Specimen	Stress (MPa)	Strain (%) Loading e_l	Transient e_{pc}	Primary e_1	Secondary e_2	0.2% Offset e_s	Fracture e_f	Time (h) Primary t_1	Secondary t_2	0.2% Offset t_s	Rupture t_r	Minimum creep rate, $\dot{e}_m$ (%/h)	Reduction of area (%)	Stable creep strain $t_r \cdot \dot{e}_m$ (%)
								482°C							
	7T[a]	276										>14,213			
								538°C							
22134	2T[b]	234	0.12	0.50	0.75	2.88	3.50	22.48	250.0	2,150.0	2,475.0	3,352.6	1.12 E-3	84.32	3.77
	8T[a]	165										>14,112			
								593°C							
	9T[a]	124						22.3				14,732		83.8	
	39T[c]	124										>11,400			
	36T[c]	117										>15,400			
	35T[c]	110										>15,400			
								649°C							
22092	1T[b]	103	0.13	0.45	0.50	2.25	2.75	30.56	25.0	345.0	400.0	632.3	5.55 E-3	89.73	3.51
								677°C							
	38T[c]	41.4										>13,000			
	37T[c]	27.6										>13,000			

[a]Tested at BMI.

[b]Tested at ORNL.

[c]Tested at W-ARD.

Table 1.18. Creep data on 16-mm plate made by hot forging and hot rolling from ESR ingot 30394 of heat 2 of two 15-ton heats procured from CarTech. The plate was normalized at 1040°C for 1 h and tempered at 760°C for 1 h

ORNL test	Specimen	Stress (MPa)	Strain (%)						Time (h)				Minimum creep rate, $\dot{e}_m$ (%/h)	Reduction of area (%)	Stable creep strain $t_r \cdot \dot{e}_m$ (%)
			Loading e_l	Transient e_{pc}	Primary e_1	Secondary e_2	0.2% Offset e_s	Fracture e_f	Primary t_1	Secondary t_2	0.2% Offset t_s	Rupture t_r			
427°C															
21822	7T	414	0.16									>20,185.2			
538°C															
21769	4T	186	0.15									>20,831.0			
593°C															
21774	5T	159	0.17	0.75	1.00	2.625	3.25	24.47	275	1,850	2,150	2,907.9	1.0 E-3	88.50	2.98
649°C															
21758	3T	103	0.12	0.425	0.500	3.00	3.50	27.81	22.5	465.0	525.0	756.3	5.5 E-3	89.74	4.16
21894	8T	90	0.12	0.25	0.30	2.75	3.25	30.06	37.5	1,375.0	1,575.0	2,340.4	1.8 E-3	84.71	4.21
21818	6T	62	0.09					19.53				21,028		68.63	

Table 1.19. Creep data on 25-mm plate made by hot forging and hot rolling from ESR ingot 30394 of heat 2 of two 15-ton heats procured from CarTech. The plate was normalized at 1040°C for 1 h and tempered at 760°C for 1 h

ORNL test	Specimen	Stress (MPa)	Strain (%) Loading e_l	Strain (%) Transient e_{pc}	Strain (%) Primary e_1	Strain (%) Secondary e_2	Strain (%) 0.2% Offset e_s	Strain (%) Fracture e_f	Time (h) Primary t_1	Time (h) Secondary t_2	Time (h) 0.2% Offset t_s	Time (h) Rupture t_r	Minimum creep rate, $\dot{e}_m$ (%/h)	Reduction of area (%)	Stable creep strain $t_r \cdot \dot{e}_m$ (%)
								454°C							
22770	16T	379										>8,378.4			
								482°C							
	7T[a]	276										>14,213			
								538°C							
	8T[a]	165										>14,112			
								593°C							
	9T[a]	124										>14,593			
	39T[b]	124										>11,200			
	36T[b]	117										>15,400			
	35T[b]	110										>15,400			
								649°C							
22090	1T[c]	103	0.06	0.50	0.75	2.50	3.00	27.67	100.0	650.0	780.0	1,155.2	3.0 E-3	84.09	3.47
								677°C							
	38T[b]	41.4										>13,000			
	37T[b]	27.6										>13,000			

[a]Tested at BMI.

[b]Tested at W-ARD.

[c]Tested at ORNL.

Table 1.20. Creep data on 51-mm plate made by hot forging and hot rolling from AOD ingot 30383 of heat 2 of two 15-ton heats procured from CarTech. The plate was normalized at 1040°C for 1 h and tempered at 760°C for 1 h

ORNL test	Specimen	Stress (MPa)	Strain (%)						Time (h)				Minimum creep rate, $\dot{e}_m$ (%/h)	Reduction of area (%)	Stable creep strain $t_r \cdot \dot{e}_m$ (%)
			Loading e_l	Transient e_{pc}	Primary e_1	Secondary e_2	0.2% Offset e_s	Fracture e_f	Primary t_1	Secondary t_2	0.2% Offset t_s	Rupture t_r			
								482°C							
	25T[a]	276										>14,091			
								538°C							
22243	16T[b]	234	0.14	1.125	1.625	3.125	3.75	21.47	250.0	880.0	1,025.0	13,513.2	2.31 E-3	80.01	31.22
	26T[a]	165										>13,969			
								593°C							
	27T[a]	124										>14,597			
								593°C							
22855	41T[b]	110	0.12									>7,560.9			

[a]Tested at BMI.

[b]Tested at ORNL.

Table 1.21. Creep data on 16-mm plate made at ORNL by hot forging, tempering, and hot rolling a part of the ingot from heat 10148 melted by the AOD process at Electralloy. The plate was normalized at 1040°C for 1 h and tempered at 760°C for 1 h

ORNL test	Specimen	Stress (MPa)	Strain (%)						Time (h)				Minimum creep rate, $\dot{e}_m$ (%/h)	Reduction of area (%)	Stable creep strain $t_r \cdot \dot{e}_m$ (%)
			Loading e_l	Transient e_{pc}	Primary e_1	Secondary e_2	0.2% Offset e_s	Fracture e_f	Primary t_1	Secondary t_2	0.2% Offset t_s	Rupture t_r			
								482°C							
	7T[a]	276										>14,261			
								538°C							
22443	1T[b]	234	0.23									>11,884.5			
22502	4T[b]	186	0.14									>7,612.5			
	8T[a]	165										>14,426			
								593°C							
22450	3T[b]	159	0.17	0.7875	1.00	2.375	2.875	24.68	350.0	2,125.0	2,525.0	3,790.0	9.0 E-4	79.75	3.41
22710	6T[b]	145	0.11									>8,472.2			
	9T[a]	124										>14,620			
								649°C							
22444	2T[b]	90	0.32	0.30	0.375	2.875	3.375	26.25	75.0	2,250.0	2,450.0	3,167.44	1.14 E-3	79.75	3.61

[a]Tested at BMI.

[b]Tested at ORNL.

Table 1.22. Creep data on 51-mm plate made by hot forging and hot rolling from AOD-ESR heat 10148 procured from Electralloy. The plate was normalized at 1040°C for 1 h and tempered at 760°C for 1 h

ORNL test	Specimen	Stress (MPa)	Strain (%)						Time (h)				Minimum creep rate, $\dot{e}_m$ (%/h)	Reduction of area (%)	Stable creep strain $t_r \cdot \dot{e}_m$ (%)
			Loading e_l	Transient e_{pc}	Primary e_1	Secondary e_2	0.2% Offset e_s	Fracture e_f	Primary t_1	Secondary t_2	0.2% Offset t_s	Rupture t_r			
593°C															
22874	1T	193	0.57	0.625	0.875	2.875	3.50	24.75	70.0	630.0	730.0	1049.6	3.56 E-3	86.40	3.74
22909	2T	172	0.22	0.625	0.75	1.75	2.125	24.68	187.5	1187.5	1325.0	2458.7	9.65 E-4	82.56	2.37
22913	3T	152	0.20									>6300.2			
649°C															
22876	5T	103	0.14	0.25	0.25	2.00	2.50	32.62	0.0	430.0	465.0	779.6	4.25 E-3	88.48	3.31
22919	4T	90	0.25	0.25	0.275	2.50	3.25	27.24	10.0	1130.0	1380.0	1918.8	2.0 E-3	86.51	3.84
677°C															
22975	14T	69	0.09	0.25	0.30	3.00	3.50	31.49	20.00	700.0	760.0	1151.5	3.88 E-3	87.20	4.46
23007	15T	41	0.99									>4417.4			
704°C															
23006	16T	41	0.64	0.30	0.375	3.25	3.75	25.65	50.0	1437.5	1575.0	2280.6	1.98 E-3	84.46	4.52

Table 1.23. Creep data on 51-mm-OD by 8-mm-wall centrifugally cast and cold-pilgered finished tube (heat XA3602) of modified 9 Cr-1 Mo steel

(Heat-treated at 1177°C for 10 min, 1040°C for 1 h, 760°C for 1 h)

ORNL Test	Specimen	Stress (MPa)	Strain (%)						Time (h)					Minimum Creep Rate, $\dot{e}_m$ (%/h)	Reduction of Area (%)	Stable Creep Strain $t_r \cdot \dot{e}_m$ (%)
			Loading e_l	Transient e_{pc}	Primary e_1	Secondary e_2	0.2% Offset e_s	Fracture e_f	Primary t_1	Secondary t_2	0.2% Offset t_s	1% Strain $t_{1\%}$	Rupture t_r			
								649°C								
21541	14L	117	0.20	0.375	0.50	2.50	2.875	32.12	5.00	104.0	110.0	33.0	173.2	2.06 E-2	90.78	3.57
21546	15L	83	0.09	0.275	0.375	2.25	3.00	30.42	50.0	1,950.0	2,350.0	700.0	3,515.3	9.95 E-4	80.48	3.50
21628	25L	69	0.24	0.3125	0.375	2.75	3.50	24.81	400.0	10,000	11,900		16,996.9	2.41 E-4	62.38	4.10
								677°C								
21542	13L	97	0.10	0.25	0.375	3.375	4.00	31.86	3.0	120.0	135.0	27.0	177.4	2.63 E-2	91.07	4.67
21640	24L	55	0.11	0.40	0.50	3.50	4.00	31.80	250.0	5,100.0	5,450.0	1,150.0	7,185.1	6.1 E-4	52.19	4.38

CarTech Heat 30394 — One long-term creep test failed on this heat after 21,028 h. Eleven additional long-term creep tests are currently in progress. Two of these tests have reached 20,000 h and seven are in the range from 13,000 to 16,000 h.

CarTech Heat 30383 — This heat has the same chemical composition as heat 30394 except that 30383 represents the AOD part of the heat and 30394 represents the AOD-ESR part. One creep test failed on this heat after 13,513.2 h. Four additional creep tests are currently in progress. Three of the four tests have reached test times in the range from 13,000 to 15,000 h.

Electralloy Heat 10148 — Several short-term creep tests have been completed on this heat, and eight are currently in progress. Three of the tests in progress have exceeded 14,000 h.

Tubes Installed in TVA Kingston Plant (Heat XA3602) — The last long-term creep test on this heat failed after 16,996.9 h. Creep testing of this heat is considered complete.

The stress-rupture data from Tables 1.15 through 1.23 are plotted and compared with the ASME Code Case N-47 minimum curve for type 304 stainless steel in Figs. 1.40 through 1.47. These plots show that all heats are still performing to expectation, namely, matching the creep strength of type 304 stainless steel through 600°C. Data on all the commercial heats were collected for inclusion in the ASME code data package, which was submitted during June 1982.

1.6 Fatigue Behavior

C. R. Brinkman, J. P. Strizak, and V. K. Sikka

Strain-controlled and limited load-controlled testing of modified 9 Cr-1 Mo steel is continuing. The objective of this effort is to obtain sufficient continuous low- and high-cycle fully reversed fatigue

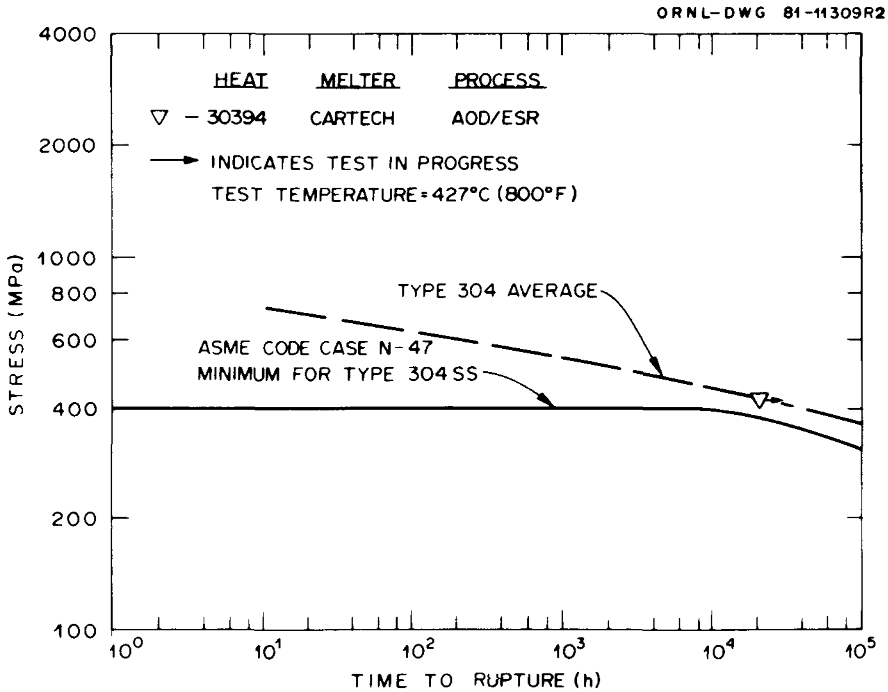

Fig. 1.40. Creep rupture data at 427°C (800°F) on commercial heats of modified 9 Cr-1 Mo steel. ASME Code Case N-47 minimum for type 304 stainless steel is included for comparison.

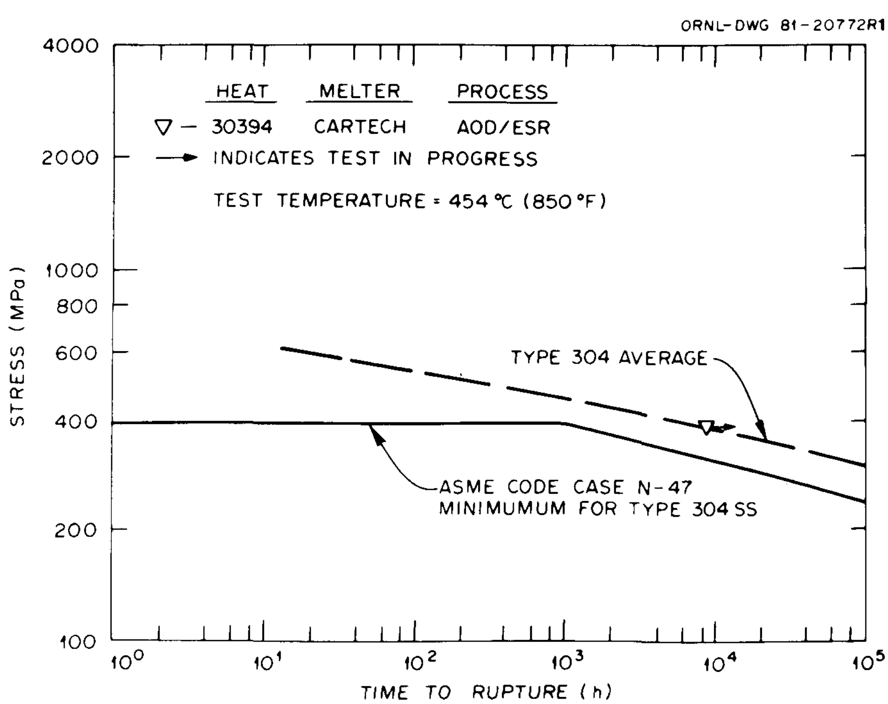

Fig. 1.41. Creep rupture data at 454°C (850°F) on commercial heats of modified 9 Cr-1 Mo steel. ASME Code Case N-47 minimum for type 304 stainless steel is included for comparison.

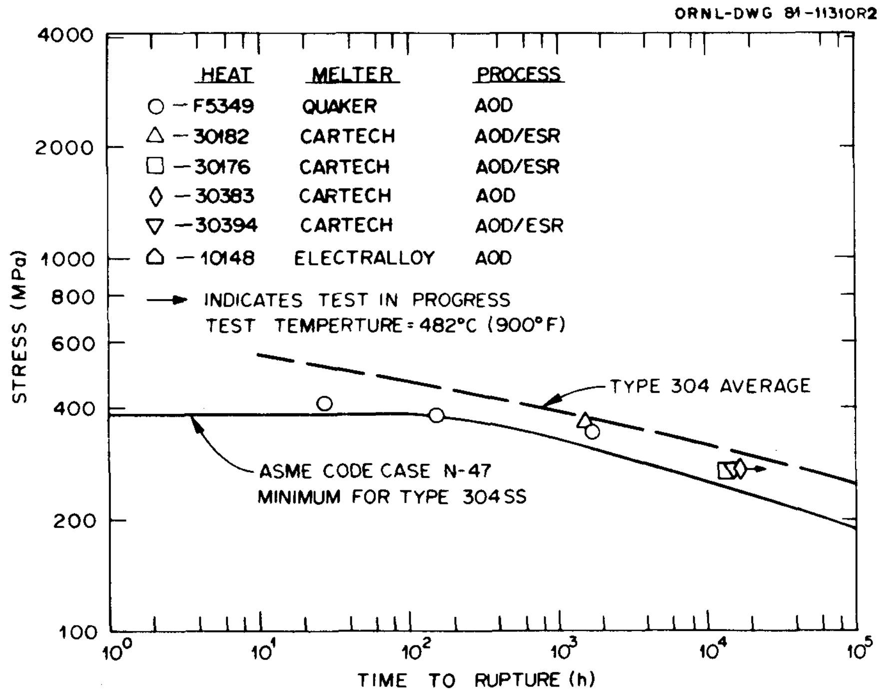

Fig. 1.42. Creep rupture data at 482°C (900°F) on commercial heats of modified 9 Cr-1 Mo steel. ASME Code Case N-47 minimum for type 304 stainless steel is included for comparison.

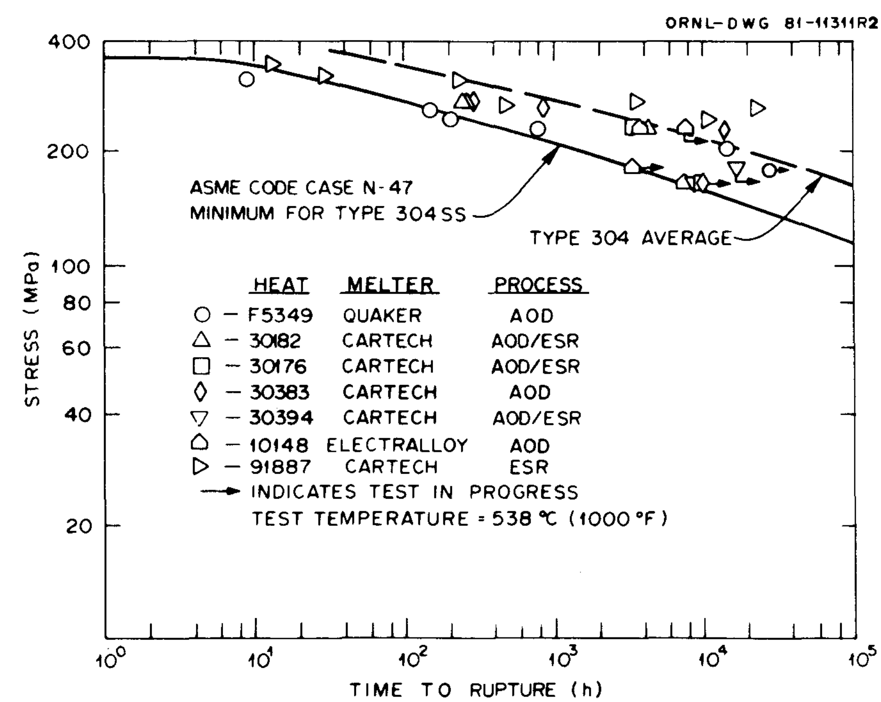

Fig. 1.43. Creep rupture data at 538°C (1000°F) on commercial heats of modified 9 Cr-1 Mo steel. ASME Code Case N-47 minimum for type 304 stainless steel is included for comparison. Several additional data points are available at this temperature on experimental and small commercial heats.

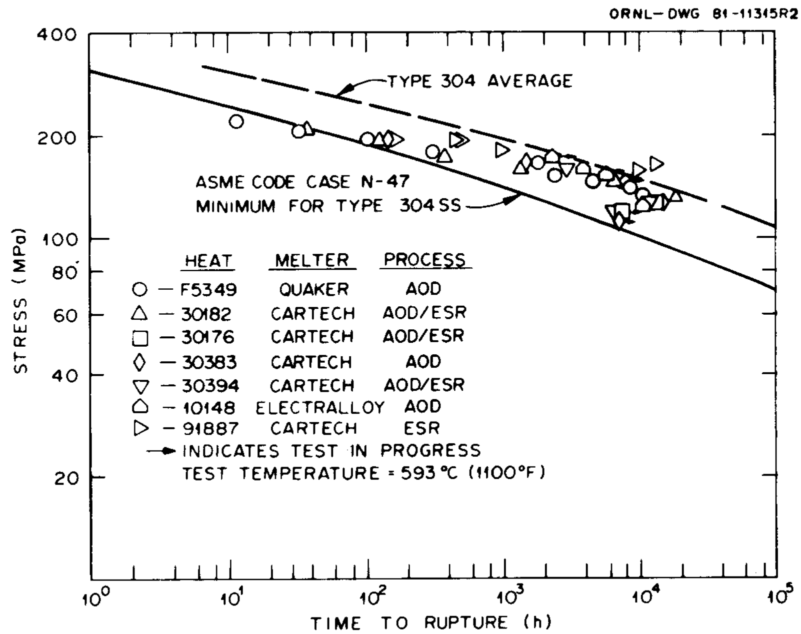

Fig. 1.44. Creep rupture data at 593°C (1100°F) on commercial heats of modified 9 Cr-1 Mo steel. ASME Code Case N-47 minimum for type 304 stainless steel is included for comparison. Several additional data points are available at this temperature on experimental and small commercial heats.

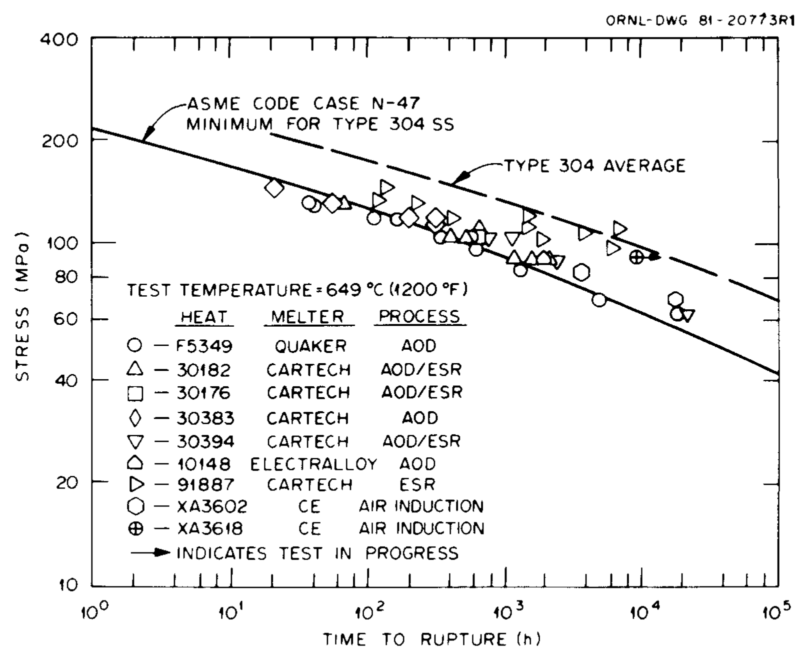

Fig. 1.45. Creep rupture data at 649°C (1200°F) on commercial heats of modified 9 Cr-1 Mo steel. ASME Code Case N-47 minimum for type 304 stainless steel is included for comparison. Several additional data points are available at this temperature on experimental and small commercial heats.

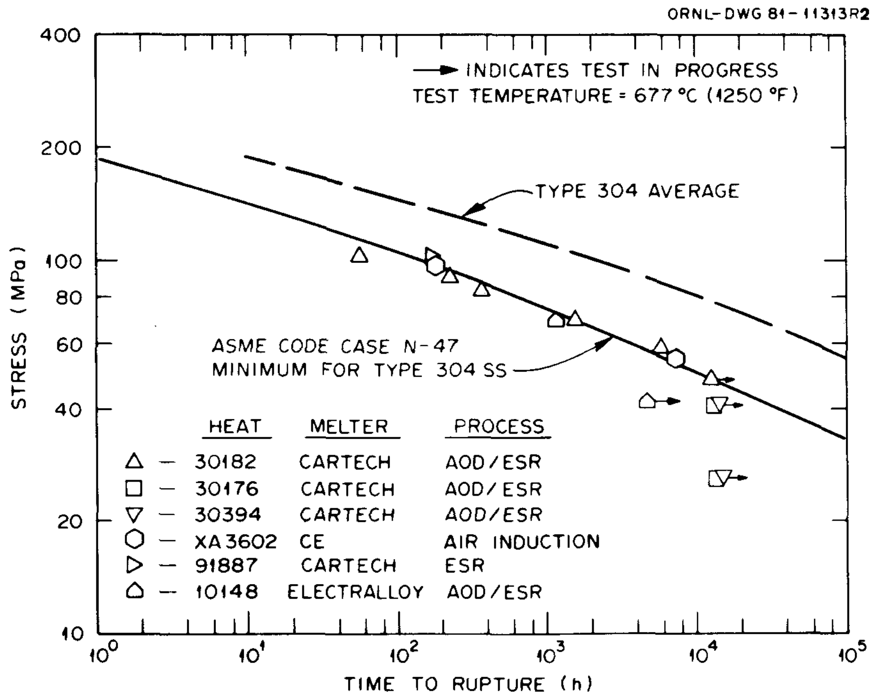

Fig. 1.46. Creep rupture data at 677°C (1270°F) on commercial heats of modified 9 Cr-1 Mo steel. ASME Code Case N-47 minimum for type 304 stainless steel is included for comparison.

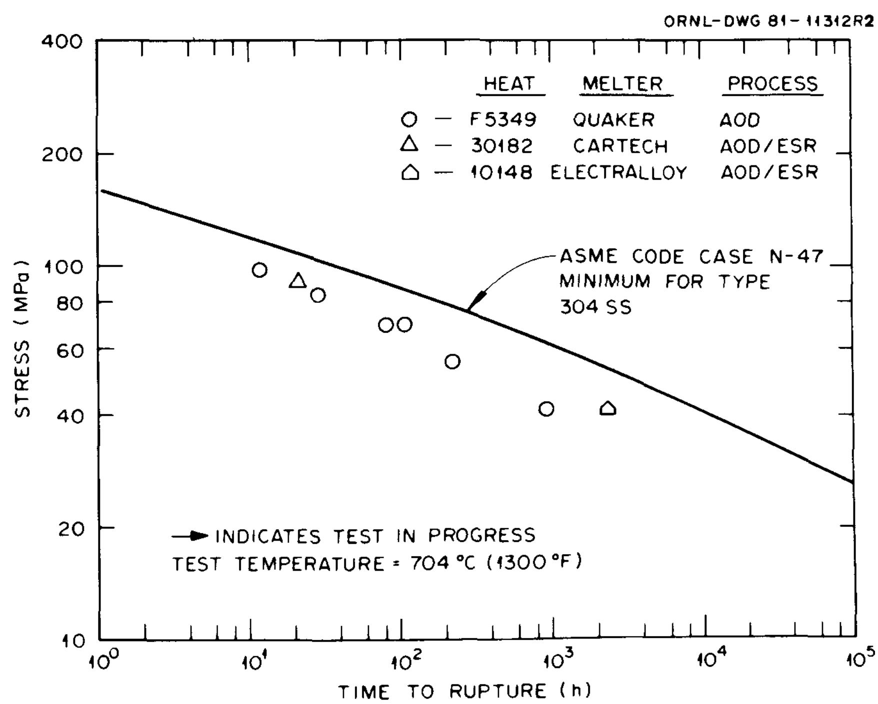

Fig. 1.47. Creep rupture data at 704°C (1300°F) on commercial heats of modified 9 Cr-1 Mo steel. ASME Code Case N-47 minimum for type 304 stainless steel is included for comparison.

data to establish appropriate ASME design fatigue curves. Sufficient time-dependent fatigue data must also be obtained to determine the influence of environment (air) and creep damage (primarily, relaxation) on the fatigue behavior of this material at temperatures of interest to design.

During this reporting period, a number of strain-controlled fatigue tests were conducted at 538 and 593°C with a compressive hold period of the same duration introduced each cycle until failure. The objective of these tests was to test several heats of material and compare cyclic lives of specimens subjected to identical test conditions. Table 1.24 compares representative tensile properties of the heats tested during this reporting period. The tensile properties do not show significant scatter, and the yield strength values (0.2% offset) are only 5 to 10% lower than the ultimate tensile strengths, as is characteristic of the behavior of this material.

Results of recently completed fatigue tests in which compressive holds were introduced into each cycle are given in Table 1.25. Tables 1.26 through 1.28 report results of all fatigue tests conducted on this material to date.

Figure 1.48 shows results of recent long-term time-dependent fatigue tests in which compressive hold periods were introduced at peak strain amplitude values each cycle until failure. Data comparisons given in Fig. 1.48 indicate the following.

1. Compressive hold periods appear to be more deleterious to fatigue life at low strain ranges (0.5%) than at higher strain ranges (1.0%).

2. Increasing the length of the hold period results in a decrease in fatigue life (cycles), particularly at the lower strain range (0.5%).

3. Heat-to-heat variations do not appear to be significant in terms of cycle life where comparisons are possible ($\Delta\varepsilon_t$ = 1.0%).

4. Increasing the duration of a compressive hold time results in an increase in tensile mean stress. Further, the effect appears to be more pronounced at lower strain ranges, as shown in Fig. 1.49. This may explain why compressive hold periods are more deleterious than tensile

Table 1.24. Representative tensile properties of several heats of modified 9 Cr-1 Mo steel

(Strain rate 6.7 × 10^{-5}/s).

Heat	Temperature (°C)	Strength (MPa)		Reduction of area (%)
		Yield (0.2% offset)	Utimate tensile	
30176	538	413.7	434.4	83
30383	538	393.0	441.3	84
91887	538	406.8	448.2	
30394	593	310.3	344.8	88
91887	593	365.4	386.1	

Table 1.25. Time-dependent fatigue tests

Test	Heat	Temperature (°C)	Total strain range (%)	Hold time and mode[a] (h)	Cycle life, N_f (cycles)
1	91887	593	1.0	1.0, C	934
2	30394	593	0.5	1.0, C	3523
3	91887	538	1.0	1.0, C	989
4	30176	538	1.0	1.0, C	1176
5	30383	538	1.0	1.0, C	1273
6	91887	538	0.5	0.5, $\sigma = 0$[b]	To be run
7	30176	538	1.0	1.0, C + T	Ongoing
8	30176	538	1.0	1.0, T	Ongoing

[a]T = a hold period at peak tension on the hysteresis loop. C = a hold period at peak compression on the hysteresis loop.

[b]Indicates zero stress hold of 0.5 h on tension-going side of the hysteresis loop.

Table 1.26. Strain-control fatigue data on modified 9 Cr-1 Mo steel at 525°C

[Fully reversed push-pull axial fatigue (R = −1), strain control and triangular waveform with strain rate = 6.7 × 10^{-4}/s; hourglass-shaped specimens with radius/diameter = 6 and 5.08-mm minimum diameter. No hold and no relaxed stress. Heat 91887, normalized (1038°C) and tempered (760°C)]

Specimen	Total strain range, $\Delta\varepsilon_t$ (%)	Stress amplitude[a] (MPa)		Stress range, $\Delta\sigma$ (MPa)	Strain range[a] (%)		Cycles to failure, N_f	Time to failure, t_f (h)
		Tensile, σ_t	Compressive, σ_c		Elastic, $\Delta\varepsilon_e$	Plastic, $\Delta\varepsilon_p$		
40T[b]	0.35	186	205	391	0.23	0.12	1,033,075	1,243.0
41T	0.35	189	201	390	0.22	0.13	>1,158,498	>1,307.3[c]
38T	1.20	285	296	581	0.34	0.86	1,824	18.2
37T	1.82	294	321	615	0.36	1.46	910	13.8
39T	0.80	257	278	536	0.32	0.48	7,853	52.4

[a] $N_f/2$ properties.

[b] Part 1 $\dot{\varepsilon}$ = 6.7 × 10^{-4}/s from start to 281,946 cycles.
Part 2 $\dot{\varepsilon}$ > 3.5 × 10^{-3}/s from 281,946 cycles to 852,720 cycles.
Part 3 $\dot{\varepsilon}$ > 3.5 × 10^{-3}/s, $\Delta\varepsilon_e$ = 0.37%, 852,720 to 1,025,070 cycles.
Part 4 $\dot{\varepsilon}$ > 3.5 × 10^{-3}/s, $\Delta\varepsilon_e$ = 0.55%, 1,025,070 to 1,033,075 cycles.

[c] Test terminated before failure.

Table 1.27. Strain-control fatigue data on modified 9 Cr-1 Mo steel at 593°C

Heat	Specimen[a]	Total strain range,[b] $\Delta\varepsilon_t$ (%)	Hold time and mode[c] (h)	Stress amplitude[d] (MPa)		Stress range, $\Delta\sigma$ (MPa)	Strain range[d] (%)		Relaxed stress, σ_r (MPa)	Cycles to failure, N_f	Time to failure, t_f (h)
				Tensile, σ_t	Compressive, σ_c		Elastic, $\Delta\varepsilon_e$	Plastic, $\Delta\varepsilon_p$			
91887	72T	1.00	None	223	238	461	0.32	0.68		7,432	10.30
91887	73T	0.50	None	184	195	379	0.27	0.23		110,377	81.25
91887	74T	0.45	None	176	188	364	0.26	0.19		139,477	86.50
91887	30T[e]	1.75	None	262	243	505	0.22	1.53		1,303	3.13
91887	26T[e]	1.01	None	254	291	545	0.32	0.69		2,818	3.87
91887	27T[e]	0.81	None	245	275	520	0.31	0.50		3,726	4.13
91887	31T[e]	0.65	None	208	189	397	0.24	0.41		10,916	5.93
91887	28T[e]	0.51	None	210	199	409	0.25	0.26		29,136	20.02
91887	32T[e]	0.41	None	140	155	295	0.18	0.23		299,707	164.75
91887	29T[e,f]	0.30	None	143	119	262	0.16	0.14		11,800,000	513.95
91887	34T[e]	1.00	0.1, T	227	283	510	0.18	0.82	71	1,584	160.60
91887	36T[e]	1.00	0.1, C	182	186	368	0.19	0.81	24	1,190	119.67
91887	88760T	1.00	None	283	293	576	0.41	0.59		3,308	4.6
91887	88761T	0.50	None	218	234	452	0.32	0.18		64,362	41.0
30394	394E61T	0.50	0.25, C	259	181	440	0.23	0.27	100	6,500	1,629.5
30394	394E54T	0.50	1.00, C	319	217	527	0.31	0.19	129	3,523	3,524.5
91887	88763T	1.00	1.00, C	252	245	444	0.27	0.73	131	933	934.3

[a] Hourglass specimen, 5.08 mm minimum diameter with a radius-to-minimum-diameter ratio of 6. Product form was 25-mm-thick plate. Material normalized (1038°C) and tempered (760°C).

[b] Fully reversed, continuous-cycle strain-controlled fatigue tests were conducted by employing a triangular waveform at a constant strain rate, $\dot{\varepsilon} = 4 \times 10^{-3}$/s.

[c] T = a hold period at peak tension on the hysteresis loop. C = a hold period at peak compression on the hysteresis loop.

[d] $N_f/2$ properties.

[e] Data are by courtesy of G. E. Korth, Idaho National Engineering Laboratory.

[f] Changed to load control at 1000 strain-controlled cycles (413.95 h), cycled at 30 Hz with sine waveform in load control until failure at ±131 MPa.

Table 1.28. Strain-control fatigue data on modified 9 Cr-1 Mo steel at 538°C

Heat	Specimen[a]	Total strain range,[b] $\Delta\varepsilon_t$ (%)	Hold time and mode[c] (h)	Stress amplitude[d] (MPa)		Stress range, $\Delta\sigma$ (MPa)	Strain range[d,e] (%)		Relaxed stress, σ_r (MPa)	Cycles to failure, N_f	Time to failure, t_f (h)
				Tensile, σ_t	Compressive, σ_c		Elastic, $\Delta\varepsilon_e$	Plastic, $\Delta\varepsilon_p$			
91887	58T	1.00	None	274	286	560	0.36	0.64		2,951	4.10
91887	46T	0.51	None	272	286	558	0.37	0.14		22,316	15.50
91887	68T	0.50	None	238	241	479	0.31	0.19		25,775	17.89
91887	53T	0.50	0.01, T	193	241	434	0.26	0.24	159	>40,911[f]	>437.10[f]
91887	50T	0.50	0.01, C	231	224	455	0.28	0.22	200	12,368	132.10
91887	52T	0.50	0.10, C	241	200	441	0.26	0.24	162	9,917	998.50
91887	57T	0.50	0.10, $\sigma = -0$[g]	241	238	479	0.31	0.19	0	8,135	817.00
91887	48T	0.40	None	210	224	434	0.28	0.12		260,770	144.90
30182	182E4T	1.00	None	279	286	565	0.37	0.63		2,907	4.04
30182	182E2T	0.50	None	283	307	590	0.38	0.12		5,708	3.96
30182	182E3T	0.40	None	224	243	467	0.30	0.10		62,227	34.57
30182	176-52T	0.40	None	232	265	497	0.32	0.07		52,129	29.00
30182	176-53T	0.30	None	183	283	466	0.25	0.05		4,456,920	
30394	394C4T	1.00	None	305	314	619	0.40	0.60		3,827	5.31
30394	394C3T	0.50	None	259	262	521	0.34	0.16		52,400	36.39
30394	394E60T	0.50	0.25, C	272	203	475	0.26	0.24	134	8,840	2,216.14
30394	394C2T	0.40	None	241	241	482	0.31	0.09		382,381	192.90
30394	394E59T	0.40	None	234	307	541	0.35	0.10		218,889	121.61
30394	394E62T	0.50	0.50, C	298	221	519	0.30	0.20	165	5,173	2,588.7
30394	394E50T	0.50	0.01, C	286	261	547	0.34	0.16	239	19,291	206.3
30394	394E49T	0.50	None	283	284	567	0.37	0.13		43,038	27.4
30394	394E51T[h]	0.63[i]	None	399	399	798	0.52	0.11		6,812	
		0.50[i]	None	291	313	604	0.39	0.11		1,681	2.4
30394	394E52T	0.50[i]	None	296	307	603	0.39	0.11		29,883	8.3

Table 1.28. (Continued)

Heat	Specimen[a]	Total strain range,[b] $\Delta\varepsilon_t$ (%)	Hold time and mode[c] (h)	Stress amplitude[d] (MPa)		Stress range, $\Delta\sigma$ (MPa)	Strain range[d] (%)		Relaxed stress, σ_r (MPa)	Cycles to failure, N_f	Time to failure, t_f (h)
				Tensile, σ_t	Compressive, σ_c		Elastic, $\Delta\varepsilon_e$	Plastic, $\Delta\varepsilon_p$			
91887	88759T	0.55	None	288	303	591	0.38	0.17		134,606	93.8
30182	182E5T	0.50	None	246	263	509	0.33	0.17		21,810	13.9
91887	88764T	1.00	1.00, C	300	279	579	0.31	0.69	172	989	989.5
30176	17646T	1.00	1.00, C	312	281	593	0.33	0.67	190	1,176	1,175.8
30383	383B64T	1.00	1.00, C	332	300	632	0.32	0.68	159	1,278	1,278.3
30176	17647T	1.00	1.00, T + C							> 785[j]	>170[j]

[a]Hourglass specimen, 5.08-mm minimum diameter with a radius-to-minimum-diameter ratio of 6. Product form was 25-mm-thick plate except for specimens 394C2T-4T, which were from 232-mm-diam bar, and 182E5T, which was hot-forged billet. Material normalized (1038°C) and tempered (760°C).

[b]Fully reversed, continuous-cycle strain-controlled fatigue tests were conducted by employing a triangular waveform at a constant strain rate, $\dot{\varepsilon} = 4 \times 10^{-3}$/s.

[c]T = a hold period at peak tension on the hysteresis loop. C = a hold period at peak compression on the hysteresis loop.

[d]$N_f/2$ properties.

[e]Calculated values using Young's modulus E of 154 GPa; $\Delta\varepsilon_e = \Delta\sigma/E$, and $\Delta\varepsilon_p = \Delta\varepsilon_t - \Delta\sigma/E$.

[f]Test terminated before failure.

[g]$\sigma = -0$ means that the strain hold period was introduced near the point on the hysteresis loop where the stress is approximately zero on the tension-going side of the hysteresis loop.

[h]$\Delta\varepsilon_t = 0.5\%$ was desired, but because of a recorder problem the test was conducted at $\Delta\varepsilon_t = 0.63\%$ for 6812 cycles. Then the strain range was lowered to 0.5% and the test was continued for another 1681 cycles to specimen failure.

[i]Strain rate, $\dot{\varepsilon} = 0.01$/s.

[j]Test in progress.

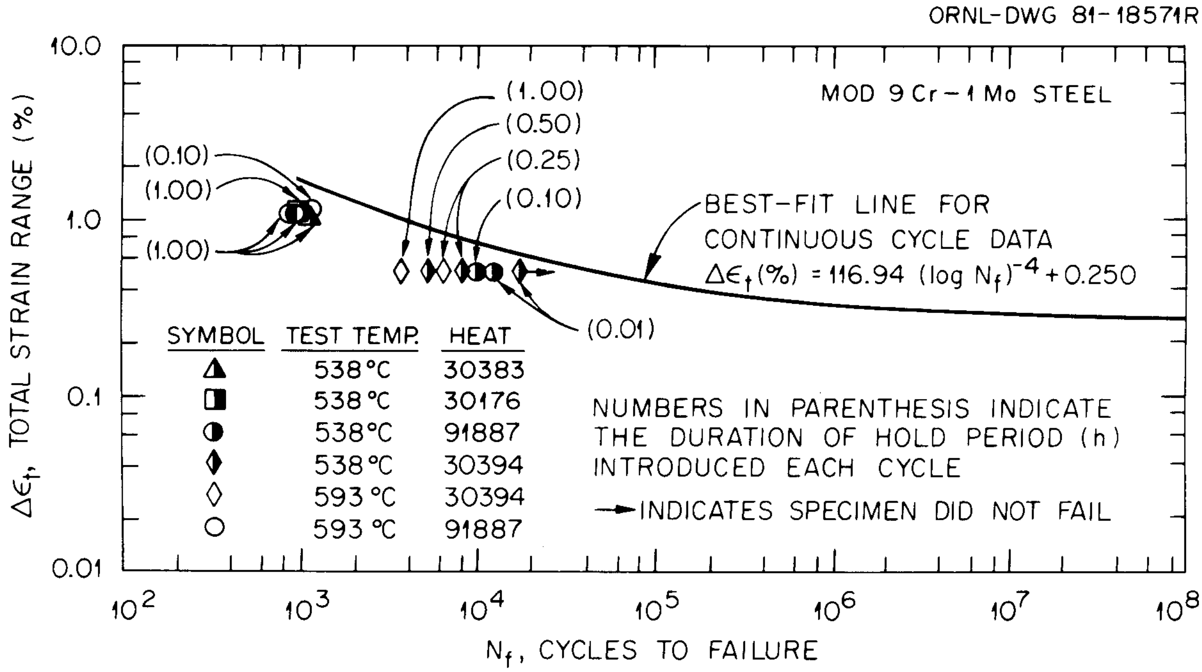

Fig. 1.48. Compressive hold periods reduce the strain-controlled fatigue life (cycles to failure) of modified 9 Cr-1 Mo steel. The magnitude of reduction depends on the hold period duration, particularly at low strain ranges.

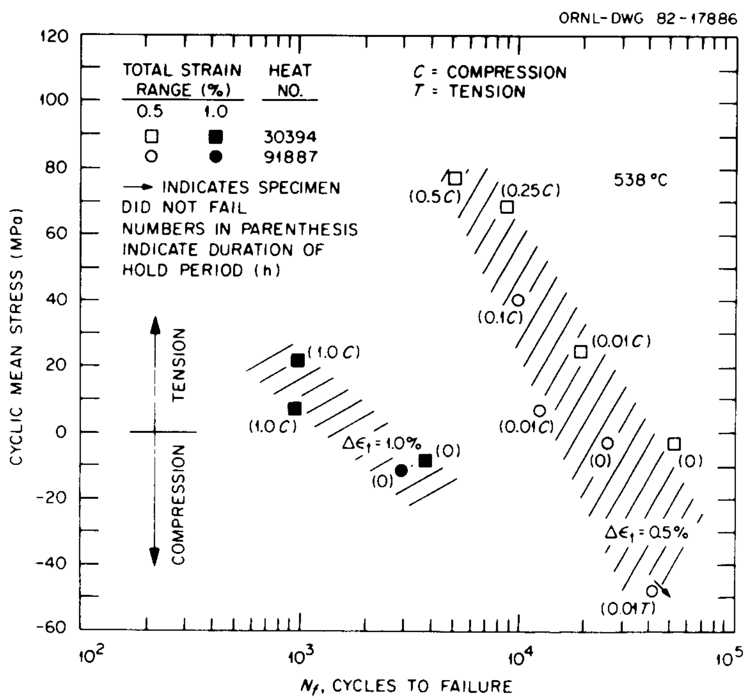

Fig. 1.49. Compressive hold periods result in a cyclic mean tensile stress, the magnitude of which depends on the duration of the hold period and on the strain range.

hold periods and why the greatest reduction in cyclic life occurs at lower strain ranges. This observation suggests that the compressive hold time effect in this material may be accounted for by use of one of the classical linear or nonlinear methods used in design for accounting for mean tensile stresses (e.g., Goodman or Soderburg method). Alternatively, a ratchetting correction may be required.

Figure 1.50 shows specimens of modified 9 Cr-1 Mo steel subjected to time-dependent fatigue tests in air at the indicated temperatures of 538 and 593°C. The test times were about 933 and 1176 h. Figure 1.51 shows the surface of a 2 1/4 Cr-1 Mo specimen tested in air for about 1006 h. Note the rather severe oxidation and exfoliation on the surface of the 2 1/4 Cr-1 Mo specimen in comparison with the modified 9 Cr-1 Mo steel specimens shown in Fig. 1.50.

Table 1.29 compares cyclic lives at a given temperature, strain range, and wave form for both modified 9 Cr-1 Mo and 2 1/4 Cr-1 Mo steels. Note that, although modified 9 Cr-1 Mo steel shows a higher continuous-cycle fatigue life (zero hold time) than 2 1/4 Cr-1 Mo steel, the limited data indicate that the fatigue lives of the two materials tend to approach one another as the duration of the compressive hold time is increased. Hardnesses in the gage section and in the head or shoulder region are also given for the modified 9 Cr-1 Mo steel. These values indicate strain softening of the gage section of the specimens near the point of fracture. Strain softening characteristics are further demonstrated by the curves given in Figs. 1.52 and 1.53. Figure 1.53 compares cyclic stress-strain curves generated at 538°C.

Work planned for the near term will involve the following:

1. conduct additional room-temperature continuous-cycle fatigue tests,
2. determine the influence of mean tensile stresses on the continuous-cycle behavior of this material at both room and elevated temperatures,
3. determine the influence of test frequency on the cyclic relaxation and high-cycle fatigue characteristics of this material, and
4. continue long-term time-dependent fatigue testing of this material.

Y-186840

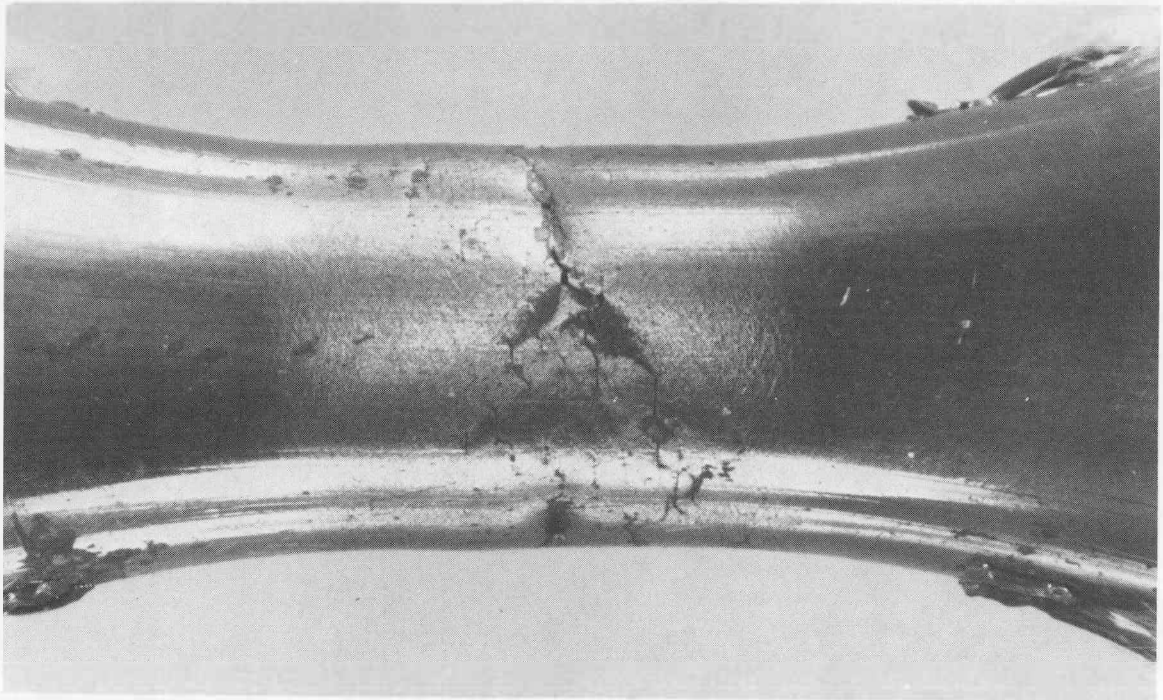

(a)

Y-186839

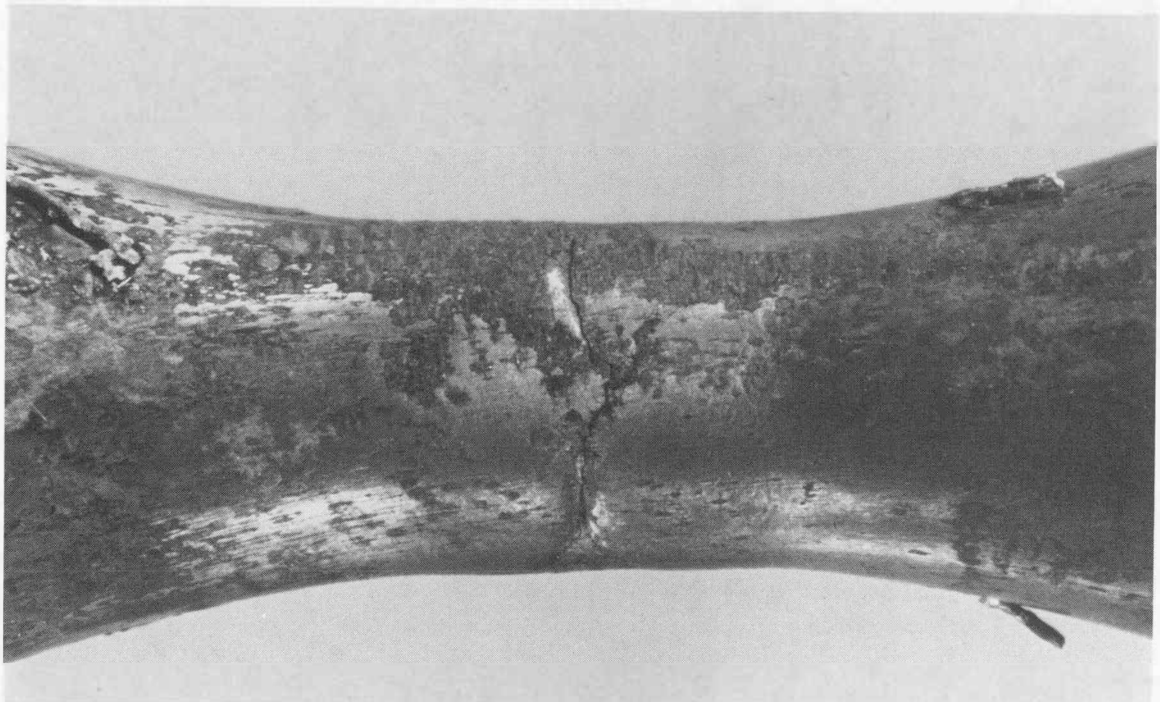

(b)

Fig. 1.50. Fatigue specimens of modified 9 Cr-1 Mo steel tested in air and in strain control. Total strain range = 1.0%, 1-h compressive hold each cycle. (*a*) 538°C, N_f = 1176 cycles. (*b*) 593°C, N_f = 933 cycles.

ORNL-Photo 4203-82

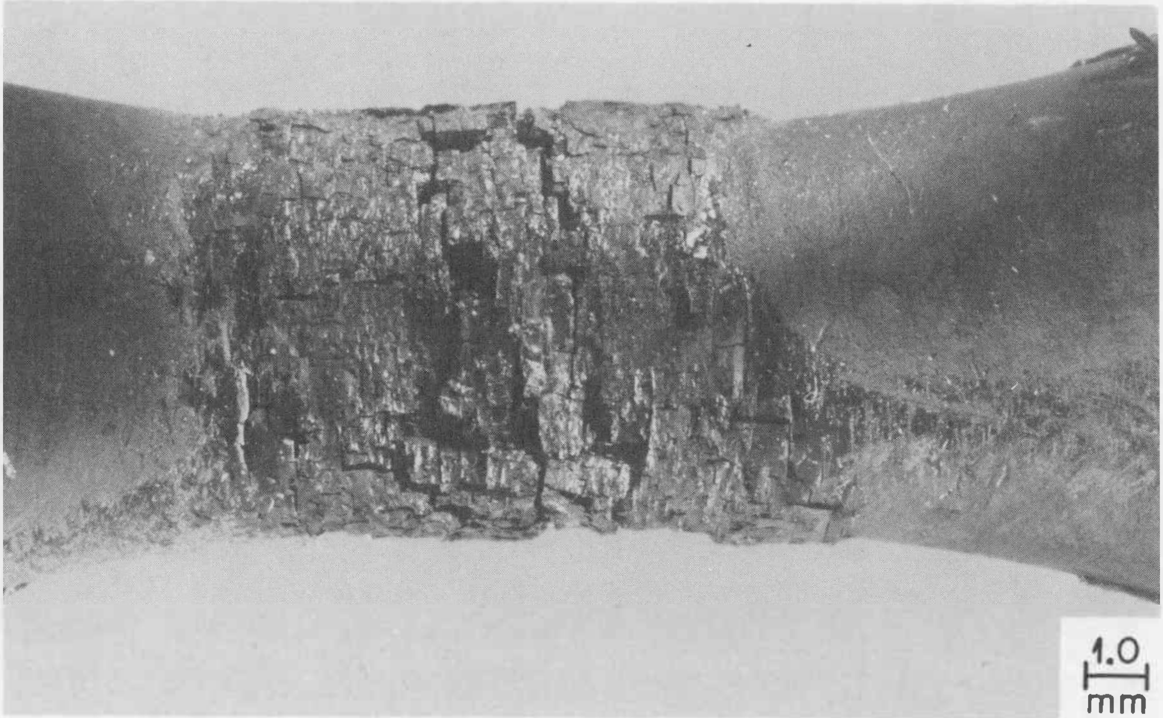

Fig. 1.51. Fatigue specimen of annealed 2 1/4 Cr-1 Mo steel tested in air and in strain control. Total strain range = 0.5%, 0.25-h tensile and compressive hold periods, 482°C, N_f = 1950 cycles (1006 h).

Table 1.29. Comparison of the fatigue life of 2 1/4 Cr-1 Mo steel (annealed) and modified 9 Cr-1 Mo steel (normalized and tempered) at 538°C and at a strain range of 0.5%

Compressive hold period (h)	Fatigue life (h)		Hardness (DPH) of 9 Cr-1 Mo[b]	
	2 1/4 Cr-1 Mo[a]	9 Cr-1 Mo[b]	Gage	Head
0	17,329	52,400	196	267
0.01	6,775	19,291	198	223
0.1	4,496			
0.25		8,840	207	223
0.5		5,173	196	219
1.0	4,133			

[a]Annealed heat 3P5601.

[b]Modified heat 30394.

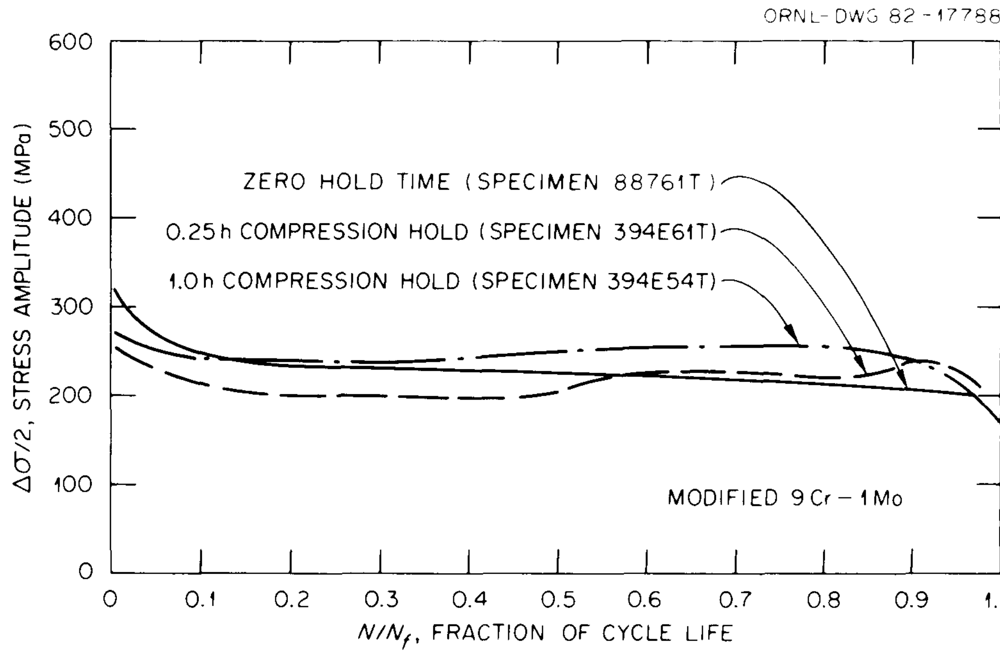

Fig. 1.52. Cyclic stress amplitude as a function of fraction of cyclic life and duration of compressive hold period for modified 9 Cr-1 Mo steel tested at 593°C and at a strain range of 0.5%.

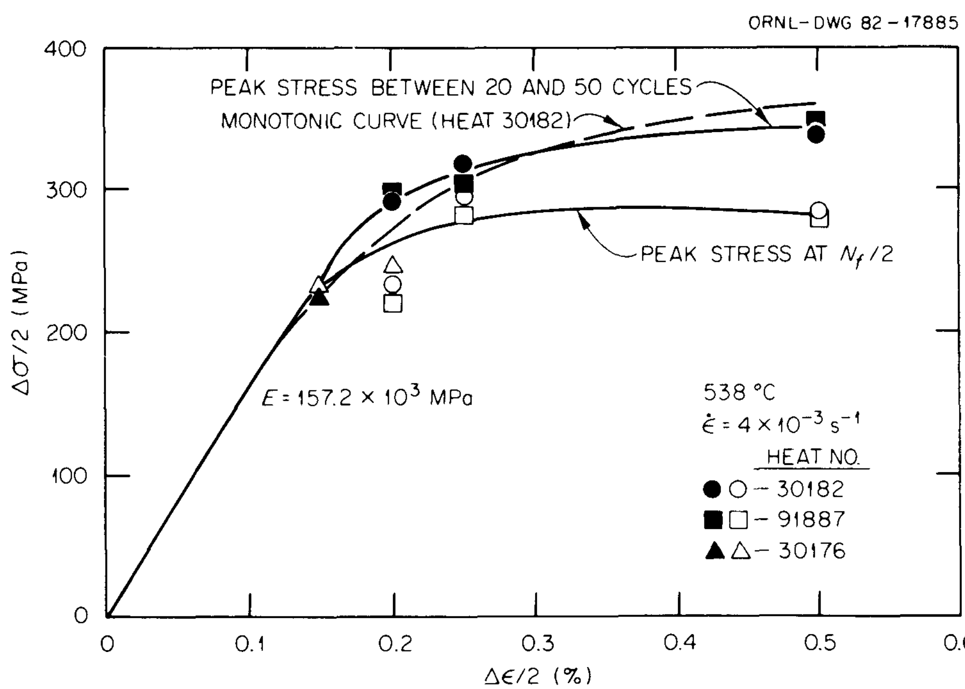

Fig. 1.53. Comparison of the cyclic stress-strain curves for modified 9 Cr-1 Mo steel tested at 538°C in continuous cycling.

1.7 Charpy V-Notch Toughness Studies

W. J. Stelzman and R. K. Nanstad

1.7.1 Thermal Aging of Plate Materials

We have continued to investigate the effects of extended periods of aging on the Charpy V-notch (C_V) impact properties of hot-forged and hot-rolled modified 9 Cr-1 Mo steel plate: 27-mm-thick (1 1/16-in.) plate from CarTech electroslag-remelted (ESR) ingot 30176 (0.2% Si) and 52-mm-thick (2 1/16-in.) plate from CarTech argon-oxygen-deoxidized (AOD) ingot 30383 (0.4% Si). We have reported the effects of aging the plate from ingot 30176 after 1200 and 5000 h at five aging temperatures: 482, 538, 593, 649, and 704°C (900, 1000, 1100, 1200, and 1300°F).[3,4] The C_V results from the as-tempered (unaged) plates have also been reported.[5] Both plates were normalized and tempered for 1 h at 1040 and 760°C (1900 and 1400°F), respectively, with air cooling to room temperature before aging. The specimen orientation was WR in all cases.[6]

1.7.1.1 Electroslag remelted ingot 30176 plate

The C_V toughness results from ESR 30176 plate (0.2% Si) after aging for 10,000 h are presented in Table 1.30 and plotted in Figs. 1.54 through 1.58. Each figure compares the toughness obtained after 10,000 h with the as-tempered and the 1200- and 5000-h aging results for each aging temperature. A comparison with the 5000-h results after aging an additional 5000 h (10,000 total) at 482, 538, and 593°C indicates a further decrease

Table 1.30 Summary of Charpy-V toughness of commercial 14-Mg (15-ton) heats of modified 9 Cr-1 Mo steel after aging

(WR orientation)

Aging temperature (°C)	Aging temperature (°F)	Temperature [°C (°F)]: 68-J (50-ft-lb) energy	Temperature [°C (°F)]: 0.89-mm (35-mil) Lateral expansion	Temperature [°C (°F)]: 50% Shear	Temperature [°C (°F)]: 100% Shear	Energy [J (ft-lb)]: 21°C (70°F)	Energy [J (ft-lb)]: Upper-shelf at 121°C (250°F)
CarTech ESR ingot 30176 (0.2% Si) aged 10,000 h							
As tempered[a]		–26 (–15)	–32 (–25)	–7 (20)	32 (90)	171 (126)	204 (150)
482	900	27 (80)	21 (70)	43 (110)	77 (170)	64 (47)	163 (120)
538	1000	35 (95)	27 (80)	43 (110)	77 (170)	48 (35)	152 (112)[b]
593	1100	24 (75)	18 (65)	32 (90)	71 (160)	64 (47)	166 (122)[b]
649	1200	–32 (–25)	–37 (–35)	–4 (25)	32 (90)	175 (129)	242 (178)[b]
704	1300	–23 (–10)	–29 (–20)	10 (50)	41 (105)	174 (128)	292 (215)[b,c]
CarTech ingot 30383 (0.4% Si) aged 1200 h							
As tempered[a]		18 (65)	24 (75)	10 (50)	43 (110)	82 (60)	95 (70)
482	900	32 (90)	32 (90)	32 (90)	49 (120)	49 (36)	106 (78)
538	1000	35 (95)	35 (95)	20 (85)	54 (130)	41 (30)	102 (75)
593	1100	35 (95)	35 (95)	27 (80)	52 (125)	45 (33)	102 (75)
649	1200	54 (130)	54 (130)	43 (110)	74 (165)	41 (30)	90 (66)

[a]Normalized 1 h at 1040°C (1900°F), tempered 1 h at 760°C (1400°F), air cooled.

[b]Upper-shelf values still increasing.

[c]Exceeded machine capacity (326 J) near 149°C (300°F).

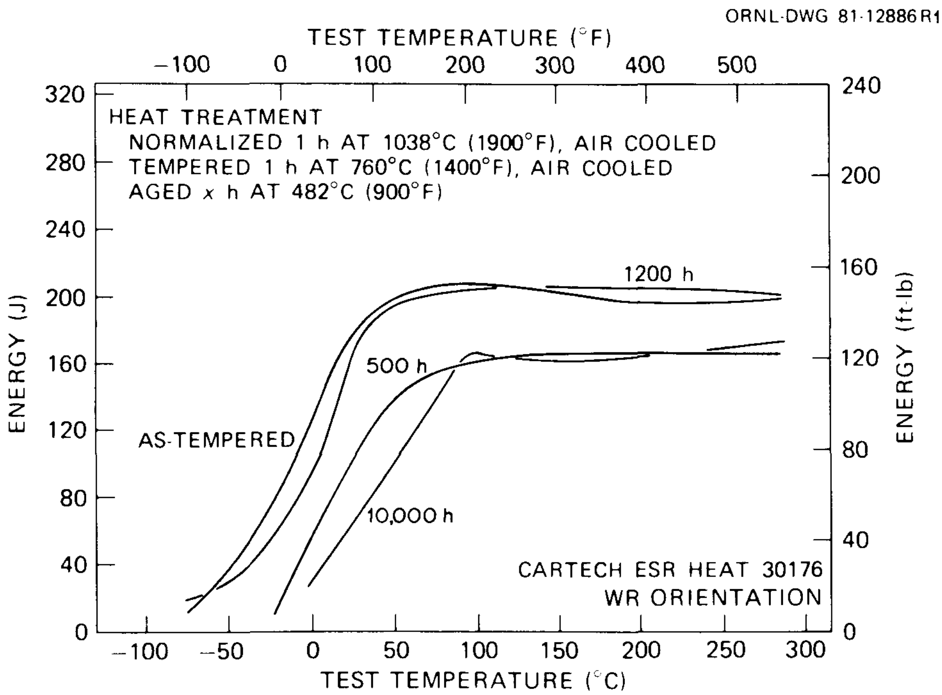

Fig. 1.54. Effect of aging at 482°C on the Charpy-V energy of 27-mm-thick (1 1/16-in.) commercially processed modified 9 Cr-1 Mo steel plate, CarTech ESR 30176.

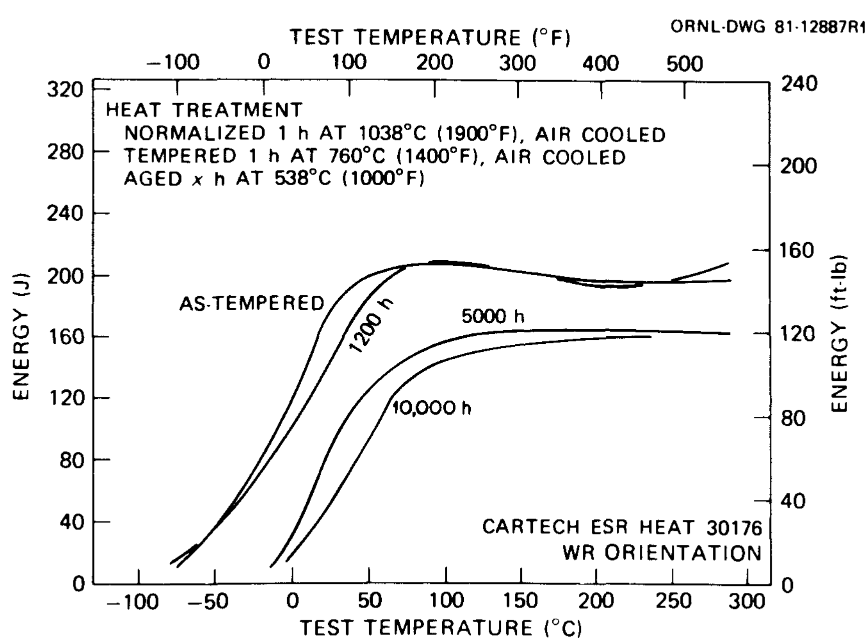

Fig. 1.55. Effect of aging at 538°C on the Charpy-V energy of 27-mm-thick (1 1/16-in.) commercially processed modified 9 Cr-1 Mo steel plate, CarTech ESR 30176.

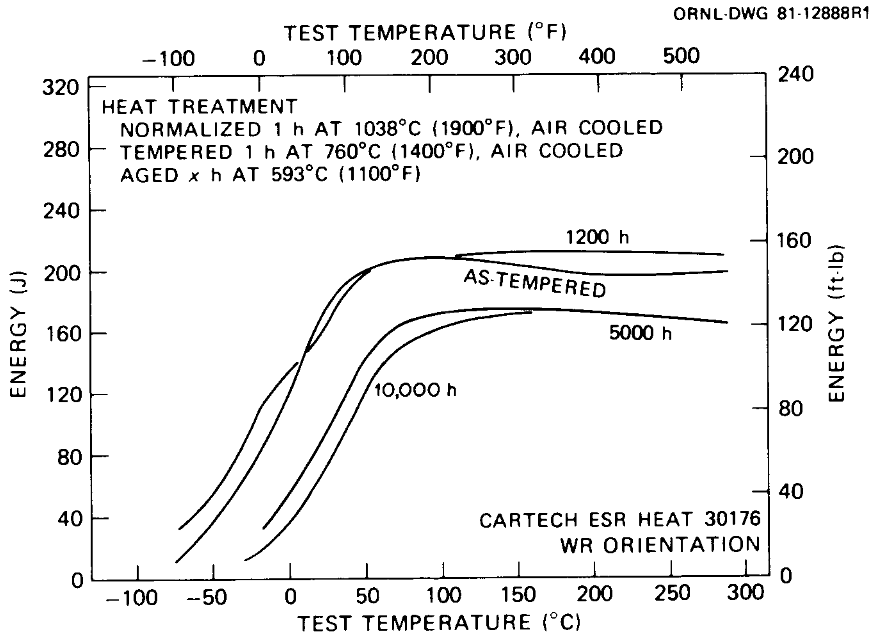

Fig. 1.56. Effect of aging at 593°C on the Charpy-V energy of 27-mm-thick (1 1/16-in.) commercially processed modified 9 Cr-1 Mo steel plate, CarTech ESR 30176.

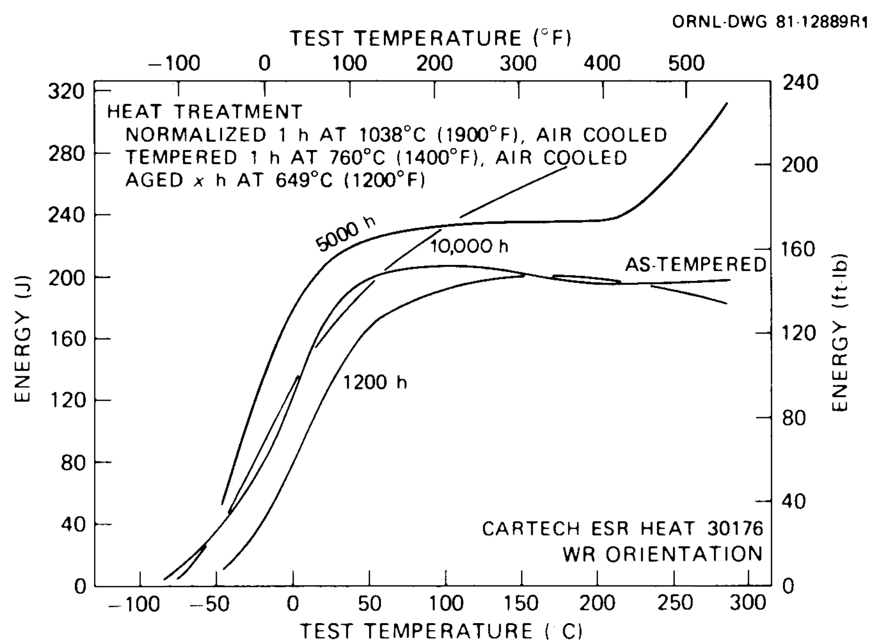

Fig. 1.57. Effect on aging at 649°C on the Charpy-V energy of 27-mm-thick (1 1/16-in.) commercially processed modified 9 Cr-1 Mo steel plate, CarTech ESR 30176.

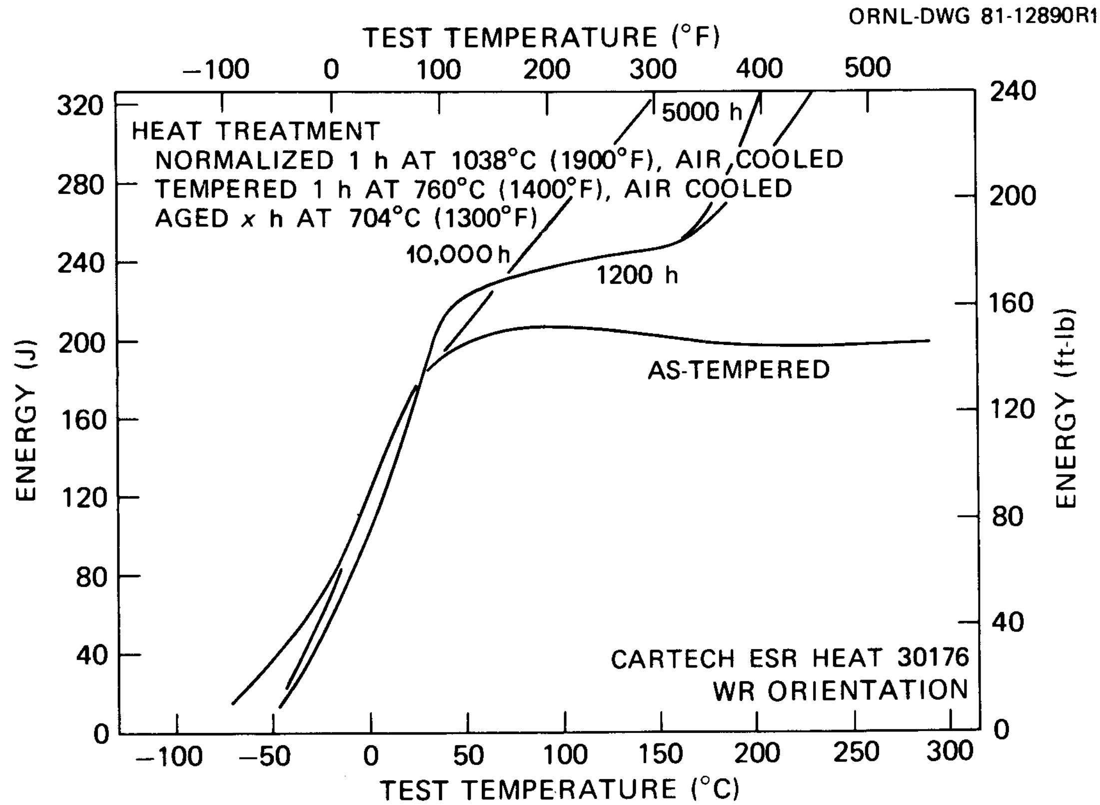

Fig. 1.58. Effect of aging at 704°C on the Charpy-V energy of 27-mm-thick (1 1/16-in.) commercially processed modified 9 Cr-1 Mo steel plate, CarTech ESR 30176.

in toughness in the transition regime (lower energies at a given test temperature) but little or no further decrease in the upper-shelf energies. Aging for 10,000 h at 649°C results in a decrease in the transition toughness obtained after aging for 5000 h but a return to the toughness values of as-tempered plate. The upper-shelf energies continue to improve. A shortage of specimens prevented the determination of energies above 204°C (400°F). Additional aging at 704°C still has altered the as-tempered transition toughness significantly, but the upper-shelf energies are still improving, exceeding the machine capacity of 326 J (240 ft-lb) near 149°C (300°F). The upper-shelf energies exceeded the machine capacity near 204°C (400°F) after 5000 h. The trends of the C_V transition energies at 21°C (70°F) after aging for 10,000 h at the aging temperature together with the 1200- and 5000-h agings are listed in Table 1.30 and shown in Fig. 1.59.

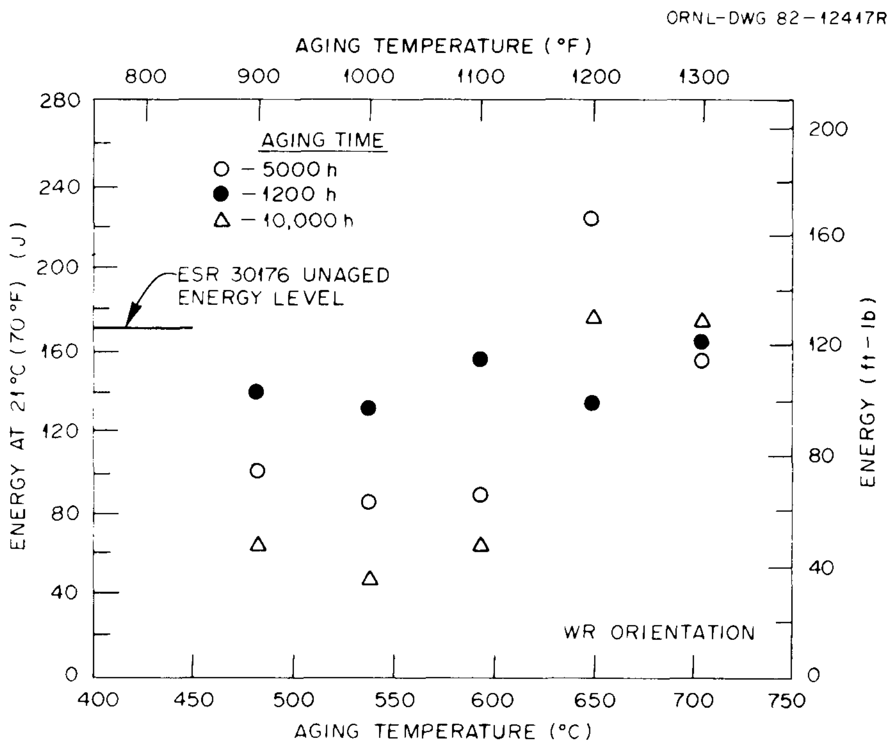

Fig. 1.59. Effect of aging time on the Charpy-V impact energy at room temperature of 27-mm-thick commercially processed modified 9 Cr-1 Mo steel plate from CarTech ESR 30176.

1.7.1.2 Argon-oxygen decarburized ingot 30383 plate

The C_V toughness results from WR-oriented specimens from AOD 30383 plate (0.4% Si) after aging for 1200 h are listed in Table 1.30 and plotted in Fig. 1.60. For obscure reasons, the AOD melt has poor impact properties when compared with the ESR melts. Part of the reduced toughness is attributed to the higher silicon content (0.4% for the AOD and 0.2% for the ESR). Aging at 482, 538, 593, and 649°C (900, 1000, 1100, and 1200°F) for 1200 h degrades the C_V toughness in the transition region; it drops from 82 J (60 ft-lb) at 21°C (70°F) for the as-tempered plate to 41 J (30 ft-lb) at 21°C after exposure at 649°C. When compared at 121°C (250°F), the upper-shelf energies increased at the lower aging temperatures (482–593°C), but decreased at the highest aging temperature used (649°C), a total spread of 16 J (12 ft-lb). The small differences indicate a minimal effect of 1200-h aging on the upper-shelf energies.

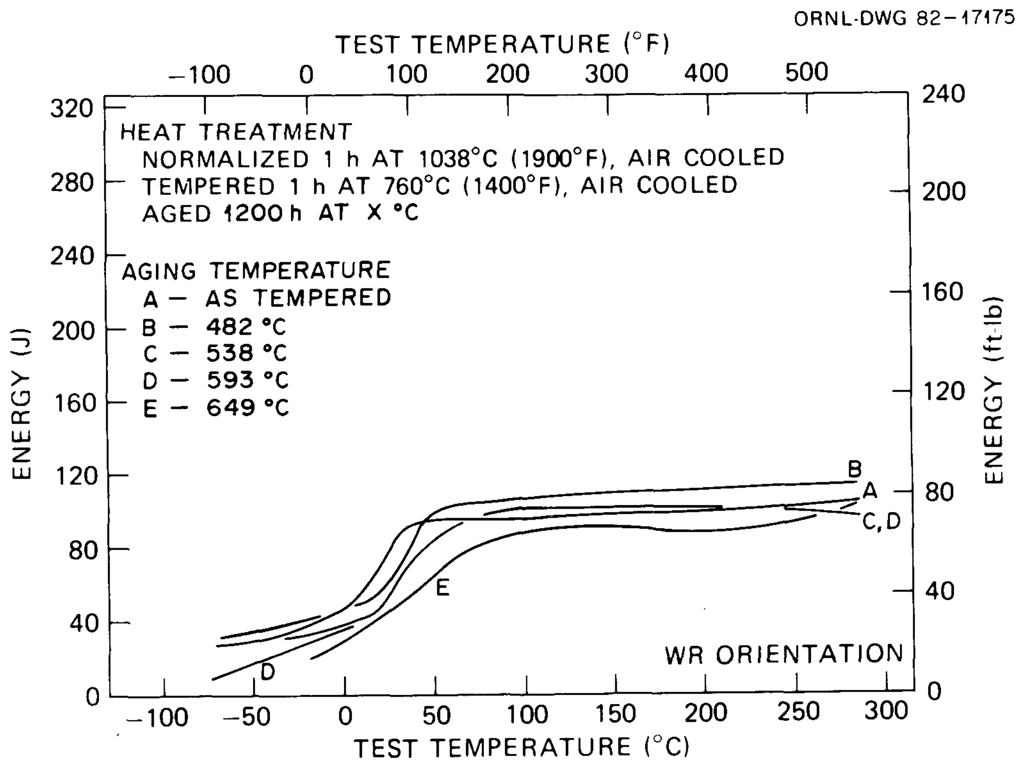

Fig. 1.60. Effect of aging for 1200 h on the Charpy-V energy of 52-mm-thick modified 9 Cr-1 Mo steel plate, CarTech AOD 30383.

1.7.2 Plate Materials

We have determined the C_V impact properties of 51-mm-thick (2-in.) plate fabricated commercially by Electralloy from modified 9 Cr-1 Mo steel ingot AOD/ESR 10148B. The ingot was melted originally by the AOD process (AOD 10148) and remelted by the ESR process. Part of the ingot was then hot forged and hot rolled to a thickness of 51 mm. The melting and chemical analysis details have been reported.[4] Before specimens were machined, the plate was normalized for 1 h at 1038°C and tempered for 1 h at 780°C (1435°F), followed after each treatment by air cooling. Charpy V-notch specimens were then machined from two depth locations (quarter and three-quarter) and in two orientations (WR and RW). The test results are listed in Table 1.31 and plotted in Fig. 1.61. We found little difference

Table 1.31. Summary of Charpy-V toughness of commercial 14-Mg (15-ton) heats of modified 9 Cr-1 Mo steel

Orientation	Temperature [°C (°F)] 68-J (50-ft-lb) energy	0.89-mm (35-mil) Lateral expansion	50% Shear	100% Shear[a]	Upper-shelf energy at 121°C (250°F) (J)	(ft-lb)
	Electralloy AOD/ESR 10148B[b]					
WR	−65 (−85)	−62 (−80)	−26 (−15)	10 (50)	*c*	
RW	−73 (−90)	−68 (−90)	−18 (0)	21 (70)	*d*	
	Electralloy AOD 10148[e]					
WR	−34 (−30)	−29 (−20)	−15 (5)	10 (50)	211	155
RW	−46 (−50)	−40 (−40)	−15 (5)	18 (65)	204	150

[a]Estimated temperature.

[b]One-quarter and three-quarter depth specimens, 51-mm-thick plate.

[c]316 J (233 ft-lb) at 66°C (150°F).

[d]326 J (240 ft-lb) near 54°C (130°F).

[e]One-half depth specimens, 16-mm-thick plate.

ORNL-DWG 82-17178

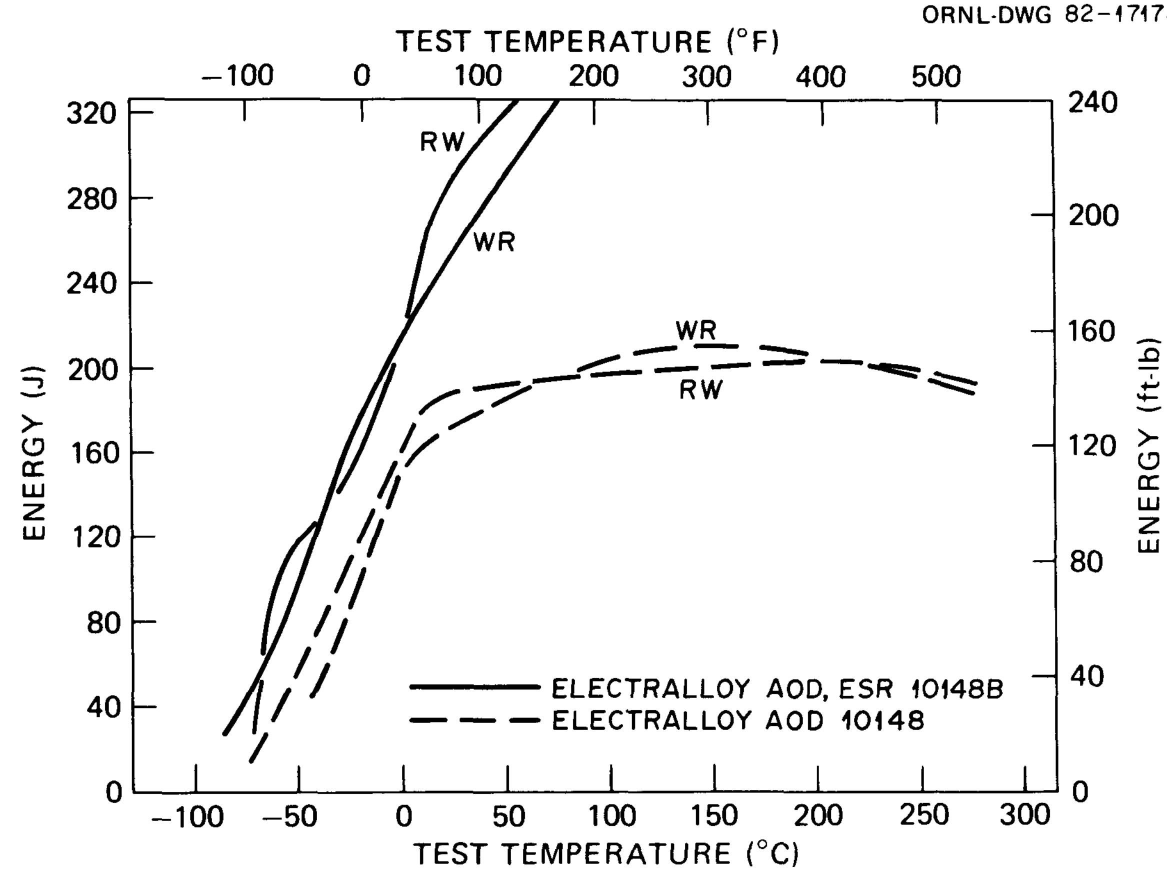

Fig. 1.61. Effect of specimen orientation on the Charpy-V energy from 51-mm-thick (2-in.) Electralloy AOD/ESR 10148B and 16-mm-thick (5/8-in.) Electralloy AOD 10148 modified 9 Cr-1 Mo steel plate.

due to depth. There was also little difference between orientations in the transition region, with the C_V energy exceeding 326 J (240 ft-lb) near 66°C (150°F).

The results from 16-mm-thick plate from AOD 10148 have been included in Fig. 1.61 to assess the value of the ESR remelt. These results have been reported[5] and are relisted in Table 1.31. The C_V toughness of the plate fabricated from AOD/ESR (ESR remelt) is clearly superior. Part of the difference can be attributed to the difference in plate thickness (cooling rate) and the depth location from which the specimens were taken: quarter and three-quarter thickness in the 51-mm-thick AOD/ESR and one-half thickness in the 16-mm-thick AOD plate.

1.8 Weldability

J. F. King, V. K. Sikka, and W. J. Stelzman

The welding development program for modified 9 Cr-1 Mo steel has been determining the effects of weld composition and welding process on the properties of weld metal and weldments in this alloy. Filler metal compositions have included both standard 9 Cr-1 Mo and the modified composition of the same analysis as the base metal. Weldments for testing have been made with the gas tungsten arc (GTA), shielded metal arc (SMA), and submerged arc (SA) welding processess. The weld metals and weldments have been evaluated and characterized by tensile, creep, and Charpy-V impact testing. The results of this testing to date are summarized in this report.

1.8.1 Gas Tungsten Arc Welding

Weldments in the modified 9 Cr-1 Mo steel alloy have been made with the GTA process and several different heats of modified 9 Cr-1 Mo filler wire. Two heats of standard 9 Cr-1 Mo, type ER505, have also been used to weld the modified alloy. Table 1.32 lists the compositions of the filler metals used in the testing to date. This section summarizes the results of the GTA welding evaluation, which included tensile, creep, and Charpy V-notch toughness testing.

Gas tungsten arc weldments in the modified 9 Cr-1 Mo used in this study have been made predominantly in flat plate specimens 16 or 25 mm thick. These welds were produced with the automatic GTA process and cold-wire filler addition. Either 75 or 60°-included-angle V-grooves were used

Table 1.32 Chemical analyses of filler metals used in gas tungsten arc welding of modified 9 Cr-1 Mo

Element	Content (wt %) for each heat					
	F5349	30394	30182	30383	Y3738F 505	A1977F 505
C	0.10	0.074	0.088	0.090	0.076	0.07
Mn	0.39	0.47	0.37	0.45	0.411	0.42
P	0.007	0.01	0.011	0.010	0.008	0.11
S	0.015	0.005	0.004	0.005	0.015	0.016
Si	0.35	0.48	0.19	0.42	0.35	0.28
Ni	0.10	0.10	0.09	0.09	0.43	0.16
Cr	8.80	8.38	8.47	8.29	8.66	9.5
Mo	0.94	1.04	0.88	1.00	1.04	0.98
V	0.205	0.197	0.21	0.02		
Nb	0.060	0.077	0.07	0.07		
Ti	0.006	0.005	0.001	0.002		
Co	0.018	0.063	0.017	0.054		
Cu	0.09	0.04	0.03	0.04	0.023	
Al	<0.001	0.018	0.009	0.001		
B	0.001	<0.001		<0.001		
W	<0.01	0.05		0.04		
As	0.002	<0.001		<0.001		
Sn	0.004	<0.001		0.002		
Zr	<0.001	<0.001		<0.001		
N	0.011	0.038	0.054	0.050		
O	0.012	0.004		0.007		

on the weld plates. All plates were preheated to 204°C before the multipass welds. The completed weldments have the appearance shown in Fig. 1.62. After welding, the weldments are typically given a postweld heat treatment (PWHT) of 732°C for 1 h. The hardness variation across a modified 9 Cr-1 Mo GTA weldment before and after PWHT is plotted in Fig. 1.63. The large difference in hardness between the weld metal, heat-affected zone (HAZ), and base metal in the as-welded condition is greatly reduced by the PWHT, but variations do exist. Microstructural variations are also observed as shown in Fig. 1.64, weld metal, and Fig. 1.65, the fusion line and HAZ. Specimens have been obtained from many weldments similar to that described here. The results of tensile, creep, and Charpy

Y-182416

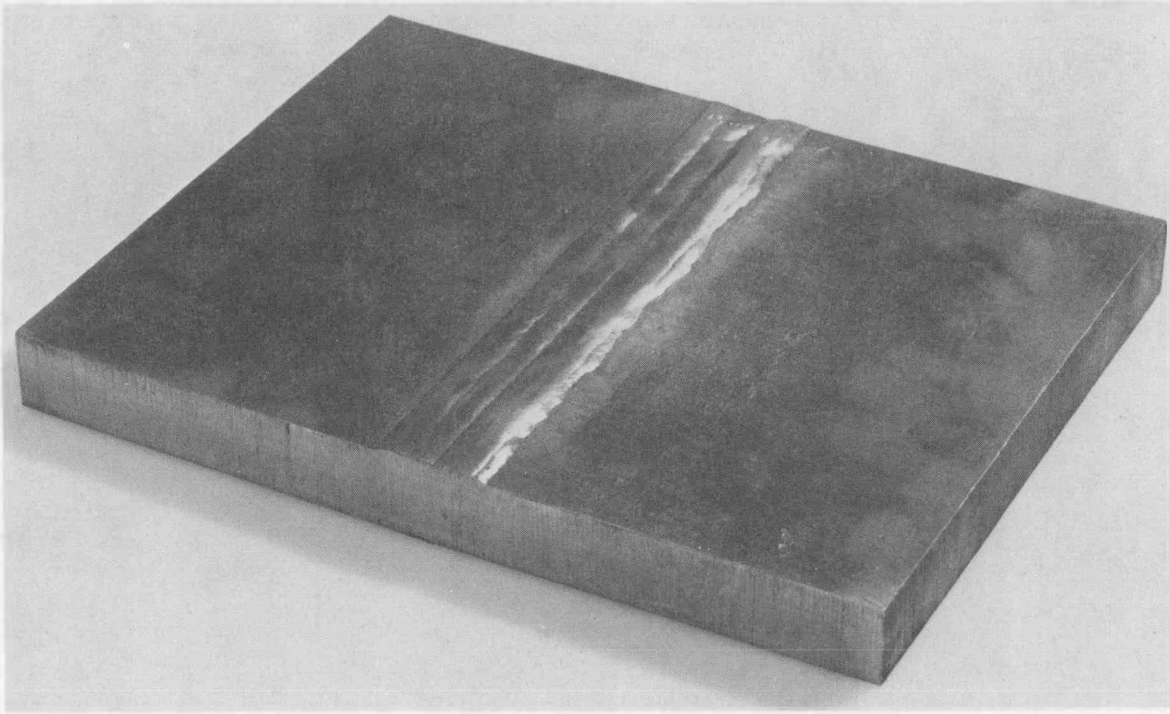

Fig. 1.62. Typical gas tungsten arc weldment of modified 9 Cr-1 Mo used in the characterization studies.

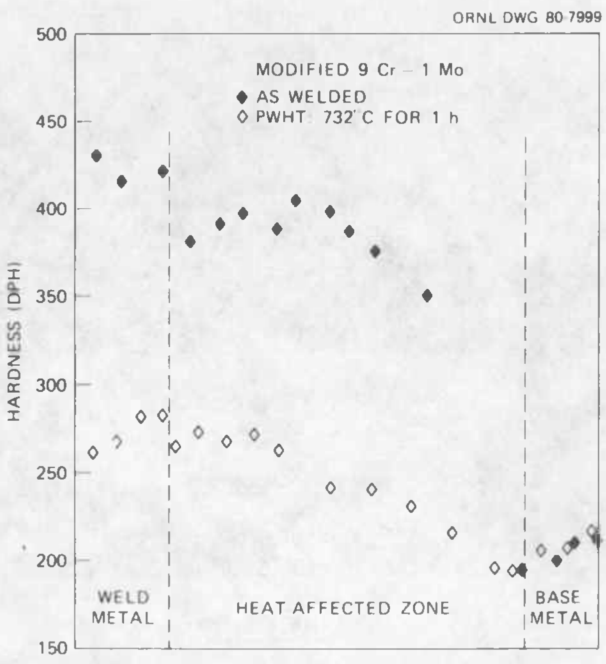

Fig. 1.63. Hardness variation across weldment is modified 9 Cr-1 Mo alloy as welded and after postweld heat treatment.

Y-176787

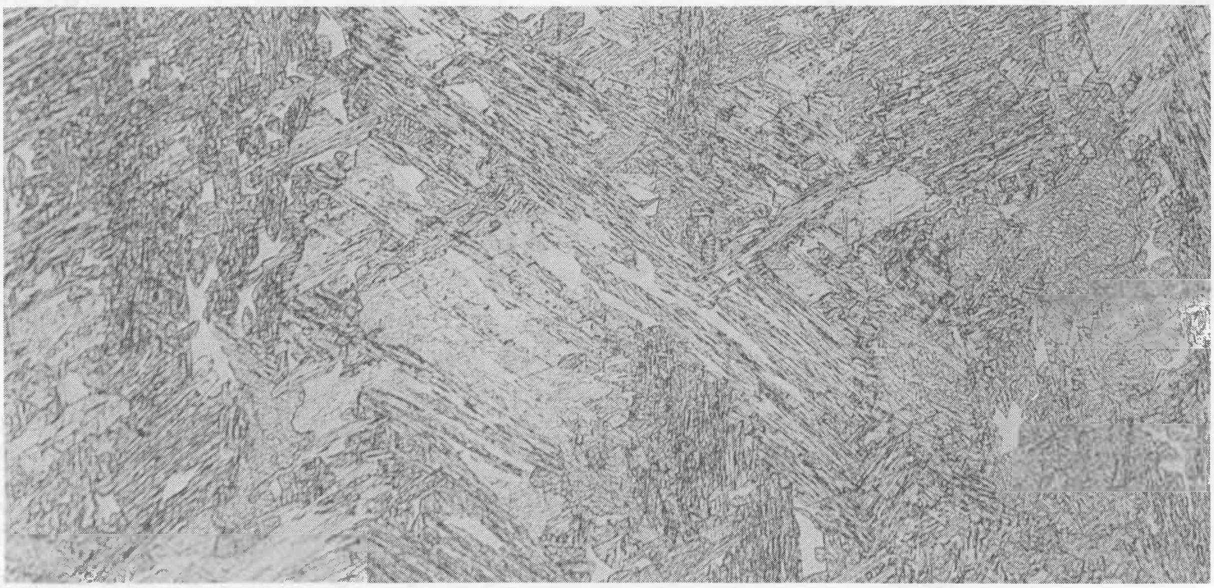

400 μm

Fig. 1.64. Microstructure of heat 30394 weld metal after a postweld heat treatment at 732°C for 1 h.

Y-176788

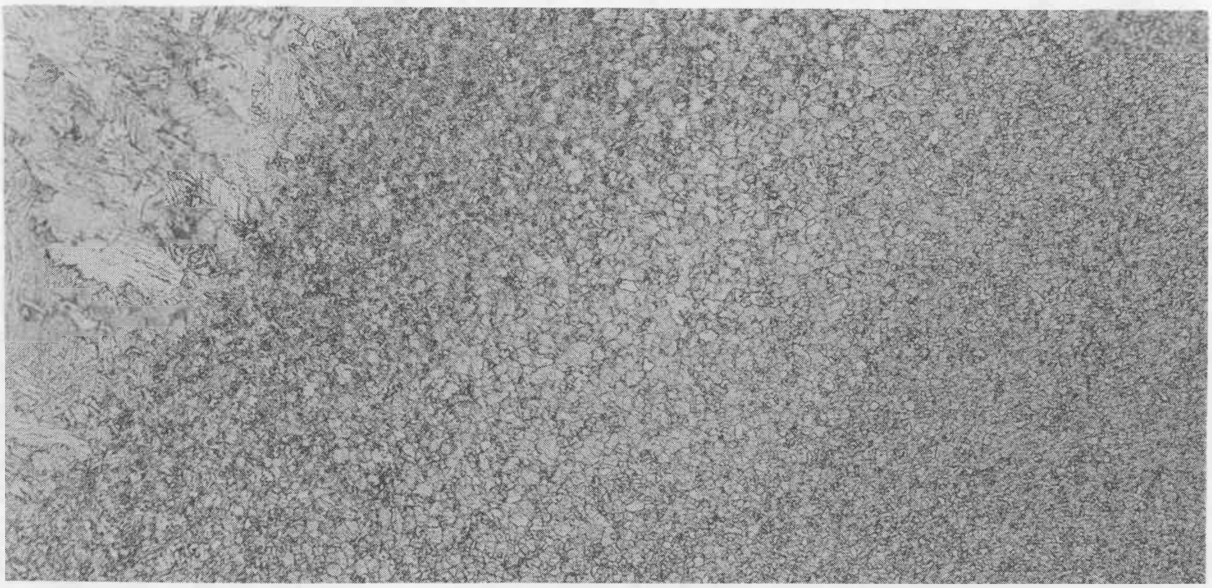

400 μm

Fig. 1.65. Microstructure of fusion line and heat-affected zone in heat 30394 weldment after postweld heat treatment.

V-notch (C_V) tests are reported in the following paragraphs. These data are plotted as specimens from weldments indicated by the weldment designation. Table 1.33 lists the filler metal and base metal heats that were used in each weldment.

Tensile properties of various GTA weldments of modified 9 Cr-1 Mo steel are compared with the average property curves for the base metal in Figs. 1.66 through 1.69. The minimum property curves based on the room-temperature specified minima are also included in these figures. The following observations are possible from these figures.

1. The yield strength data for various weldments match the average curve observed for the base metal.

Table 1.33. Filler metal and base metal heat combinations used in gas tungsten arc weldment characterizations

Weld	Filler metal heat	Base metal heat
PC-4	F5349	F5349
PC-5	F5349	F5349
PC-9	F5349	F5349
PC-10	Y3738 F505	30394
PC-32	30182	30182
PC-36	30394	30394
PC-37	30394	30394
PC-38	30182	30394
PC-39	30394	30394
PC-45	30394	30394
PC-49	A1977 F505	K4860-3F (std 9 Cr-1 Mo)
PC-52	30383	30394
PC-53	30383	30176
PC-58	A1977 F505	30394
394L[a]	30394	30394

[a]Weldment prepared by Leighton Industries.

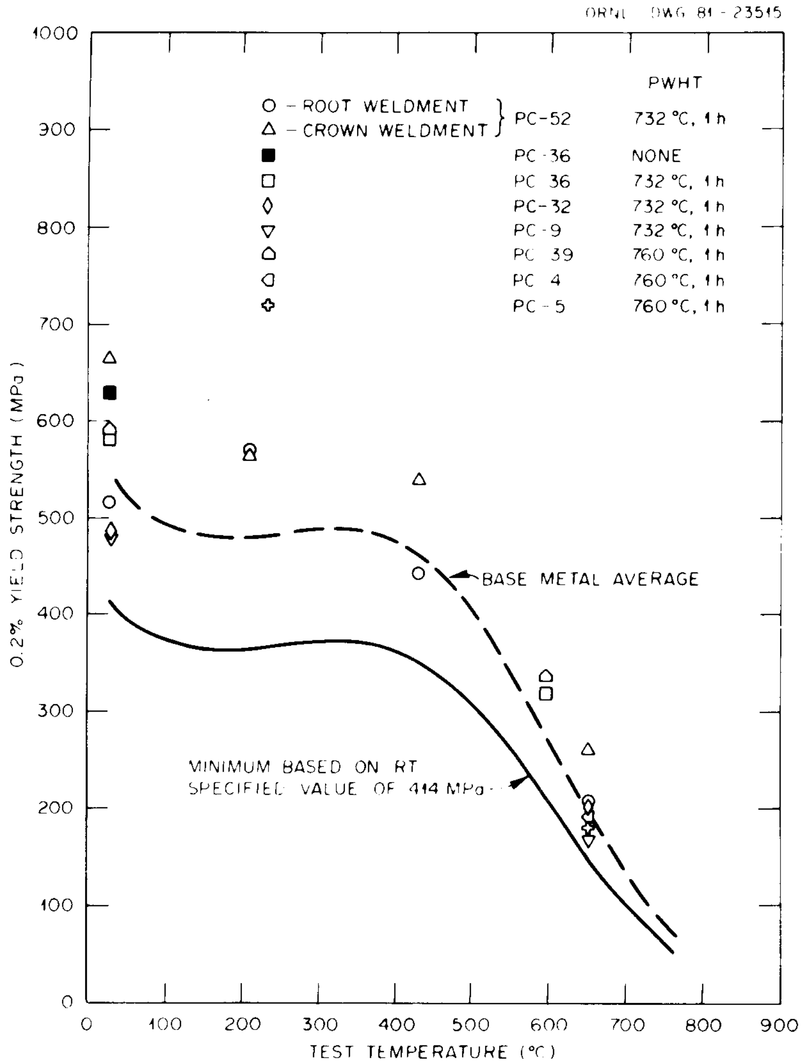

Fig. 1.66. Yield strength data for various weldments of modified 9 Cr-1 Mo steel match the average curve observed for the base metal data.

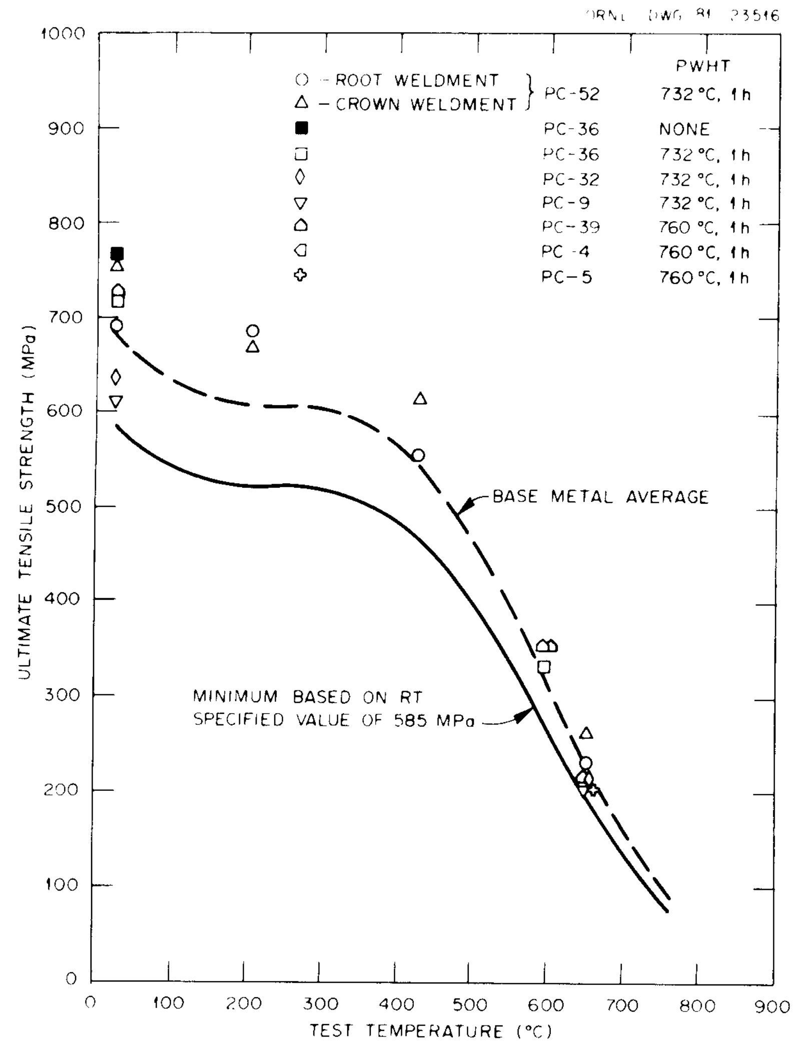

Fig. 1.67. Ultimate tensile strength data for various weldments of modified 9 Cr-1 Mo steel match the average curve observed for the base metal data.

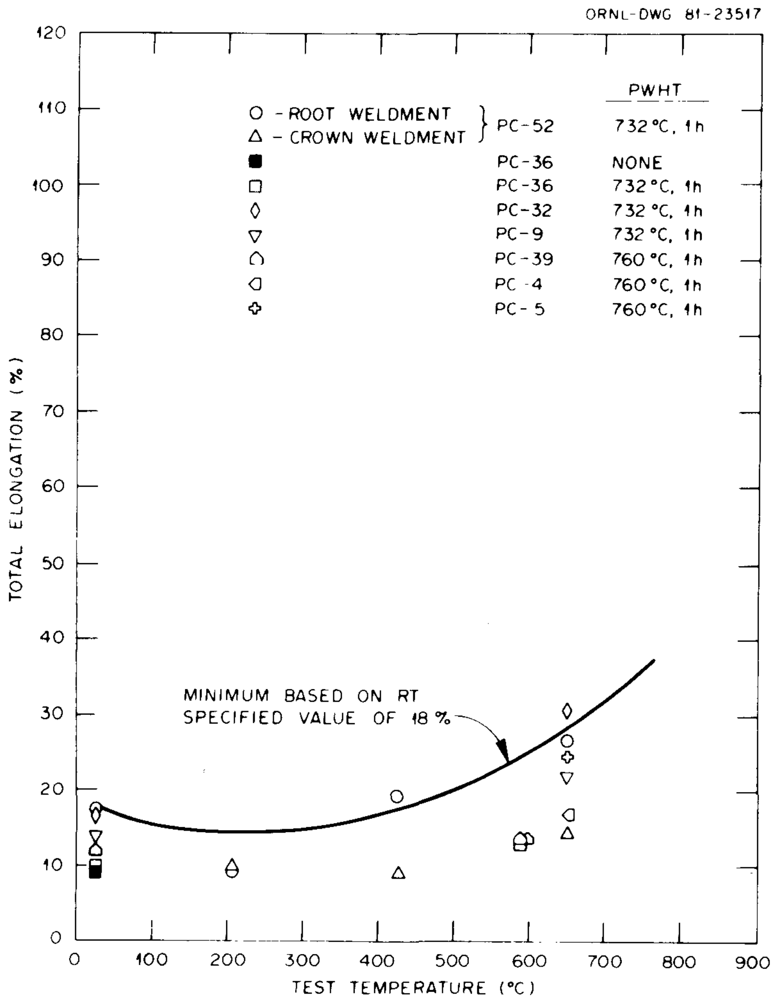

Fig. 1.68. Total elongation values for various weldments of modified 9 Cr-1 Mo steel fall below the minimum value curve for the base metal. Note, however, that values are still about 10% or more for the entire temperature range.

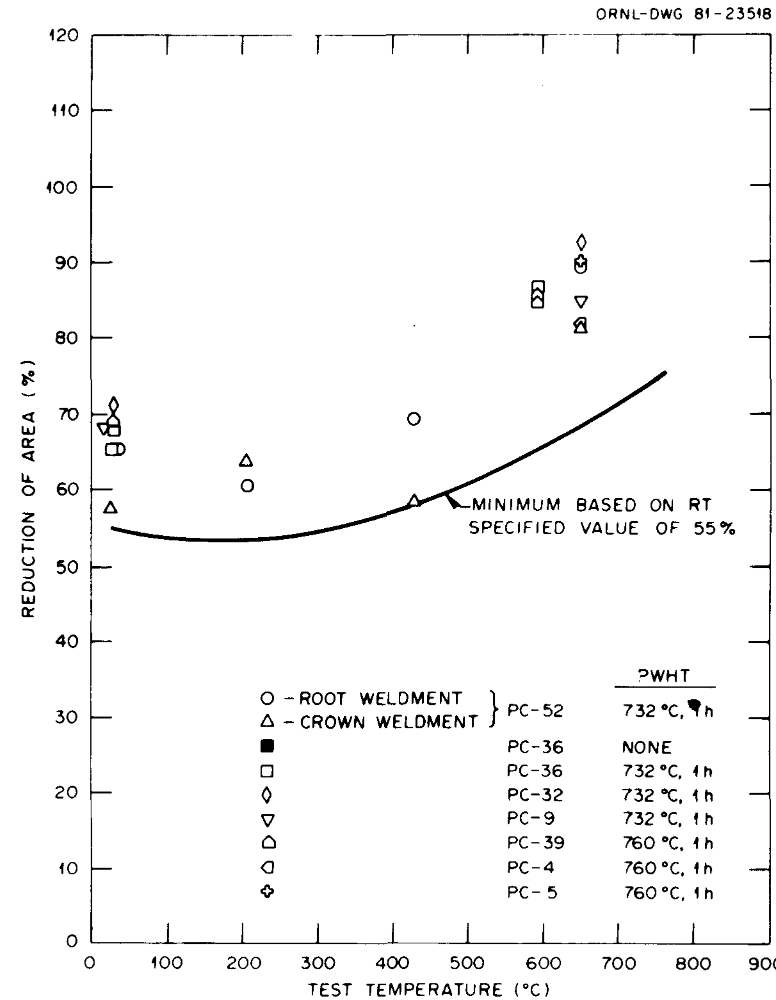

Fig. 1.69. Reduction of area values for various weldments of modified 9 Cr-1 Mo steel are on or above the minimum curve for the base metal.

2. The ultimate tensile strength data for various weldments match the average curve observed for the base metal.

3. The total elongation values for various weldments fall below the minimum value for the base metal. However, the weldment values are still about 10% or more for the entire temperature range.

4. The reduction of area values for various weldments of modified 9 Cr-1 Mo steel are on or above the minimum curve for the base metal.

Creep data on tests ruptured thus far and tests in progress are compared with the average and average — 1.65 SEE (standard error of estimate) stress rupture curves for the base metal in Figs. 1.70 through 1.72. These figures show that the rupture times for weldment tests fall between the average and average — 1.65 SEE for the base metal. At 593°C, the weldment data are closer to the average, but at 649°C they are closer to the average — 1.65 SEE curve. Data plotted here are for weldments in the as-welded and PWHT conditions and for various filler wires. Rupture in all cases was within the HAZ. Several long-term tests are in progress, and we expect that for them the rupture time will approach the base metal average values. This approach is expected because during the long-term tests the base metal, HAZ, and weld metal properties tend to equalize.

Charpy V-notch (C_V) impact properties have been determined for weld metals from the various heats of filler metals and for different heat treatments. Figure 1.73 shows the effect of PWHT on the C_V impact energy of weld metal from filler wire of heat 30394. Also, the silicon content in the weld deposit had an effect on the impact properties, as shown in Fig. 1.74, with lower silicon being beneficial. Weld PC-49 was made with the GTA process using standard 9 Cr-1 Mo filler metal, as shown in Table 1.33. After welding, the weldment received a PWHT of 732°C for 1 h. The C_V toughness of the weld deposit was determined and compared with the modified-composition weld deposit data. The results are plotted in Fig. 1.75, which also shows the effect of specimen location within the weld. The C_V toughness of the standard composition weld metal is very similar to that of the modified composition.

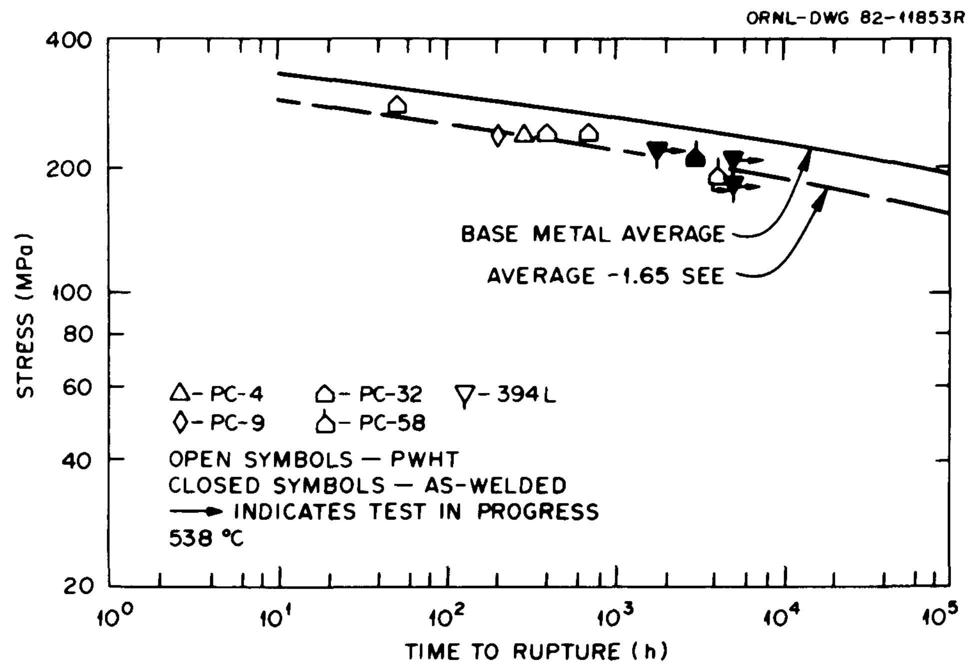

Fig. 1.70. Comparison of creep-rupture lives of modified 9 Cr-1 Mo steel weldments at 538°C with the average and average — 1.65 SEE rupture strength values for the base metal.

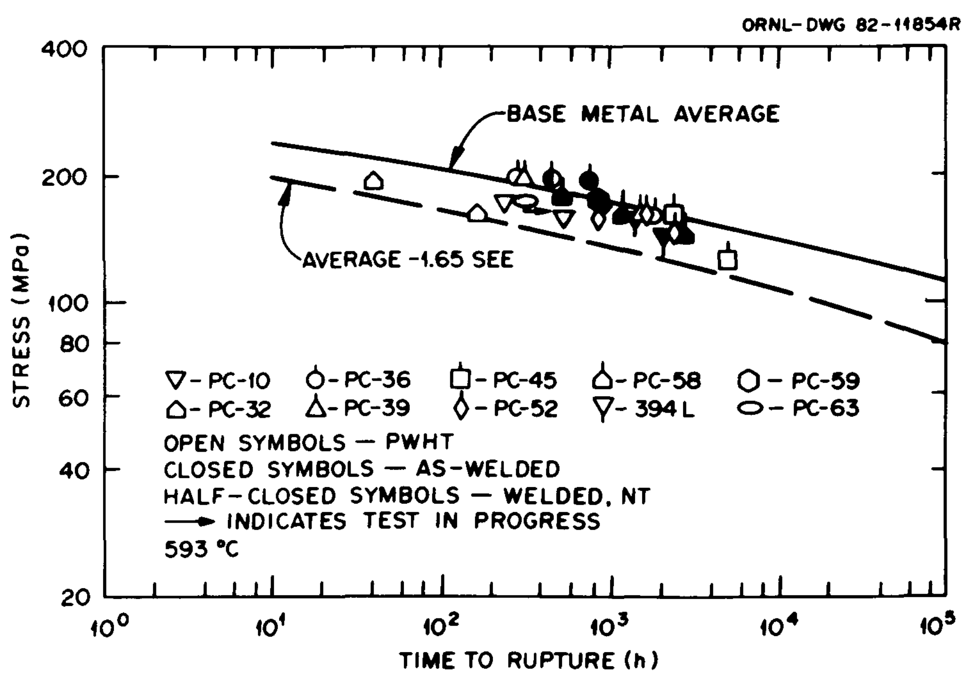

Fig. 1.71. Comparison of creep-rupture lives of modified 9 Cr-1 Mo steel weldments at 593°C with the average and average — 1.65 SEE rupture strength values for the base metal.

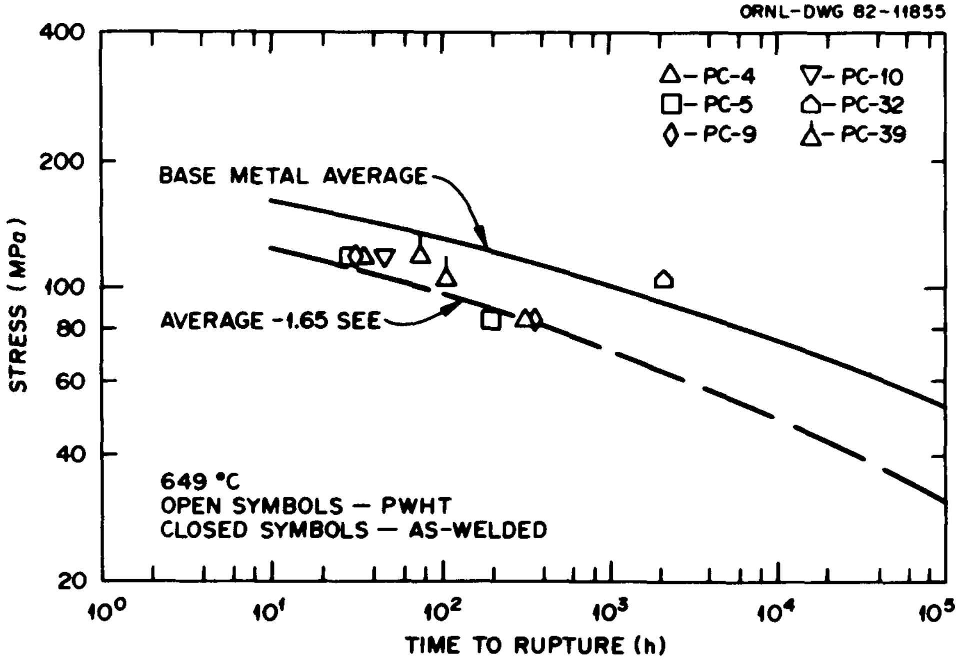

Fig. 1.72. Comparison of creep-rupture lives of modified 9 Cr-1 Mo steel weldments at 649°C with the average and average — 1.65 SEE rupture values for the base metal.

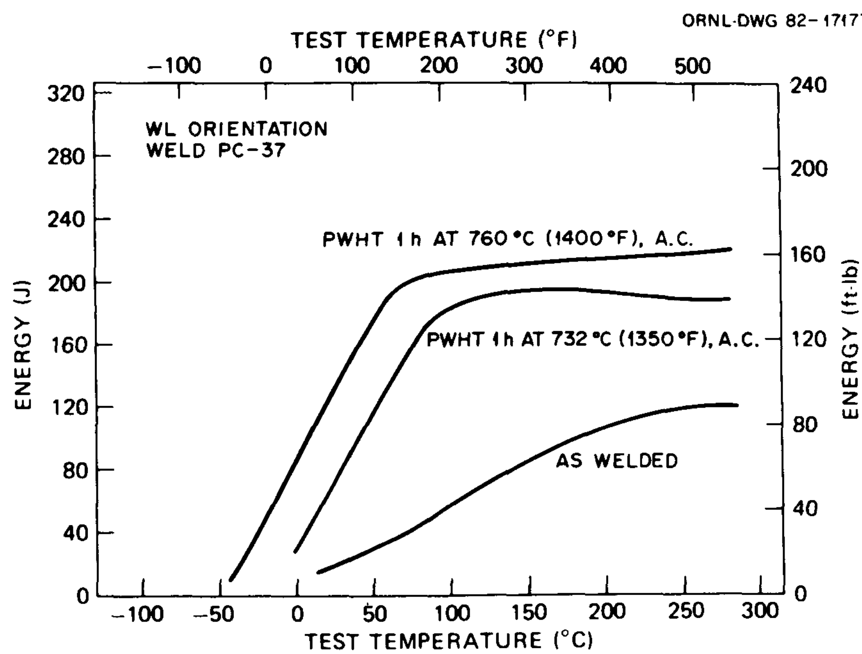

Fig. 1.73. Effect of postweld heat treatment on the Charpy-V impact energy of gas tungsten arc weld metal deposit from filler wire heat 30394.

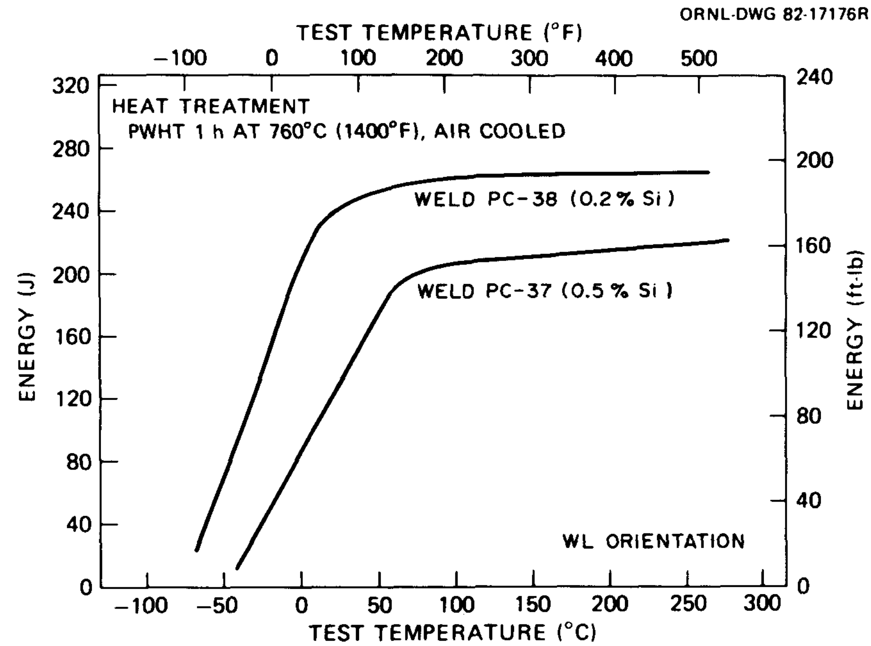

Fig. 1.74. Effect of silicon content on the Charpy-V impact energy of gas tungsten arc weld deposits.

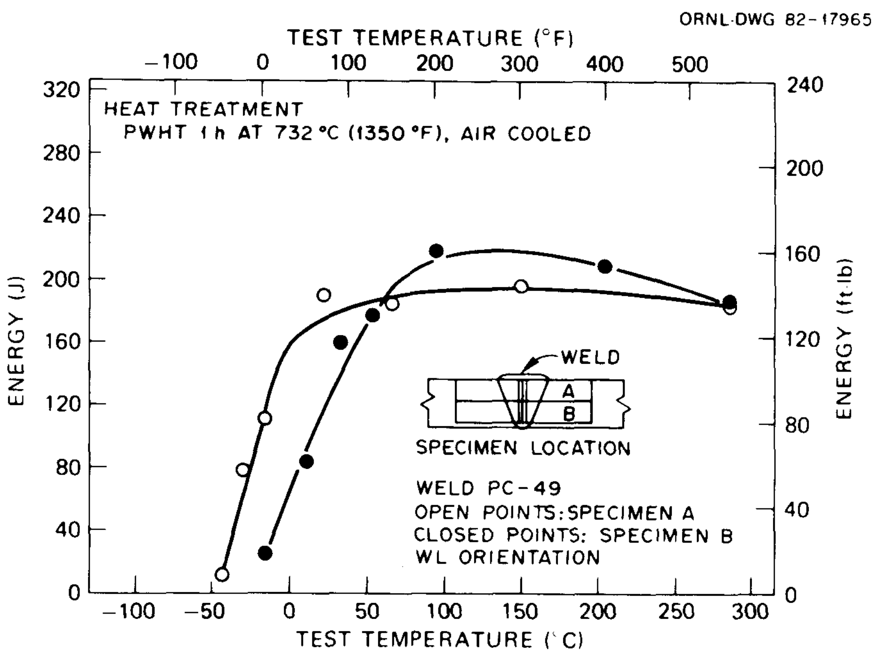

Fig. 1.75. Effect of depth in weld metal from a standard 9 Cr-1 Mo gas tungsten arc weld in 27-mm (1 1/16-in.) plate welded with Johnston type ER505 filler metal and postweld heat-treated 1 h at 732°C (1350°F).

1.8.2 Shielded Metal Arc Welding

Shielded metal arc weldments have been made in modified 9 Cr-1 Mo in both tubing and plate. Only limited work has been conducted at ORNL with this process, but additional electrodes have been received for evaluation. The weldments and deposit compositions currently in test are listed in Table 1.34. Weldments PC-63 and PC-64 were made in 76-mm-OD by 48-mm-ID tubing from Sumitomo heat YYC-9826 and are shown in Fig. 1.76. These weldments, made with a GTA root pass and an SMA fill pass, have the cross-sectional appearance shown in Fig. 1.77. Weldment PC-67 was made in flat plate but has the same general appearance.

Transverse test specimens were obtained from these weldments for mechanical property testing after a PWHT of 732°C for 1 h. Creep testing is in progress. Tensile test results have shown that the yield strength data and ultimate tensile strength data match the average curve observed for the base metal (Figs. 1.78 and 1.79).

Table 1.34. Shielded metal arc weld metal chemical analyses

Element	Content (wt%) for each electrode lot (weld No.)		
	CAOIG(PC-63)	8N9AMix19(PC-64)	8N20AMix24(PC-67)
C	0.052	0.089	0.078
Mn	0.62	0.75	0.69
P	0.005	0.011	0.015
S	0.007	0.011	0.006
Si	0.14	0.25	0.29
Ni	<0.01	0.06	0.07
Cr	9.27	8.05	8.10
Mo	0.87	0.97	0.97
V	0.03		
Cu	0.05		

Y-186114

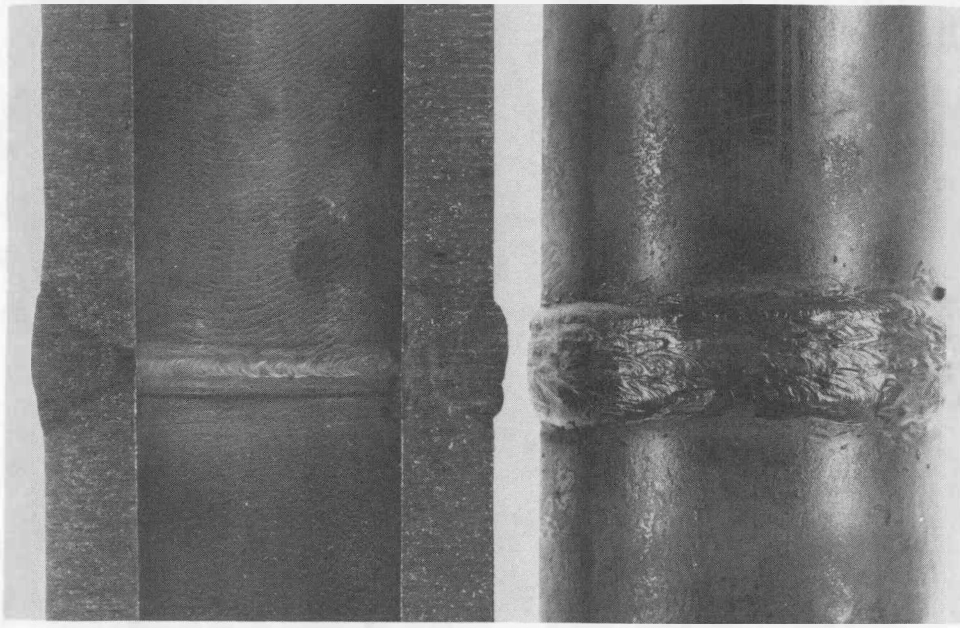

Fig. 1.76. Shielded metal arc weldment in modified 9 Cr-1 Mo steel 76-mm-OD tubing.

Y-186051

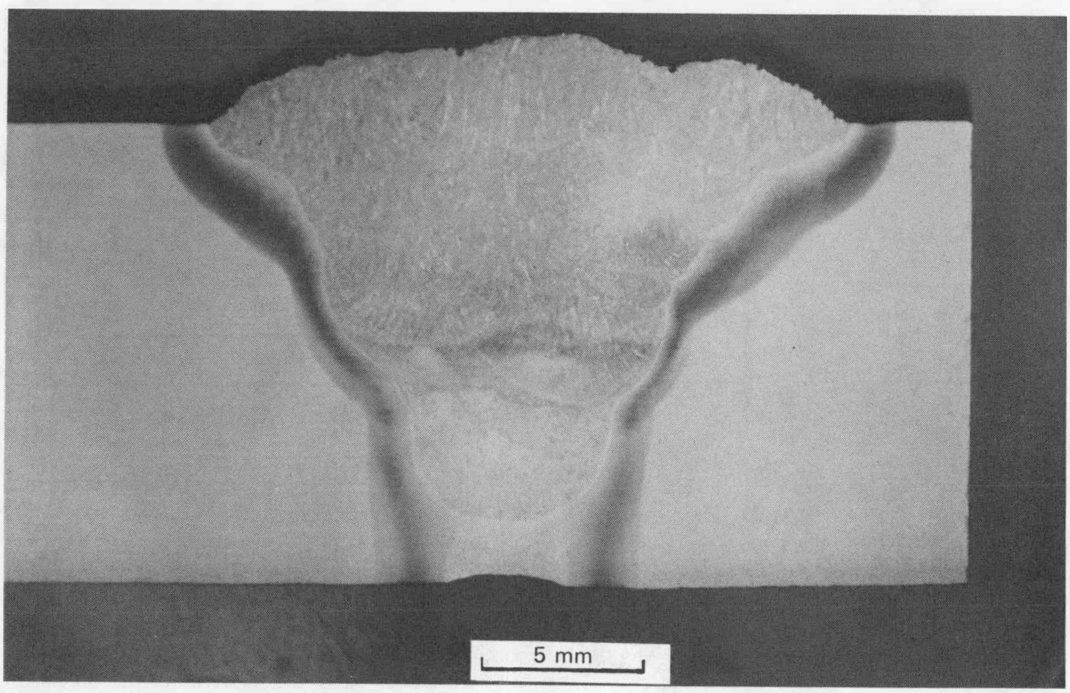

Fig. 1.77. Cross-sectional view of shielded metal arc tube weld.

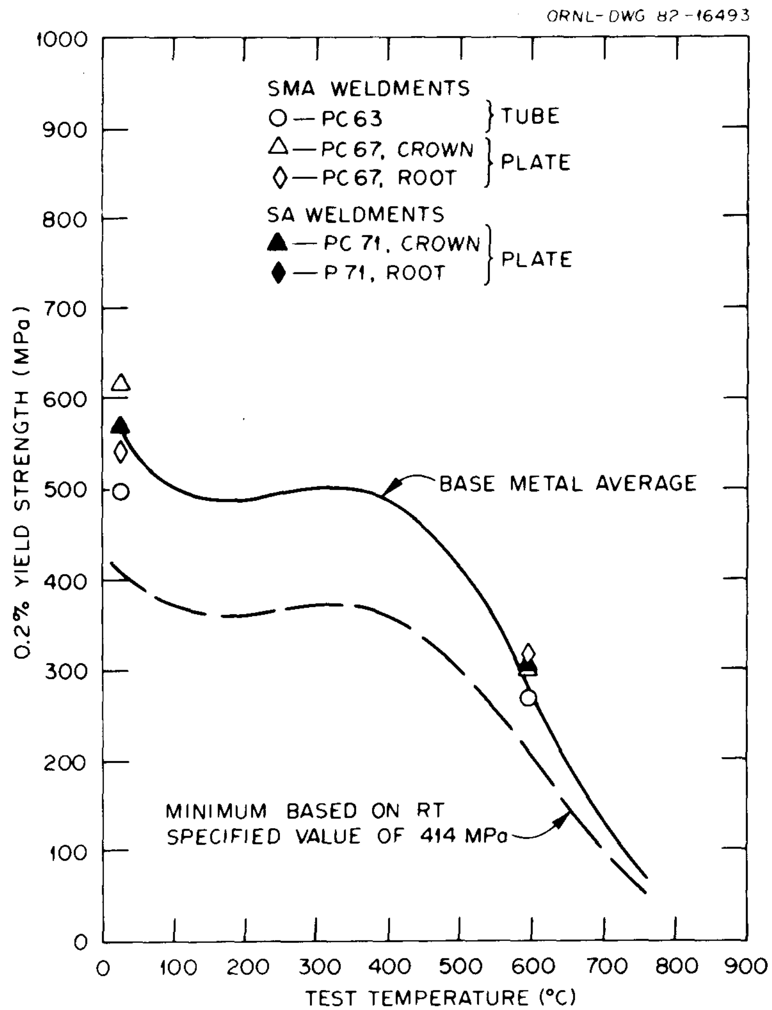

Fig. 1.78. Yield strength data for various shielded metal arc and submerged arc weldments of modified 9 Cr-1 Mo steel match the average curve observed for the base metal data.

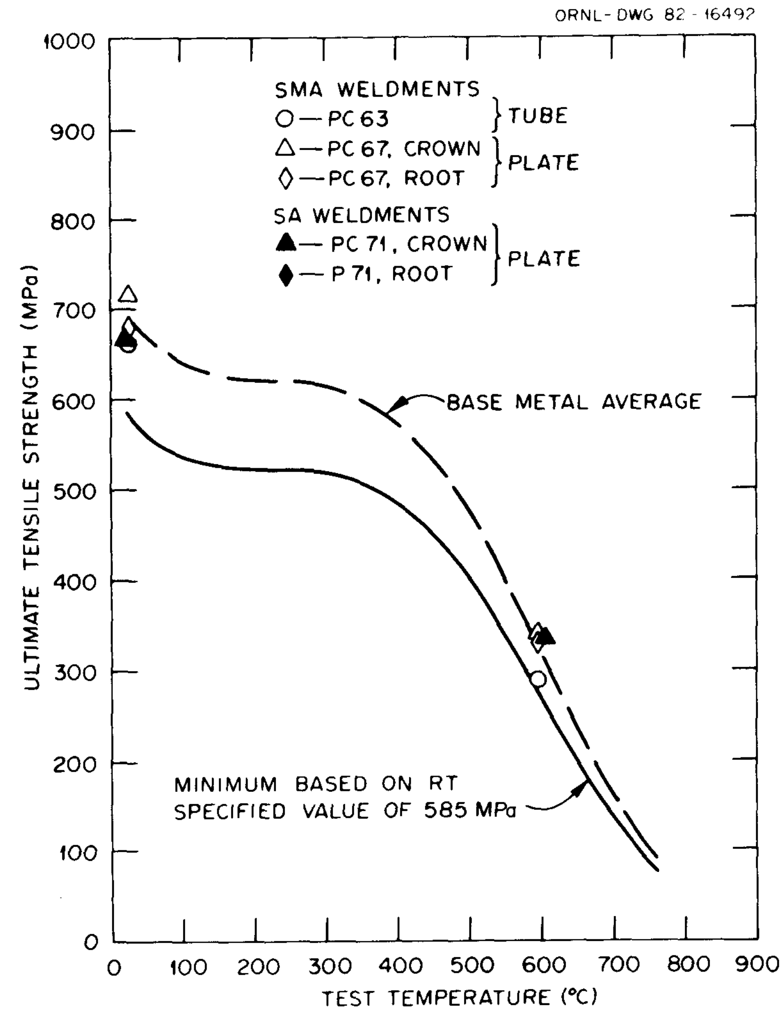

Fig. 1.79. Ultimate tensile strength data for shielded metal arc and submerged arc weldments of modified 9 Cr-1 Mo steel match the average curve observed for the base metal data.

The C_V toughness was determined for the SMA welds PC-64 and PC-67. Weld PC-64 was the SMA weld in the Japanese-fabricated tubing (Sumitomo heat YYC-9826). Standard composition E505 electrodes were used for this weld, which was given a PWHT of 732°C for 1 h before testing. We used AC-oriented specimens [specimen length parallel to the axial direction (A); fracture in the circumferential direction (C)]. The C_V toughness results for the weld metal are listed in Table 1.35 and plotted in Fig. 1.80. Weldment PC-67, a flat plate weldment, was tested both as welded and after a PWHT. Test results from the WL-oriented C_V weld metal specimens are also listed in Table 1.35 and are plotted in Fig. 1.81. The C_V toughness of the as-welded weld metal was poor, with a maximum upper-shelf energy of 46 J (34 ft-lb) at 260°C (500°F) in the temperature range examined (–18 to 288°C). The as-welded results are plotted as a band to include the scatter in C_V toughness results. The differences between the two depth positions examined was minimal. The PWHT improved the toughness, especially in the weld metal near the crown of the weld (position A). The upper-shelf energy in both welds (PC-64 and PC-67) is much less than that of the GTA weld deposits, but the development of improved electrodes is under way.

1.8.3 Submerged Arc Welding

Submerged arc welding in the modified 9 Cr-1 Mo alloy has been conducted in 27- and 50-mm-thick plates as shown in Fig. 1.82. These weldments have been made with various heat inputs and Oerlikon OP-76 flux. This flux is a basic agglomerated flux and has been found to provide excellent element transfer from the filler wire to the deposit, as shown in Table 1.36. Weldments have been produced with heat inputs ranging from 3 to 1.85 kJ/mm (Fig. 1.83). These weldments contain both standard

Table 1.35. Summary of Charpy-V toughness of several welds in modified 9 Cr-1 Mo steel plate

Depth location[a]	Temperature [°C (°F)]: 68-J (50-ft-lb) energy	0.89-mm (35-mil) Lateral expansion	50% Shear	100% Shear[b]	Upper-shelf energy at 121°C (250°F): (J)	(ft-lb)
	Weld PC-49 (gas tungsten arc)					
0.24	-29(-20)	-29(-20)	-9(15)	27(80)	197	145
0.76	2(35)	2(35)	24(75)	66(150)	218	160
	Weld PC-46 (shielded metal arc)					
0.5[c]	27(80)	16(60)	21(70)	43(110)	106	78
	Weld PC-64 (shielded metal arc)					
0.24	21(70)	16(60)	27(80)	77(170)	106	78
0.76	74(165)	63(145)	49(120)	82(180)	84	62
	Weld PC-70 (submerged arc)					
0.24	-9(15)	-7(20)	2(35)	27(80)	201	148
0.76	-1(30)	4(40)	10(50)	32(90)	196	124

[a]Fraction of thickness from crown of weld.

[b]Estimated temperature.

[c]Weld in 72-mm-OD by 48-mm-ID tubing; remainder of welds in 27-mm-thick plate.

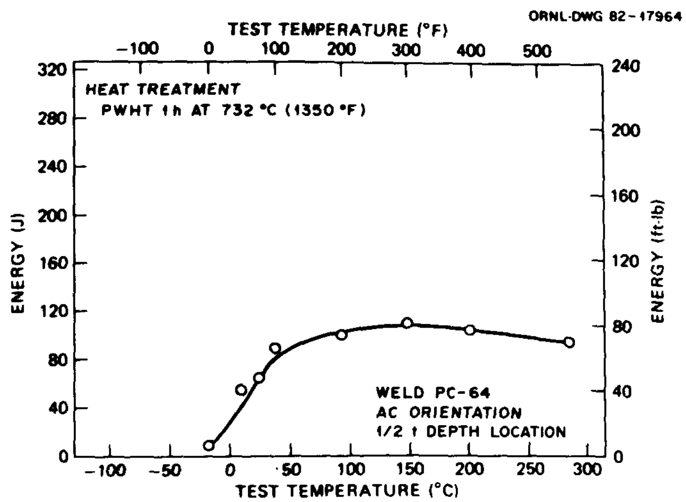

Fig. 1.80. Charpy-V impact properties of weld metal from a shielded metal arc weld in a 72-mm-OD by 48-mm-ID (3-by 1 7/8-in.) modified 9 Cr-1 Mo steel tube. Sumitomo heat YYC-9826, welded with standard 9 Cr-1 Mo electrodes and postweld heat treated 1 h at 732°C.

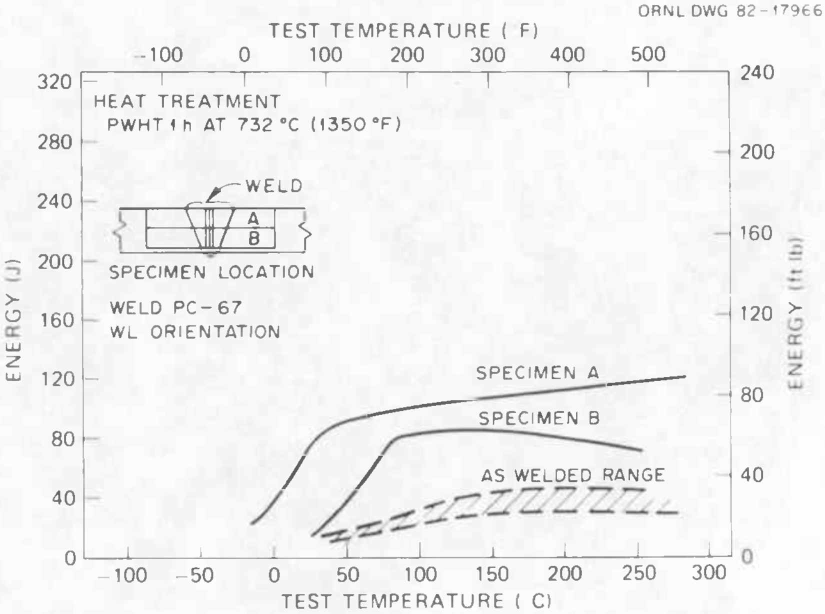

Fig. 1.81. Effect of depth and postweld heat treatment on the Charpy-V impact energy of weld metal from a shielded metal arc weld in 27-mm-thick (1 1/16-in.) modified 9 Cr-1 Mo plate, welded with standard 9 Cr-1 Mo electrodes and postweld heat-treated 1 h at 732°C.

Y-186625

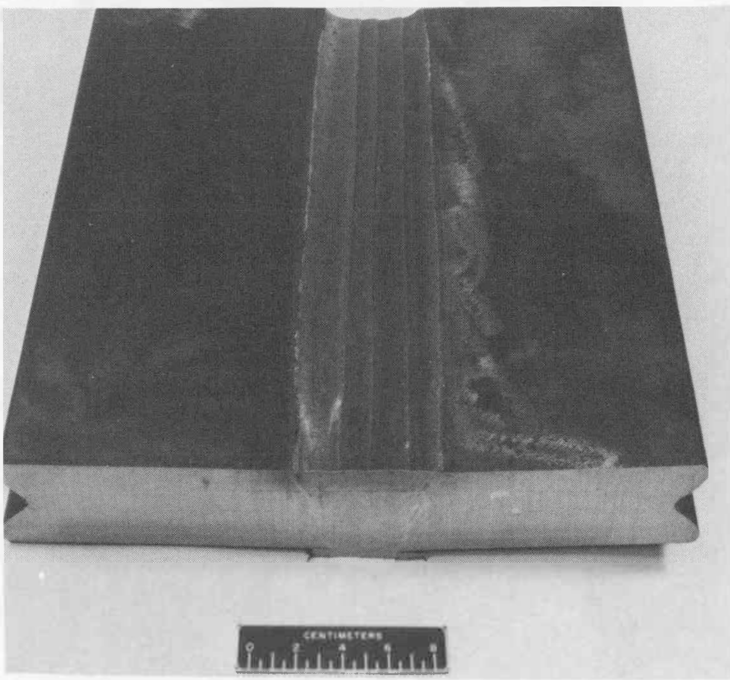

Fig. 1.82. Submerged arc weldment in 50-mm-thick plate of modified 9 Cr-1 Mo steel.

Y-186886

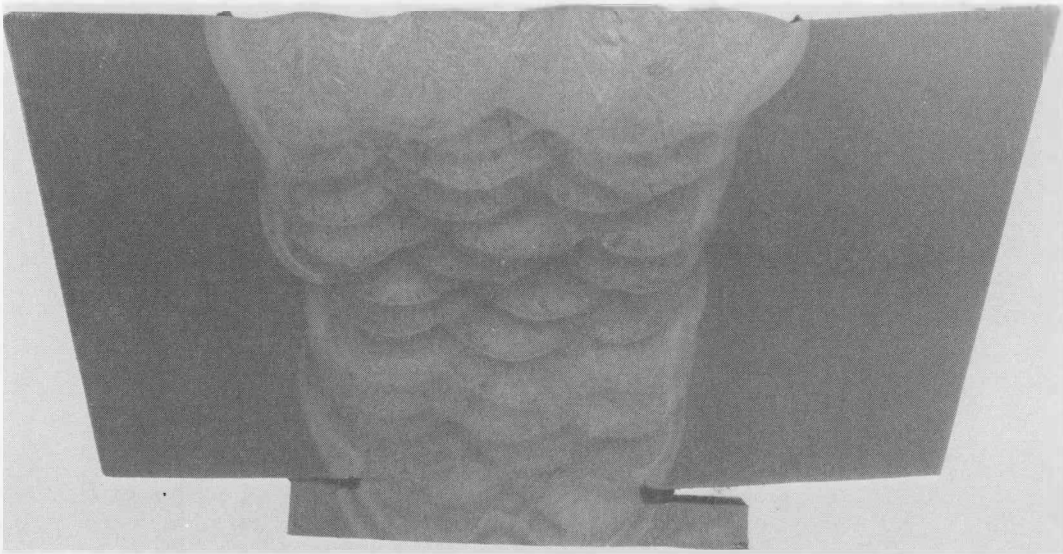

(a)

Y-186885

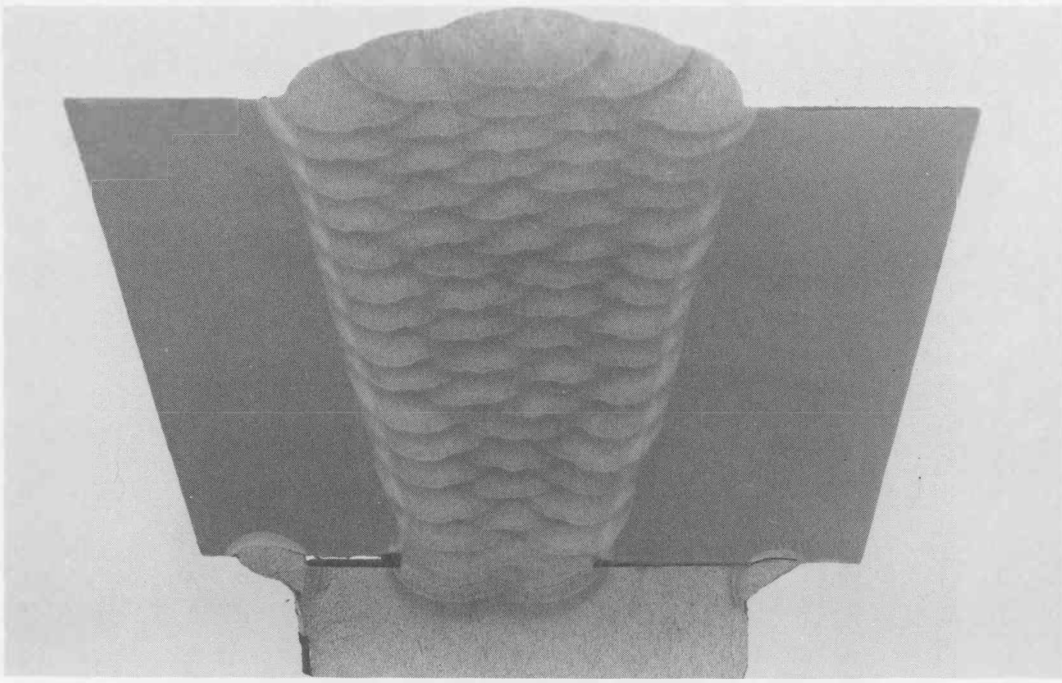

(b)

20 mm

Fig. 1.83. Cross section of submerged arc weldment in 50-mm-thick plate. (*a*) Made with a heat input of 3 kJ/mm. (*b*) Made with a heat input of 1.85 kJ/mm at Combustion Engineering, Inc.

Table 1.36. Chemical analyses of E505 filler metal and submerged arc weld deposit made with Oerlikon OP-76 flux

Element	ER505 vendor analysis	Weld deposit PC-77
C	0.08	0.082
Mn	0.51	0.54
P	0.030	0.008
S	0.019	0.008
Si	0.34	0.35
Ni	0.19	0.08
Cr	8.94	8.69
Mo	0.98	0.99
V		0.005
Nb		0.006
Ti		0.002
Co		0.025
Cu	0.06	0.04
Al		0.006
B		<0.01
W		<0.01
As		0.003
Zr		<0.001
N		0.019
Sn		0.002

composition and modified composition weld metals and are to be creep and tensile tested. Some of the first tensile results are compared with results on SMA weld metals in Figs. 1.78 and 1.79.

Weldment PC-70 is a submerged arc weld deposit made in 27-mm-thick plate with ER505 filler metal and OP-76 flux. Charpy-V impact properties of the weld metal were determined with WL-oriented specimens from two depths and in two weld conditions, as welded and PWHT. The C_V weld metal toughness results are reported in Table 1.35 and plotted in Fig. 1.84. The as-welded results are poor and similar to those for the shielded metal arc weld, but the 732°C PWHT resulted in a considerable improvement in toughness. Location in the weld has little effect on the C_V toughness in the transition region, but the upper-shelf energies near the crown of the weld are superior to the results obtained nearer the root.

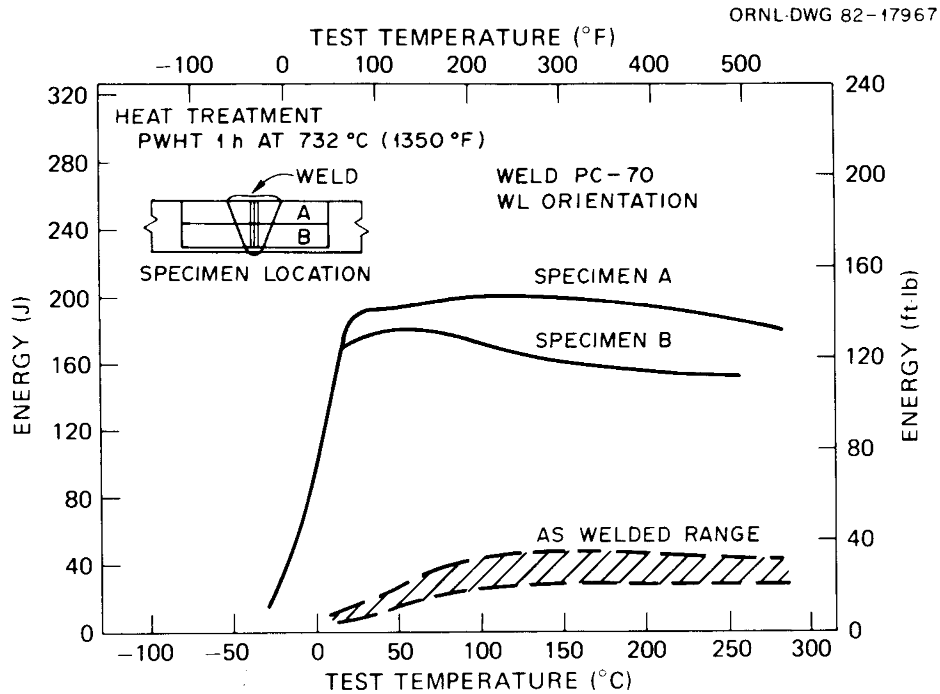

Fig. 1.84. Effect of depth and postweld heat treatment on the Charpy-V impact energy of weld metal from a submerged arc weld in 27-mm-thick (1 1/16-in.) modified 9 Cr-1 Mo steel plate welded with standard 9 Cr-1 Mo filler wire and postweld heat-treated 1 h at 732°C.

1.8.4 Discussion

The welding development program for modified 9 Cr-1 Mo has been examining three processes: GTA, SMA, and SA. We are evaluating the weldments by tensile, creep, and C_V toughness testing. Our goal is to achieve weldment properties that match or exceed the average base metal properties for tensile and creep testing. A tentative goal for the C_V toughness of weld metal is to achieve 68-J (50 ft-lb) energy at or below room temperature. Various weldments and weld metals from the three processes have been evaluated.

Gas tungsten arc weldments and weld metals appear to meet the mechanical property criteria for filler metals of both standard and modified composition. Longer term creep-rupture testing will determine if the standard-composition filler wire is satisfactory. The modified-composition GTA weld metal appears to be much stronger than the base metal. Such a strength is known to adversely affect weldment properties and indicates that a lower strength modified composition will be needed if the standard composition is found to be inadequate. A lower carbon content than the modified 9 Cr-1 Mo base metal specification should reduce the weld metal strength.

Limited testing at ORNL has been performed on SMA weldments of 9 Cr-1 Mo. Tensile test results have shown that the yield strength data and ultimate tensile strength data match the average curve observed for the base metal. Creep testing is in progress at this time. The Charpy V-notch toughness data show that this process produced weld metal with much lower values of upper-shelf energy than did the GTA process. Development of electrodes is under way to improve the weld metal toughness.

Similar to the SMA process, work on the SA process is still in the early stages of testing. Numerous weldments have been made in 27- and 50-mm-thick plate. Testing is under way to find the tensile and creep properties of these weldments. We have found that Oerlikon OP-76 flux provides excellent element transfer from the filler wire to the deposit. It also has good operating characteristics and easy slag removal. The C_V toughness of weld metal from tests to date show that it is similar to the GTA weld metal after both have been postweld heat-treated.

1.9 Design Methods

G. T. Yahr, R. C. Gwaltney,
R. L. Battiste, and D. N. Robinson

A benchmark test on a simply supported modified 9 Cr-1 Mo beam at a temperature of 593°C (1100°F) was reported previously.[7] Analytical predictions from an inelastic structural analysis performed with the finite-element program ADINA[8] were judged to be in reasonable agreement with the experimental results for the deformation-controlled test of the beam.

However, the analytical results showed less plasticity than the experimental results during loading. Subsequent investigation revealed a problem in the implementation of the Robinson nonlinear plasticity model.[9] This has now been corrected, and the 9 Cr-1 Mo beam test is being reanalyzed for comparison with experimental results. Early indications point to a very good comparison between predicted and observed behavior. A topical report is being prepared on the experimental and analytical results.[10]

1.10 References

1. V. K. Sikka, R. E. McDonald, and G. C. Bodine, "Material Procurement and Processing," *Advanced Alloy Technology Program Semiannu. Prog. Rep. Mar. 31, 1982*, ORNL/MSP/1.7-82/1, Oak Ridge National Laboratory, Oak Ridge, Tenn., pp. 1-1–4.
2. R. R. Irving, "What's this steel they're raving about down in Tennessee?," *Iron Age* 225(18), 46–50 (June 25, 1982).
3. W. J. Stelzman and R. K. Nanstad, "Charpy V-Notch Toughness Studies," *Advanced Alloy Technology Program Semiannu. Prog. Rep. Mar. 31, 1982*, ORNL/MSP/1.7-82/1, Oak Ridge National Laboratory, Oak Ridge, Tenn., pp. 1-79–98.
4. W. J. Stelzman and R. K. Nanstad, "Charpy V-Notch Toughness Studies," *Advanced Alloy Technology Program Semiannu. Prog. Rep. Sept. 30, 1981*, ORNL/MSP/1.7-81/3, Oak Ridge National Laboratory, Oak Ridge, Tenn., pp. 2-58–70.
5. W. J. Stelzman and D. A. Canonico, "Charpy V-Notch Toughness Studies," *Advanced Alloy Technology Program Semiannu. Prog. Rep. Mar. 31, 1981*, ORNL/MSP/1.7-81/1, Oak Ridge National Laboratory, Oak Ridge, Tenn., pp. 2-135–149.
6. D. A. Canonico and W. J. Stelzman, "Charpy V-Notch Toughness Studies," *Modified 9 Cr-1 Mo Steel Development Program Prog. Rep. Mar. 31, 1979*, ORNL/BRP-79/4, Oak Ridge National Laboratory, Oak Ridge, Tenn., pp. 2.74.

7. G. T. Yahr et al., "Beam Test," *Advanced Alloy Technology Program Semiannu. Prog. Rep. Sept. 30, 1981*, ORNL/MSP/1.7-81/3, Oak Ridge National Laboratory, Oak Ridge, Tenn., pp. 2-75–79.

8. Klaus-Jürgen Bathe, *Static and Dynamic Geometric and Mathematical Nonlinear Analysis Using ADINA*, Report 82448-2, Massachusetts Institute of Technology, Cambridge, May 1976.

9. D. N. Robinson, *A Nonlinear Plasticity Model for Structural Alloys at Elevated Temperatures*, ORNL/TM-6582, Oak Ridge National Laboratory, Oak Ridge, Tenn., November 1978.

10. R. C. Gwaltney et al., *Elevated Temperature Deflection Controlled Test of Modified 9 Cr-1 Mo Beam*, ORNL/TM-8254, Oak Ridge National Laboratory, Oak Ridge, Tenn., to be published.

2. COMBUSTION ENGINEERING, INC.

G. C. Bodine

2.1 Introduction

The status and progress of work conducted by Combustion Engineering, INc. (C-E) Metallurgical and Materials Laboratory (MML) for FY 1982 is described in the following sections. Work represents that subcontracted to C-E as part of the ORNL modified 9Cr-1Mo alloy steel development program.

2.2 Material Examination and Testing

Optical metallographic examination was made by MML on specimens prepared from:

a. 54 mm O.D. x 9.5 mm W.T. hot extruded/cold finished/normalized and tempered T.I. Stainless Ltd. tubing, AOD/ESR heat 10148.
b. 51 mm O.D. x 6.4 mm W.T. cold finished/normalized and tempered NKK tubing, VIM heat 59020.
c. 51 mm O.D. x 6.4 mm W.T. cold finished/normalized and tempered Sumitomo tubing, VIM heat VF0028.
d. 76.2 mm O.D. x 12.7 mm W.T. cold finished/normalized and tempered Sumitomo VIM heat VF0028.
e. 45 mm O.D. x 12.7 MM W.T. cold finished/normalized and tempered Sumitomo EF/VOD heat A231001.

Representative micrographs are shown in Figs. 2.1 through 2.7.

MML tensile testing included specimens prepared from:

a. 51 mm O.D. x 6.4 MM W.T. cold finished/normalized and tempered tubing, NKK VIM heat 59020. (full section tests)
b. 51 mm O.D. x 6.4 mm W.T. cold finished/normalized and tempered tubing, Sumitomo VIM heat VF0028. (full section tests)

O.D. Area BHN 228 (R_B95/98)

Midwall Area BHN 228 (R_B95/98)

I.D. Area BHN 228 (R_B95/98)

Fig. 2.1. Micrographs at 500X, Modified 9Cr-1Mo alloy steel, hot extruded (T.I. Chesterfield) and annealed 760/788C 1 hour at heat, furnace cool. 47.6 mm I.D. x 15.9 mm W.T., Heat No. 10148R4, AOD/ESR. Longitudinal Section (HCl/picric etch)

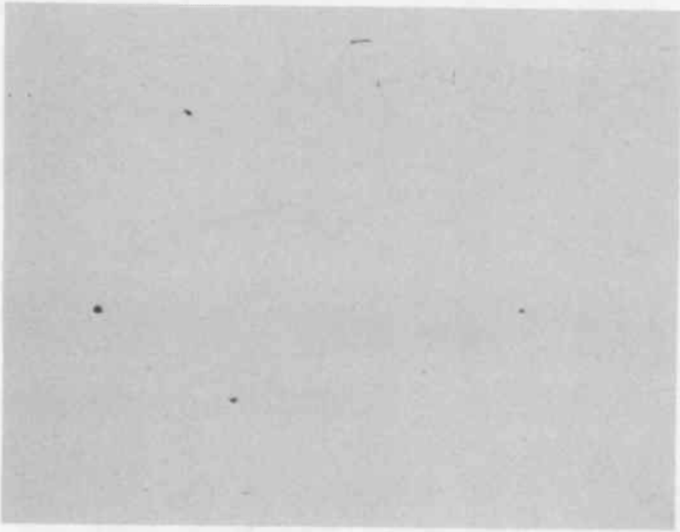

100X

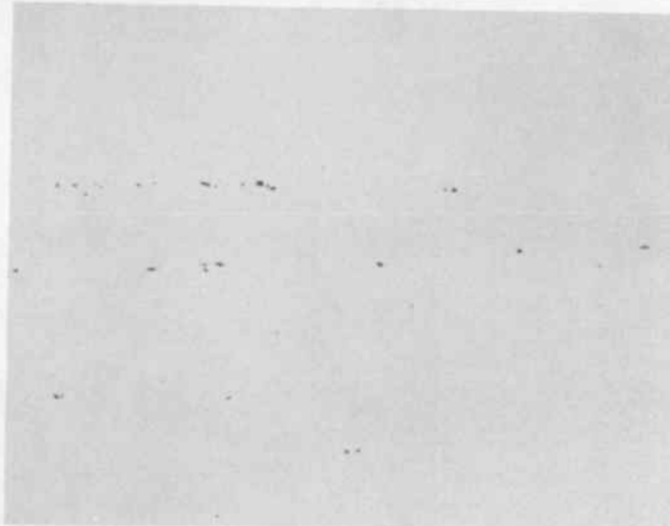

100X

500X

Fig. 2.2. Micrographs, longitudinal section, 51 mm (2") O.D. x 6.4 mm (.250") W.T., modified 9Cr-1Mo alloy steel tubing, NKK Heat No. 59020 Vac. induction melt. As-polished condition showing typical micro-cleanliness.

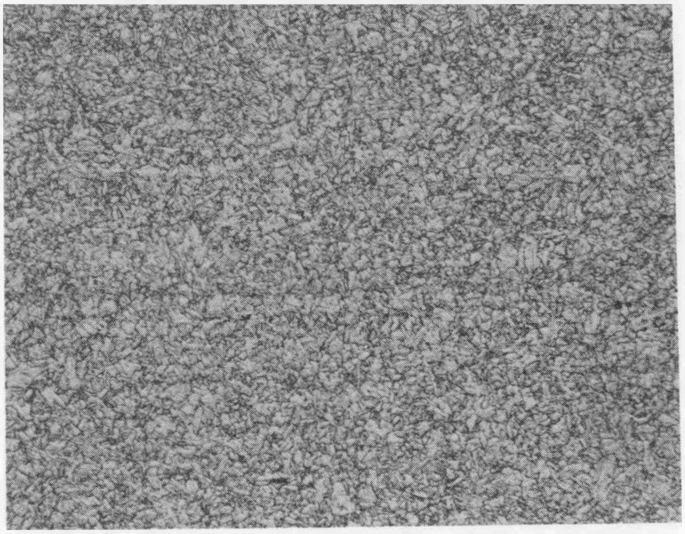

100X

500X

Fig. 2.3. Micrographs, longitudinal section, 51 mm (2") O.D. x 6.4 mm (0.250") W.T., modified 9Cr-1Mo alloy steel tubing, normalized 1038C 1 hour/tempered 760C 1 hour, NKK Heat No. 59020, vac. induction melt (HCl/picric etch) 608.7/619.8 MPa 0.5% y.s., 731/740.4 MPa U.T.S., 29% E 51 mm.

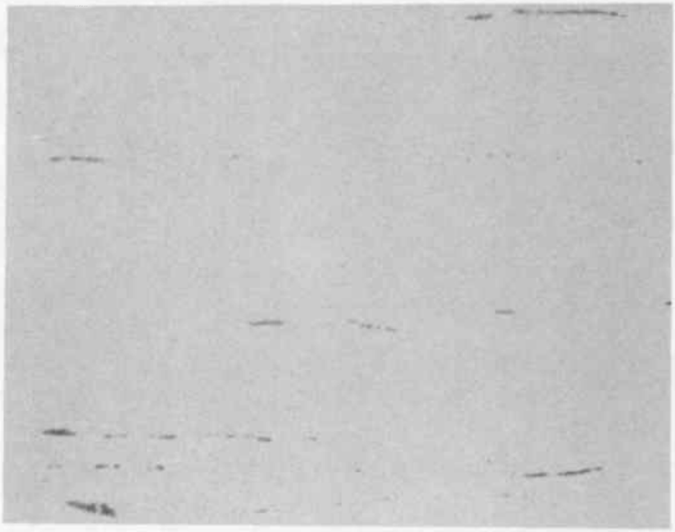

(a)

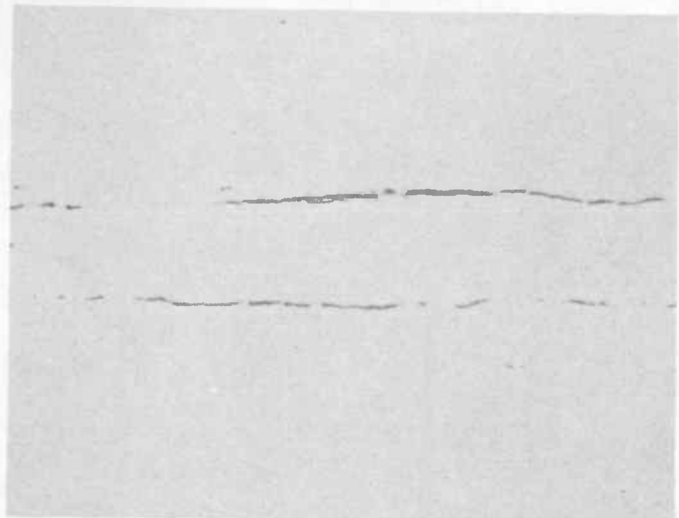

(b)

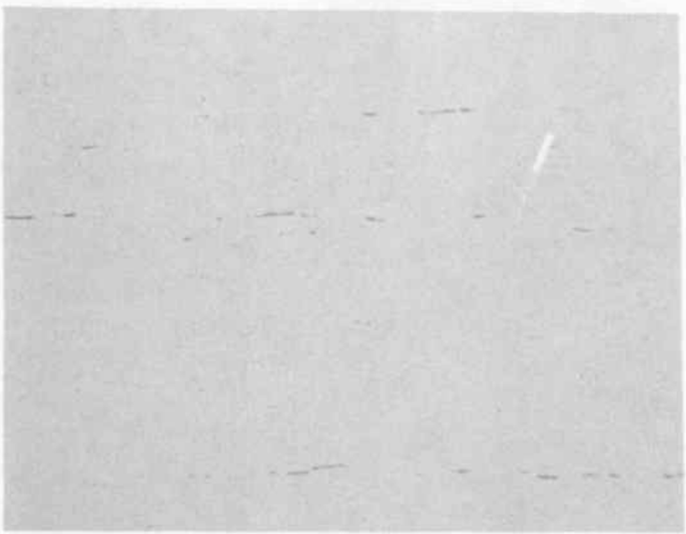

(c)

Fig. 2.4. Micrographs at 500X, longitudinal section, as-polished, showing typical inclusion type/distribution. Modified 9Cr-1Mo alloy, Sumitomo vac. induction Heat No. VF0028 (a), (b) 76.2 mm (3") O.D. x 12.7 mm (.5") W.T. tubing, (c) 50.8 mm (2") O.D. x 6.4 mm (.25") W.T. tubing.

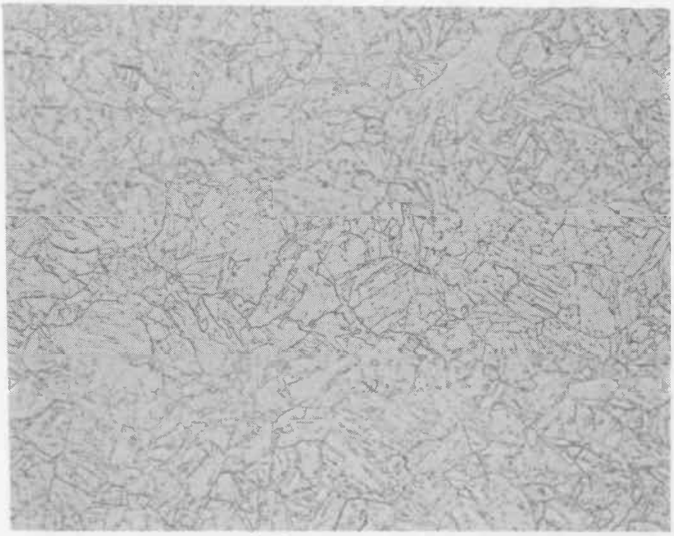

(a)

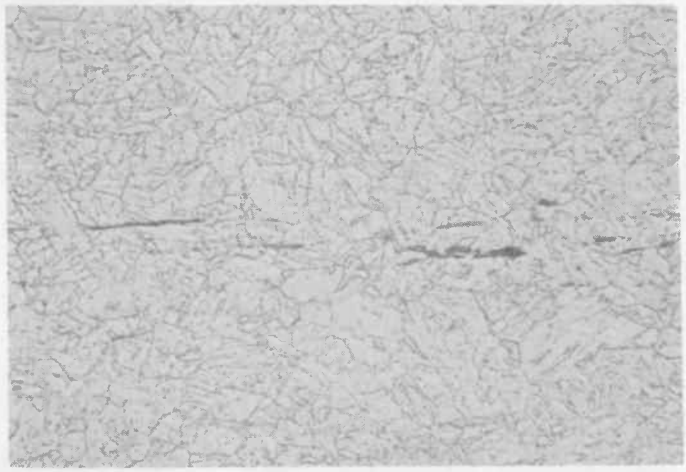

(b)

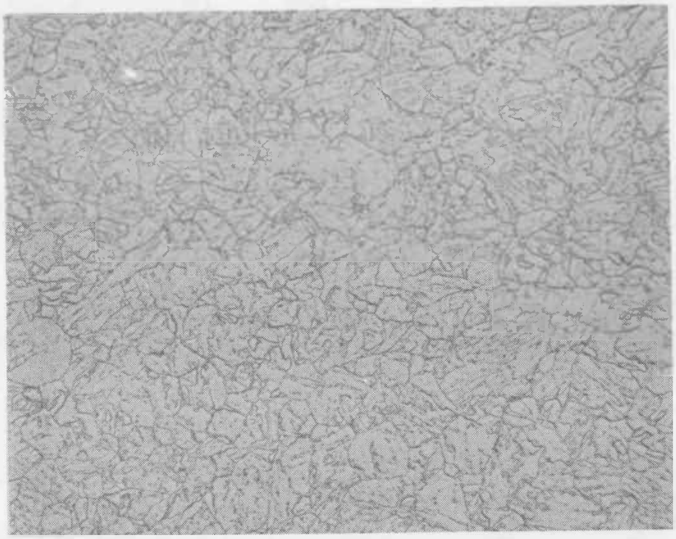

(c)

Fig. 2.5. Micrographs at 500X, longitudinal section, HCl/picric etch, showing microstructure. Modified 9Cr-1Mo alloy tubing, Sumitomo vac. induction Heat No. VF0028. Normalized 1040 C 1 hour and tempered 780 C 1 hour AC. (a) (b) 76.2 mm (3") O.D. x 12.7 mm (.5") W.T. (c) 50.8 mm (2") O.D. x 6.4 mm (.25") W. T.

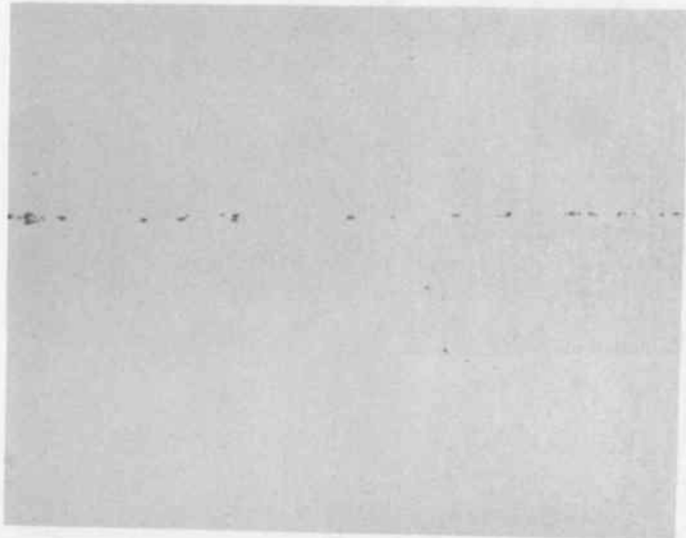

100X

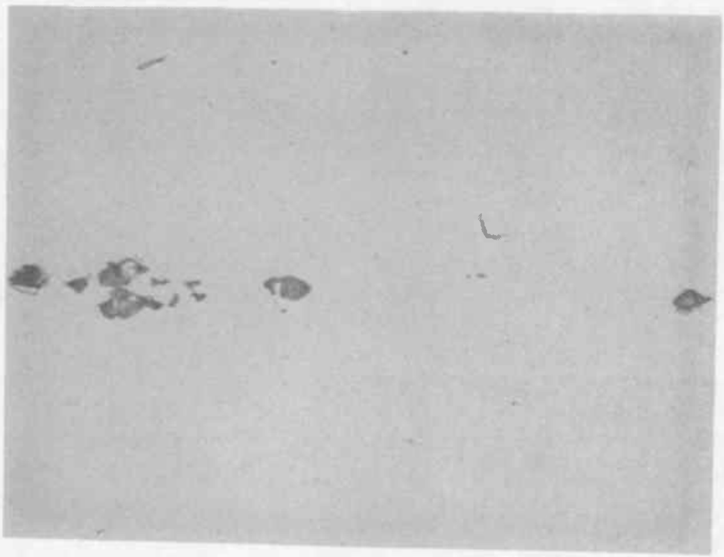

500X

Fig. 2.6. Micrographs, longitudinal section, as-polished, showing inclusion type distribution, 42 mm (1.65") O.D. x 12.7 mm (.5") W.T. modified 9Cr-1Mo alloy steel tubing, Sumitomo EF/VOD Heat No. A231001.

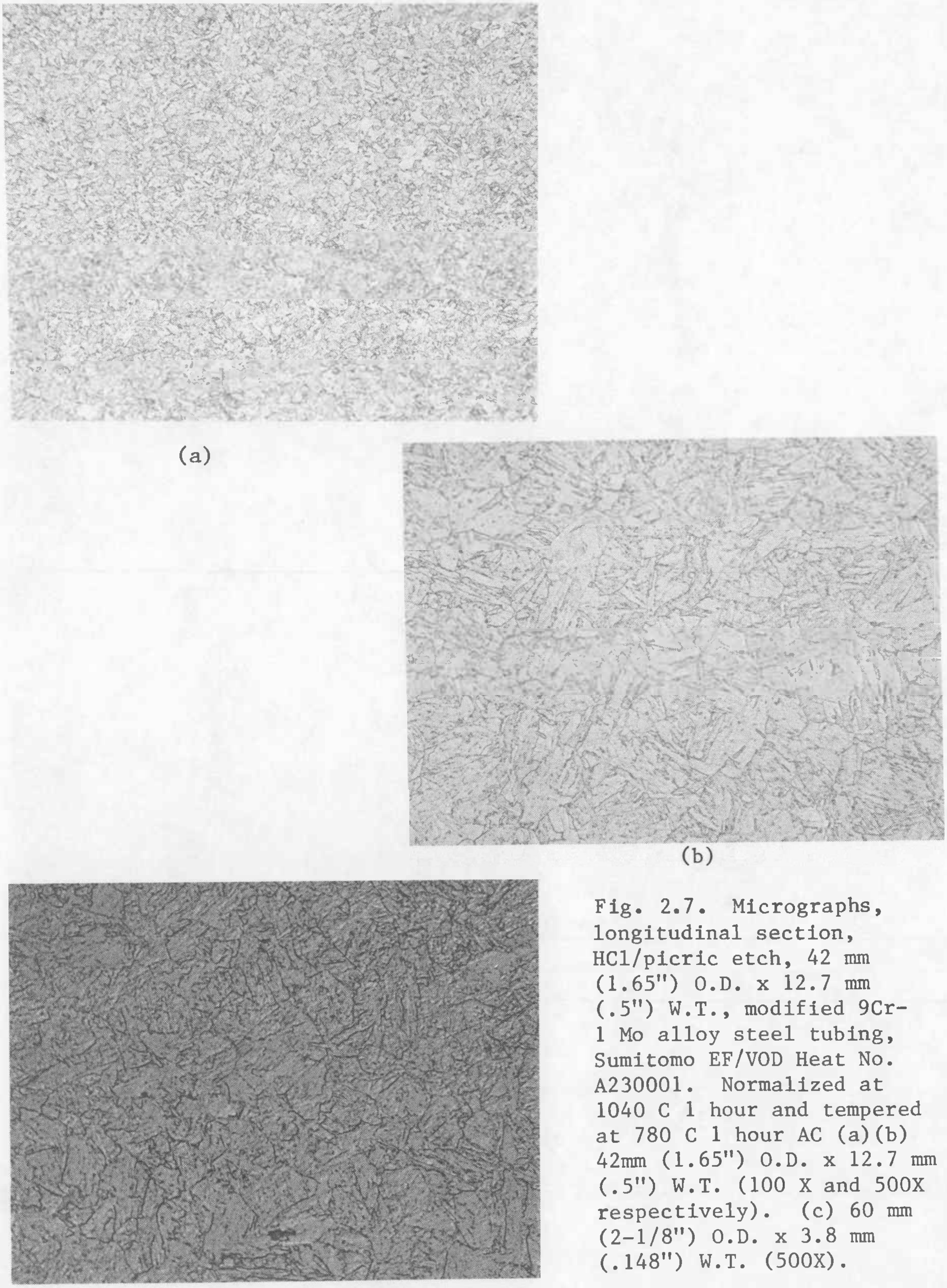

(a)

(b)

(c)

Fig. 2.7. Micrographs, longitudinal section, HCl/picric etch, 42 mm (1.65") O.D. x 12.7 mm (.5") W.T., modified 9Cr-1 Mo alloy steel tubing, Sumitomo EF/VOD Heat No. A230001. Normalized at 1040 C 1 hour and tempered at 780 C 1 hour AC (a)(b) 42mm (1.65") O.D. x 12.7 mm (.5") W.T. (100 X and 500X respectively). (c) 60 mm (2-1/8") O.D. x 3.8 mm (.148") W.T. (500X).

c. 45 mm O.D. x 12.7 mm W.T. cold finished/normalized and tempered tubing, Sumitomo EF/VOD heat A231001 (machined test specimens).

Tube flare and flattening tests were made by MML on Sumitomo 76.2 mm O.D. x 12.7 mm W.T. and 51 mm O.D. x 6.4 mm W.T. cold finished normalized/tempered tubing, VIM heat VF0028. Flattening tests were also made on 45 mm O.D. x 12.7 mm W.T. cold finished normalized/tempered tubing, Sumitomo EF/VOD heat A231001.

Tensile, flare, flattening, and hardness test results were obtained as mill test reports from T.I. Stainless Ltd. and Sumitomo Metals Ltd. for the following:

a. T. I. Stainless, 54 mm O.D. x 6.4 mm W.T., AOD/ESR heat 10148
b. Sumitomo, 76.2 mm O.D. x 12.7 mm W.T., VIM heat VF0028
c. Sumitomo EF/VOD heat A230001:

38 mm O.D. x 5.6 mm W.T.
44.5 mm O.D. x 5.5 mm W.T.
45 mm O.D. x 12.7 mm W.T.
51 mm O.D. x 8.1 mm W.T.
54 mm O.D. x 3.8 mm W.T.
54 mm O.D. x 4.6 mm W.T.
57 mm O.D. x 7.0 mm W.T.
63.5 mm O.D. x 9.5 mm W.T.
28.6 mm O.D. x 4.8 mm W.T. (rifled bore tubing)

A complete compilation of mill test chemical analyses is shown in Table 2.1 and tensile/mechanical test results are shown in Table 2.2.

Table 2.1. Chemical analyses of modified 9Cr-1Mo alloy (Sumitomo)

50T EF/VOD HT. A231001	C	Mn	P	S	Si	Cr	Ni	Mo	Cu	V	Nb	N	Sol. Al
Ladle	.100	.38	.013	.005	.38	8.39	.10	.94	.02	.21	.077	.0375	.002
38mm O.D. 5.6mm MWT ck	.097	.38	.015	.005	.40	8.52	.11	.96	.02	.23	.077	.0396	.004
45 12.7 ck	.097	.38	.015	.005	.40	8.46	.11	.96	.02	.23	.076	.0390	.005
54 4.6 ck	.096	.38	.014	.005	.41	8.53	.11	.97	.02	.23	.077	.0397	.004
57 7.0 ck	.099	.38	.014	.005	.40	8.45	.11	.96	.02	.23	.076	.0392	.005
51 8.1 ck	.096	.39	.014	.005	.41	8.58	.11	.98	.02	.23	.078	.0391	.004
64 9.5 ck	.098	.38	.015	.005	.41	8.50	.11	.96	.02	.23	.076	.0391	.005
29* 4.8 ck	.090	.39	.014	.004	.40	8.40	.10	.94	.03	.20	.080	.0385	.004

*Rifled Bore Tube

2T VIM HT. VF0028	C	Mn	P	S	Si	Cr	Ni	Mo	Cu	V	Nb	N	Sol. Al
Ladle	.105	.43	.006	.006	.42	8.52	.02	.98	.03	.20	.075	.0465	.003
76.2mm** OD 12.7 mm WT ck	.096	.46	.005	.008	.41	8.52	<.01	.97	<.01	.19	.083	.050	<.001
51** 6.4 ck	.083	.47	.005	.008	.42	8.58	<.01	.97	<.01	.20	.085	.050	<.001

**C.E. Ck analysis

Table 2.2. Tensile, hardness, and manipulation test results, modified 9Cr-1Mo alloy steel tubing

Source	Heat Type/No.	O.D. mm	W.T. mm	Y.S. MPa	U.T.S. MPa	% E	Flat/ Flare	Hard. R_B	Code
T.I. Stainless Ltd.	AOD/ESR 11048	54	9.5	675	818	19(3)	OK	-	M
NKK	VIM59020	51	6.4	608	803	-	OK	-	MX
NKK	VIM59020	51	6.4	618	812	29(2)	OK	-	MX
Sumitomo	VIM VF0028	51	6.4	556	675	39(2)	OK	-	MX
Sumitomo	VIM VF0028	51	6.4	551	675	38(2)	OK	-	MX
Sumitomo	VIM VF0028	76.2	12.7	-	-	-	OK	-	MX
Sumitomo	VIM VF0028	76.2	12.7	508	679	32(2)	OK	-	M

	Normalized	Tempered
T.I. Stainless	1038 C 1 Hr	760 C 1 Hr
NKK	1038 C 1 Hr	760 C 1 Hr
Sumitomo	1040 C 1 Hr	780 C 1 Hr

M - Mill test
MX - MML test
(2) - 50.8 mm gage
(3) - 63.5 mm gage

Table 2.2. (Continued)

Source	Heat Type/No.	O.D. mm	W.T. mm	Y.S. MPa	U.T.S. MPa	%E	Flat/ Flare	Hard. R_B	Code
Sumitomo	EF/AOD A231001	38	5.6	508	684	39(2)	OK	94.5	M
Sumitomo	EF/AOD A231001	45	5.5	518	679	38(2)	OK	-	M
Sumitomo	EF/AOD A231001	45	12.7	523	675	28(1)	OK	-	MX
Sumitomo	EF/AOD A231001	45	12.7	508	679	25(1)	OK	-	MX
Sumitomo	EF/AOD A231001	45	12.7	513	689	30(2)	OK	93.2	M
Sumitomo	EF/AOD A231001	51	8.1	523	694	30(2)	OK	94.5	M
Sumitomo	EF/AOD A231001	54	3.8	513	684	38(2)	OK	-	M
Sumitomo	EF/AOD A231001	54	4.6	504	684	39(2)	OK	95.4	M
Sumitomo	EF/AOD A231001	57	7.0	503	689	28(2)	OK	92.0	M
Sumitomo	EF/AOD A231001	63.5	9.5	504	684	28(2)	OK	94.4	M
Sumitomo	EF/AOD A231001	28.6*	4.8	508	679	27(2)	OK	(HY209)	M

	Normalized	Tempered
Sumitomo	1040 C 1 Hr	780 C 1 Hr

M - Mill test
MX - MML
(1) - 25.4 mm gage
(2) - 50.8 mm gage
* - Rifle bore tube

2.3 Fabrication (Safe-Ending) of Modified 9Cr-1Mo Boiler Tubes, Ontario Hydro Lambton and Nanticoke TGS

Twelve 54 mm O.D. x 3.8 mm W.T. modified 9Cr-1Mo tubes, Sumitomo EF/VOD heat A231001, were safe-ended at C-E MML as part of a test installation for Ontario Hydro Lambton's TGS. Six tubes 2.75 meters (9') long were safe-ended on both ends with 152 mm (6") lengths of 54 mm O.D. x 3.8 mm W.T. TP347H. stainless steel. Six tubes 2.4 meters (8') long were safe-ended on one end with a 54 mm O.D. x 3.8 mm x 152 mm TP347H; and with 63.5 mm O.D. x 7.1 mm W.T. x 152 mm SA-213 Gr T-9 on the other end. Three modified 9Cr-1Mo tubes of each length without safe-ends were provided as spares. Two 1.5 meter long tubes, 54 mm O.D. x 6 mm W.T., Sumitomo HCM9M alloy (9Cr-2Mo), heat ZWD24T3, were safe ended on both ends with 54 mm O.D. x 6.4 mm W.T. TP347. These tubes are to be used for comparative test purposes.

Safe-end welding procedure, modified 9Cr-1Mo/TP347, was gas metal arc automatic (GMAA), multiple pass, rotated tube, and single V-90° included angle using ER Ni Cr-3 (Inco 82) 0.76 mm dia. wire as filler metal. Preheat was 93° C, maximum interpass 260° C, and postheat treatment (induction coil heating) 732 + 14 -0° C for 15 min. Weld qualification guided bend tests were satisfactory, and tensile specimens broke (in weld) at 628 MPa and 651 MPa. Safe-ending procedure, modified 9Cr-1Mo/SA213 T-9, was GMAA multiple pass rotated tube, and single V using 0.76 mm dia. Class ER 505 wire as filler metal. Preheat was 93° C, maximum interpass 260° C, and 732 + 14 - 0° C for 20 minutes as postheat. Weld qualification guided bend tests were satisfactory, and tensile tests broke in base material at 671 MPa and 709 MPa. Sumitomo HCM9M/TP347H welding procedure was similar to that used for modified 9Cr-1Mo/TP347H. Weld qualification guided bend tests were satisfactory, and tensile tests broke in the weld at 663 MPa and 665 MPa. Safe-ended tubes ready for shipment are shown in Figs. 2.8 and 2.9.

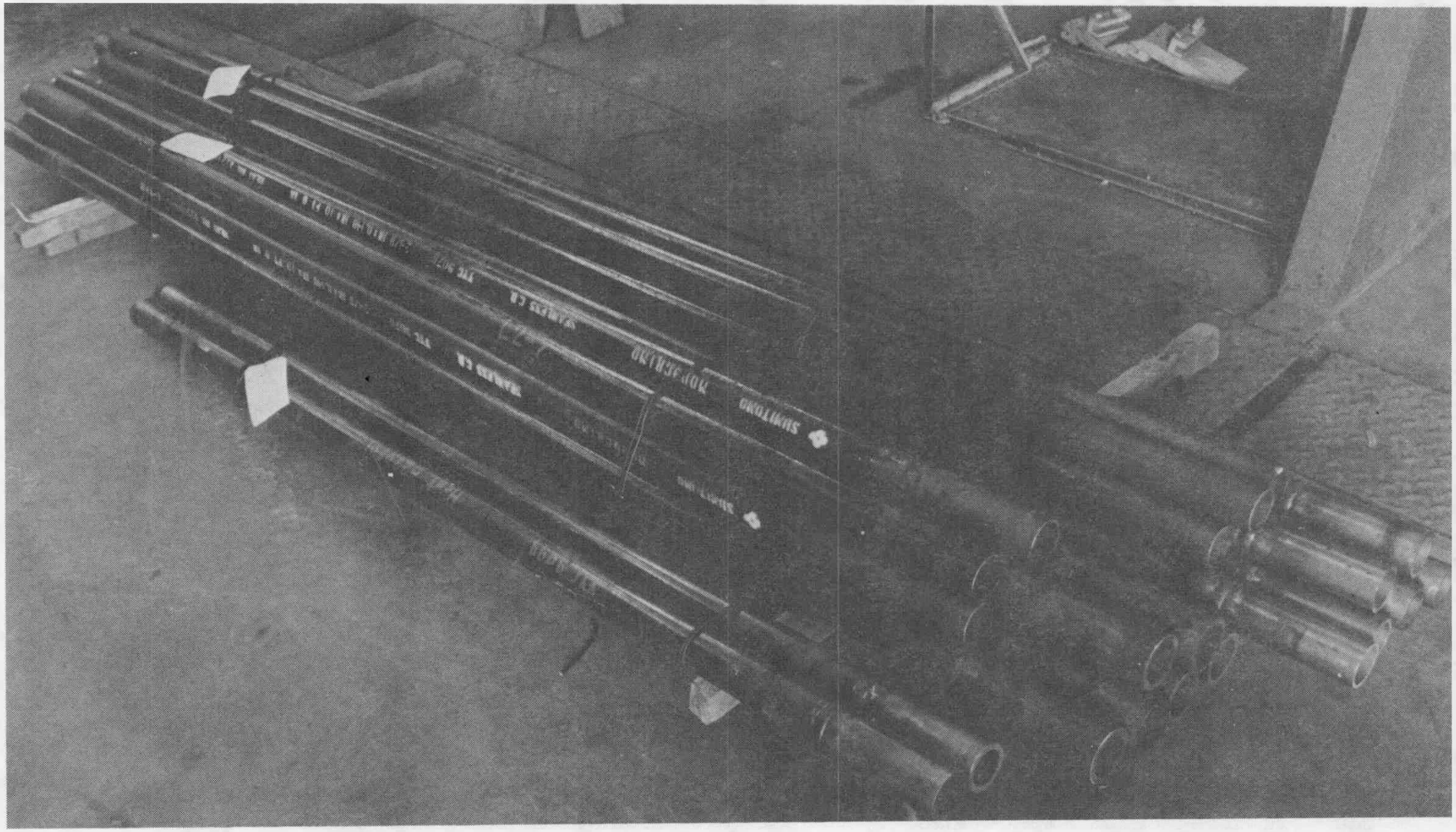

Fig. 2.8. Safe-ended modified 9Cr-1Mo tubing for Ontario Hydro Lambton TGS.

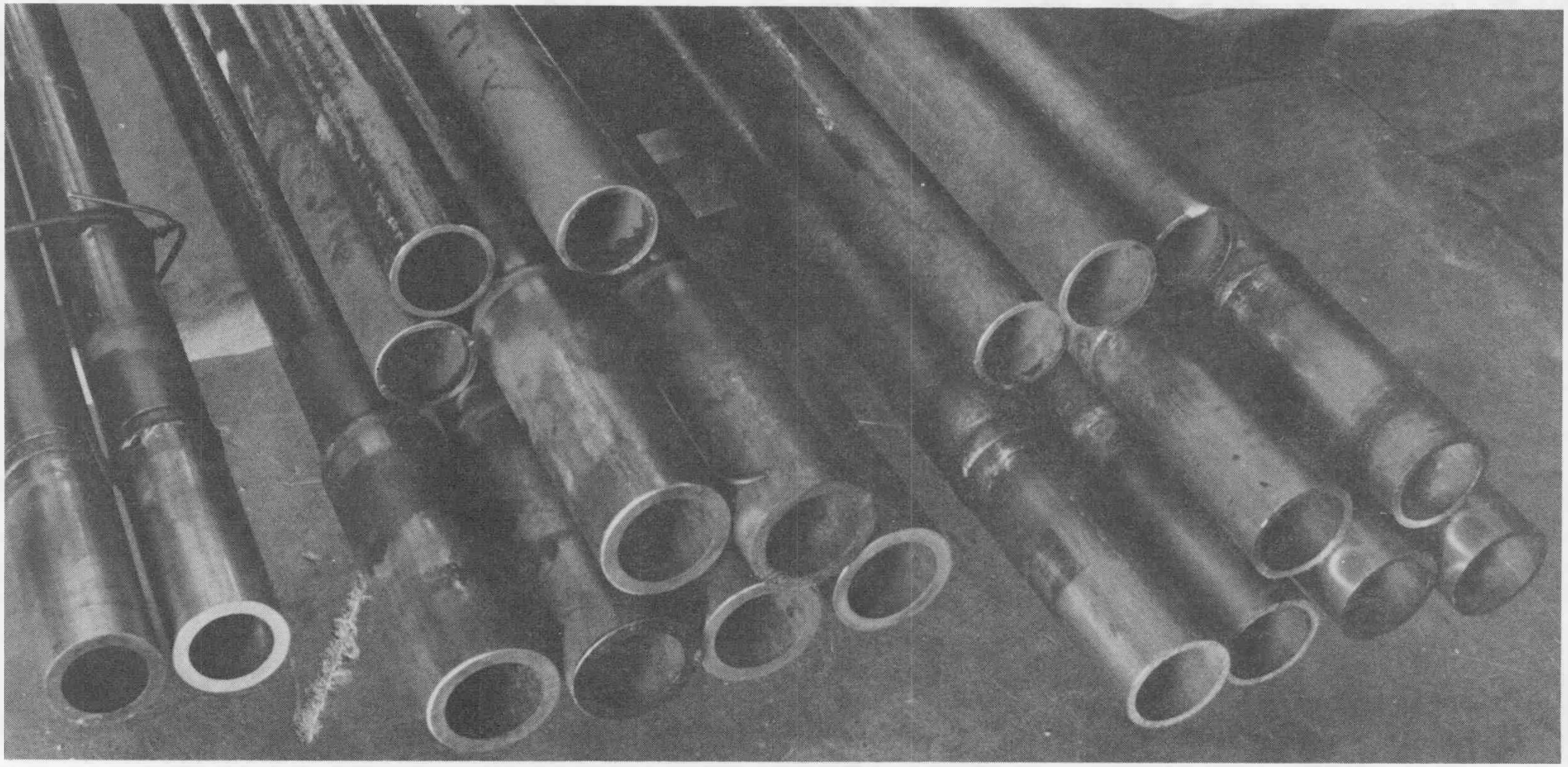

HCM9M | Modified 9Cr-1Mo/T-9 | Modified 9Cr-1Mo/TP347H

Fig. 2.9. Safe-end detail, tubing for Ontario Hydro Lambton TGS.

Eight 44.5 mm O.D. x 5.5 mm W.T. x 3 meters long modified 9Cr-1Mo alloy tubes, Sumitomo EF/VOD heat A231001 were safe-ended at C-E MML for a test installation at Ontario Hydro Nanticoke TGS. All tubes were safe-ended on both ends with SA-213 Gr T-22, 44.5 mm O.D. x 9.5 W.T. Boreside mismatch between modified 9Cr-1Mo alloy (A213 Gr T-91) and T-22 was compensated by boreside weld build-up as shown in Fig. 2.10. Weld build-up procedure consisted of depositing three shielded metal arc weld-metal-layers as multiple passes with 2.4 mm (3/32") diameter E505-15, M-11145, R-5184 electrodes. Rotated tube technique was used with D.C. reversed polarity current. Preheat temperature was 93° C, maximum interpass 260° C, and postheat 427° C (no hold time and air cool). Three tubes without safe-ends were included as spares. The safe-ended tubes are shown in Fig. 2.11.

2.4 References

1. Materials and Structures Technology Management Center, ORNL, Advanced Alloy Technology Program, Semi-annual Progress Report for Period Ending March 31, 1982.

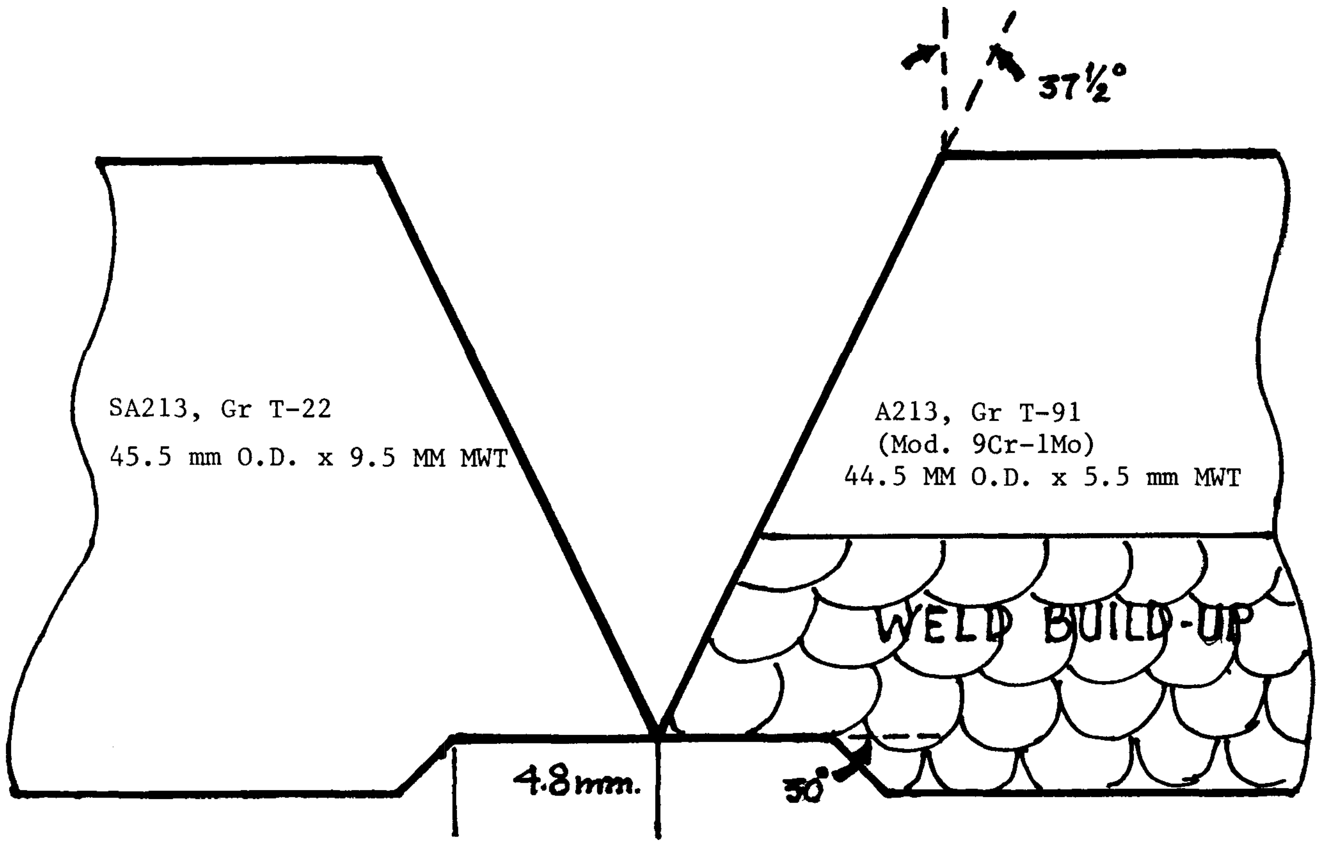

Fig. 2.10. Weld build-up detail, T-22/modified 9Cr-1Mo, safe-end joint, Nanticoke TGS.

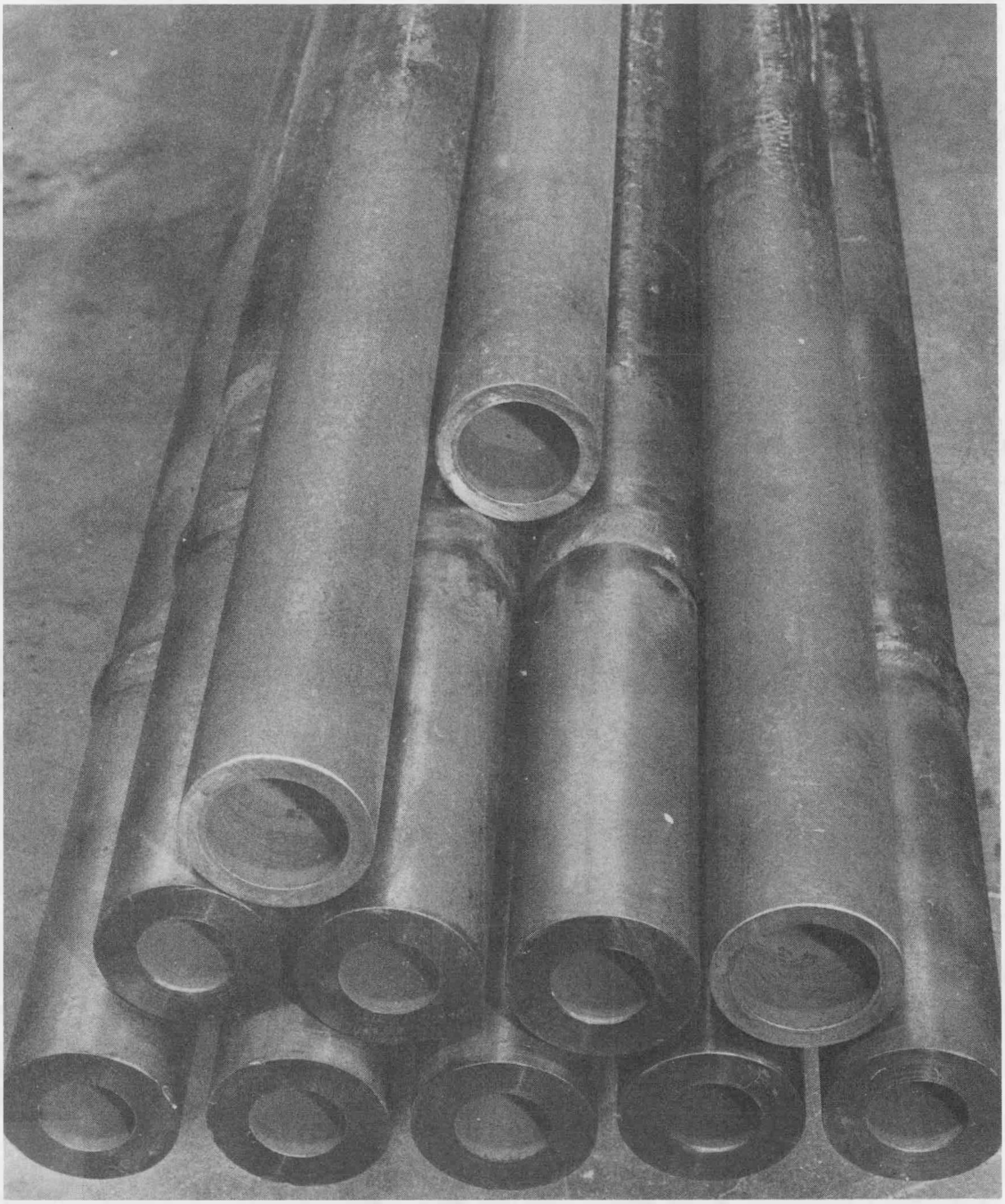

Fig. 2.11. Safe-end detail, T-22/modified 9Cr-1Mo tubing for Ontario Hydro Nanticoke TGS.

3.0 WESTINGHOUSE ADVANCED REACTORS DIVISION

M. G. Cowgill and K. C. Thomas

3.1 INTRODUCTION

The primary objective of the Westinghouse Advanced Reactors Division (WARD) program is to perform uniaxial creep and creep-rupture tests on the various heats of modified 9 Cr-1 Mo steel. The initial phase of the program involved the testing of several experimental heats of material under similar conditions of temperature and load in order to assess alloy properties relative to each other. The second phase of the program extended the testing to include prototypic commercial scale heats of material. Testing in both phases is supplemented by metallographic examination. The data produced by the program will ultimately be used to provide input for an ASME Code Case on a modified 9 Cr-1 Mo steel with optimized properties.

The program was initiated during the third quarter of FY 1978, and eleven creep-rupture tests, involving six different experimental heats of modified 9 Cr-1 Mo steel, were performed in the remaining portion of FY 1978 (Reference 1). An additional twenty four tests, involving eight different experimental heats and three prototypic commercial heats, were completed during FY 1979 (References 2 and 3). During FYs 1980 and 1981, twenty six tests were performed, involving two prototypic commercial heats, and ten long term (in excess of 15,000 hr) tests were initiated (References 4 through 7). Four additional tests were completed in the first half of FY 1982 (Reference 8).

The program was performed initially under 189a CW065 and later funded under B&R AF 15 10 15, Subtask WA-1.7. Current funding is provided under ORNL P.O. 40X-40495, issued under Union Carbide Corporation prime contract W-7405-eng-26.

3.2 SPECIMENS AND TEST EQUIPMENT

The specimens in test incorporate a cylindrical gage section of diameter 6.35 mm and length 31.75 mm. Extensometer attachment was facilitated by shoulder grooving and grip attachment by a 1/2-13 UNC thread.

All specimens were received from ORNL, machined with the gage length transverse to the rolling direction of the original plate except as noted in the text. All heats of material tested to date had received a standard normalizing and tempering treatment of 1038°C for 1 hour plus 760°C for 1 hour.

The conventional lever arm creep units used for testing during the current report period are either Applied Test Systems or Satec Instruments load frames, equipped with power positioning furnaces. The lever arm ratio for all units is 20:1. Strain is measured by extensometers attached to the shoulders of the specimen and equipped either with linear variable differential transducers or with super linear variable capacitors and digital readout. Specimen temperatures are taken from three thermocouples located along the specimen gage length and are recorded at regular intervals on a Doric Digitrend 220. In addition, periodic spot checks are carried out with a Doric Trendicator 410A.

In addition, testing with loads less than about 125 MPa is being performed on direct-loading multi-specimen units. Each unit is made up of a load frame which supports a Skutt Model 321 high temperature kiln and, in the present configuration, can accept up to four specimens simultaneously. Strain measurement is by extensometers attached to the shoulders of the specimen and equipped with a high precision dial gage. Temperatures, taken from two thermocouples located along the specimen gage length, are recorded continuously on the strip charts of a Honeywell Electronik 16 recorder and periodically checked with a Doric Trendicator 410A.

3.3 TESTING OF PROTOTYPIC COMMERCIAL HEATS

Testing is being performed on three prototypic commercial heats of modified 9 Cr-1 Mo steel: Cartech heats 30182, 30176 and 30394E. All three heats are being tested at 593°C. In addition, Cartech heats 30176 and 30394E are being tested at 677°C. The chemical analyses of the three heats are given in Table 3.1.

3.3.1 Creep-Rupture Testing of Cartech Heat 30182

The one remaining test on heat 30182 was completed with failure after 18,505.6 hours at 593°C and a stress of 131 MPa. The results

Table 3.1 Chemical Analyses of Cartech Heats Being Tested at WARD

Element	Content in wt. %		
	Cartech Heat 30182	Cartech Heat 30176	Cartech Heat 30394E
C	.087	.075	.084
Mn	.37	.40	.47
P	.012	.012	.011
S	.004	.004	.004
Si	.21	.19	.45
Ni	.10	.10	.09
Cr	8.46	8.41	8.35
Mo	.89	.90	1.03
V	.225	.204	.202
Nb	.075	.072	.08
Ti	.001	.004	.005
Co	.019	.016	.061
Cu	.03	.03	.04
Al	.012	.005	.025
B	<.001	.001	.001
W	.01	.01	.05
As	.001	.001	.001
Sn	.002	.002	.002
Ar	.001	.001	.001
N_2	.054	.054	.054
O_2	.008	.005	.004
Cr Equivalent	9.55	8.51	11.04

of the test are summarized in Table 3.2 and the creep strain-versus-time plot shown in Figure 3.1. This particular series of tests at 593°C, with stresses ranging from 131 MPa to 207 MPa, is now complete and the stress-versus-rupture time data are shown in Figure 3.2. The latest data point continues the trend established by testing at higher stresses and shorter rupture times, with the slope of the log stress versus log rupture time line being approximately -.08. As is apparent in Figure 3.2, the rupture strength of this heat at 593°C continues to exceed the ASME Code Case N47 minimum strength for Type 304 SS. Moreover, the differential between the two materials continues to increase as the stress is lowered and, in fact, the last data point falls on the expected Code Case minimum line for Type 316 SS. If this trend is continued at lower stresses and longer rupture times, the rupture strength of the modified 9 Cr-1 Mo steel will become progressively greater than the Code Case minimum for Type 316 SS, as well.

Optical metallography and microhardness measurements were performed on this most recently failed specimen. No significant changes were noted in the microstructure which retained the coarse-grained, equiaxed tempered martensite appearance of the as-received material.

Examination of the fracture cross-section revealed some void formation in the vicinity of the fracture surface, in contrast with all but one of the other specimens of this heat of material. The exception was the specimen tested for 6369.2 hours at 145 MPa. Although the void formation was not extensive in either specimen, it appeared that the void density was greater in that with the longer rupture time.

Microhardness indentations made in one of the grip cross-sections of the specimen gave an average value of 216 DPH (500g load). This is very similar to the values recorded on the other specimens in this series of tests (see Figure 3.3) and is little different from the as-received values for this heat of material recorded in Reference 6. Based on these observations and the optical metallography, it appears that this heat of modified 9 Cr-1 Mo steel is microstructurally quite stable for times out to near 20,000 hours at 593°C.

Table 3.2 Creep-Rupture Measurements on Cartech Heat 30182 at 593°C

Load (MPa)	Rupture Time (hours)	Minimum Creep Rate (% per hour)	Loading Strain (%)	Creep Strain at Fracture (%)	Reduction of Area at Fraction (%)	Time to Onset of Secondary Creep (hrs)	Time to Onset of Tertiary Creep (hrs)	Strain Intercept at Zero Time (%)[a]
131	18,505.6	1.10×10^{-4}	0.15	23.62	84.26	2000	8500	0.82

a - based on extrapolation of minimum creep rate line

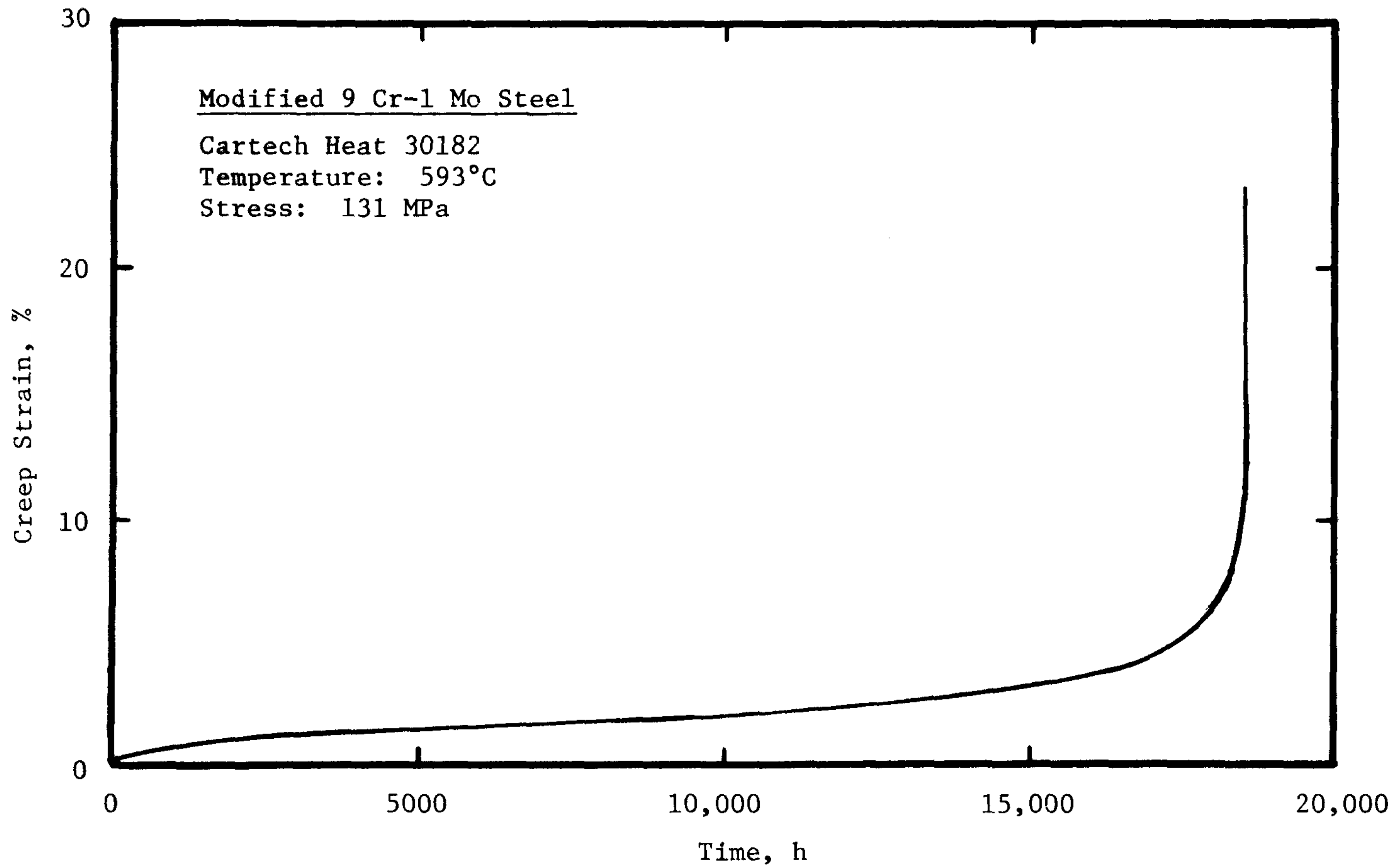

Fig. 3.1 Creep-Rupture curve for Cartech Heat 30182 at 593°C and 131 MPa

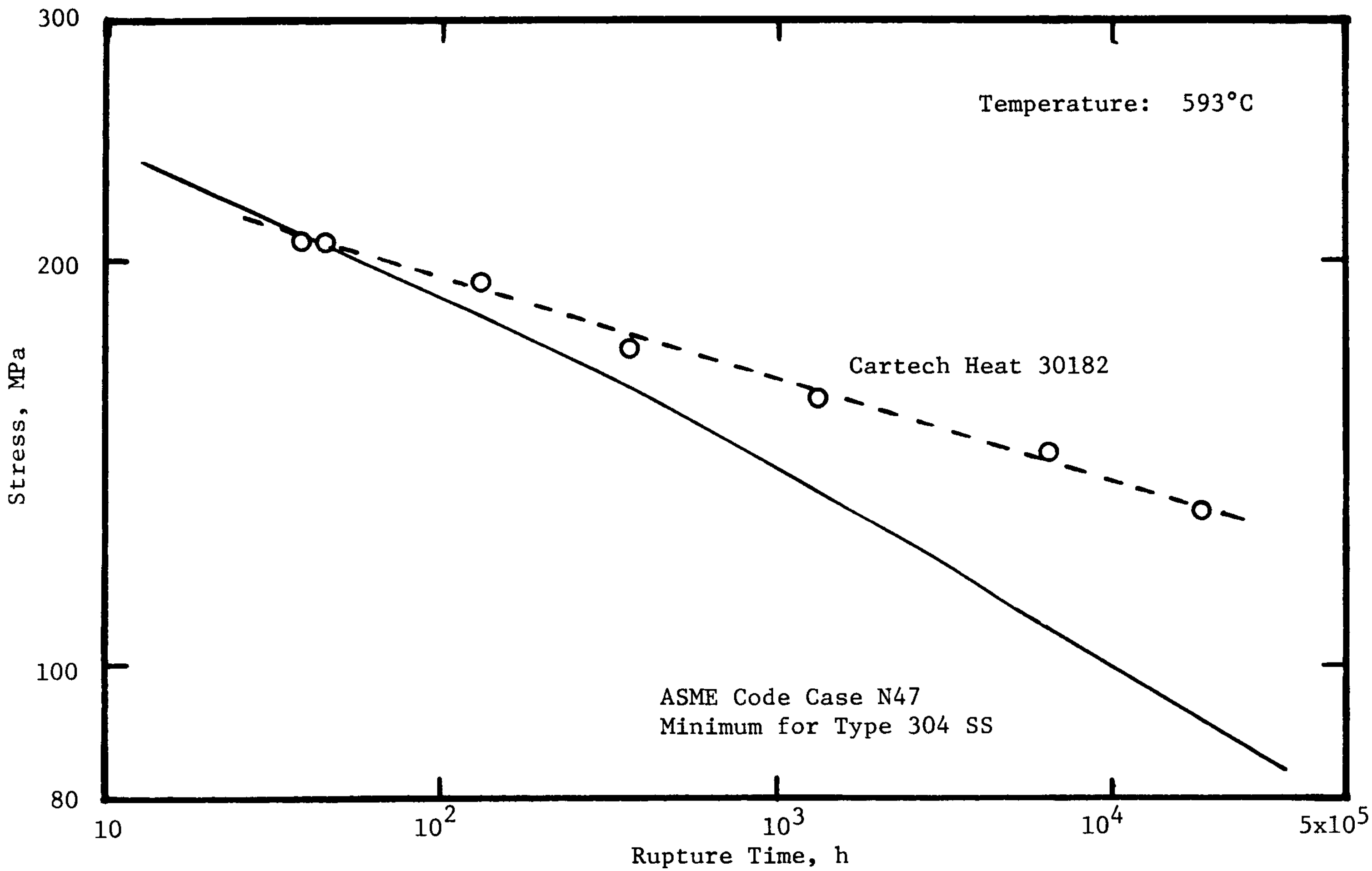

Fig. 3.2 Rupture time as a function of stress for Cartech Heat 30182 (Modified 9 Cr-1 Mo Steel) and Type 304 SS ASME Code Case N47 minimum at 593°C

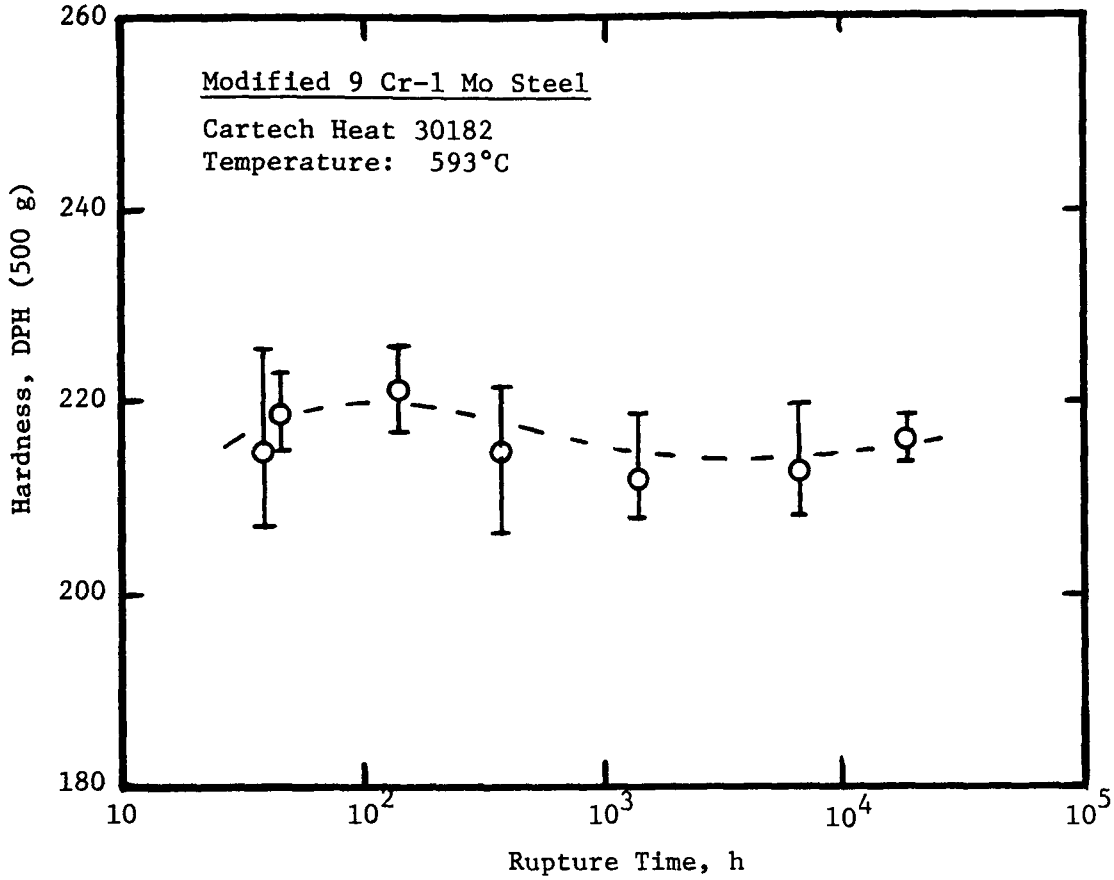

Fig. 3.3 Microhardness values as a function of rupture time at 593°C for Cartech Heat 30182

3.3.2 Creep-Rupture Testing of Cartech Heats 30176 and 30394E

Testing of these two heats is mainly confined to relatively low stress levels at 593 and 677°C, with the aim of obtaining rupture data out to 20,000 hours and beyond. Eight tests are currently in progress simultaneously in two Skutt kilns. Those at 593°C involve stress levels of 110 and 117 MPa and have accumulated 15,400 hours of exposure to date. The four tests at 677°C have been in progress for 13,000 hours and have stress levels of 27.6 and 41.4 MPa. Two other tests are in progress on lever arm machines at 593°C, with a stress level of 124 MPa, and have been on test for in excess of 11,000 hours. The creep strains acquired during the ten tests described above are given in Table 3.3. One of the tests (specimen 176-35T, 110 MPa at 593°C) has experienced very low creep strain (0.25%) relative to the other specimens at the temperature. This particular specimen demonstrated contraction of about 0.1% during the first 650 hours of test, followed by a step increase of a similar amount. Since that time the creep strain has undergone several sequences of contraction or consolidation followed by sudden step increases. The overall effect, however, has been one of strain increase at an average rate similar to that of specimen 394E-35T being tested under identical conditions. The reason for this behavior has still to be ascertained. All other tests in the series show the normally observed form of the creep strain-time curve, sometimes involving small step increases but with no significant examples of negative creep.

3.4 REFERENCES

1. J. R. DiStefano, *Modified 9 Cr-1 Mo Steel Development Program Progress Report for Period Ending September 30, 1978,* ORNL/BRP-79/2, Oak Ridge National Laboratory, Oak Ridge, TN.

2. J. R. DiStefano, *Modified 9 Cr-1 Mo Steel Development Program Progress Report for Period Ending March 31, 1979,* ORNL/BRP-79/4, Oak Ridge National Laboratory, Oak Ridge, TN.

3. J. R. DiStefano, *Modified 9 Cr-1 Mo Steel Development Program Progress Report for Period Ending September 30, 1979,* ORNL/BRP-80-1, Oak Ridge National Laboratory, Oak Ridge, TN.

4. Materials and Structures Technology Management Center, *Advanced Alloy Technology Program Semiannual Progress Report for Period Ending March 31, 1980,* ORNL/MSP.1.7-80/3, Oak Ridge National Laboratory, Oak Ridge, TN.

5. Materials and Structures Technology Management Center, *Advanced Alloy Technology Program Semiannual Progress Report for Period Ending September 30, 1980*, ORNL/MSP/1.7-80/3, Oak Ridge National Laboratory, Oak Ridge, TN.

6. Materials and Structures Technology Management Center, *Advanced Alloy Technology Program Semiannual Progress Report for Period Ending March 31, 1981*, ORNL/MSP/1.7-81/1, Oak Ridge National Laboratory, Oak Ridge, TN.

7. Materials and Structures Technology Management Center, *Advanced Alloy Technology Program Semiannual Progress Report for Period Ending September 30, 1981*, Oak Ridge National Laboratory, Oak Ridge, TN.

8. Materials and Structures Technology Management Center, *Advanced Alloy Technology Program Semiannual Progress Report for Period Ending March 31, 1982*, Oak Ridge National Laboratory, Oak Ridge, TN.

Table 3.3 Status of On-Going Creep-Rupture Tests on Cartech Heats 30176 and 30394E

Specimen Number	Temperature (°C)	Load (MPa)	Time (hrs)	Creep Strain (%)
Heat 30176				
176-35T	593	110	15,400	0.39
176-36T	593	117	15,400	1.46
176-39T	593	124	11,400	1.16
176-37T	677	27.6	13,000	0.64
176-38T	677	41.4	13,000	2.16
Heat 30394E				
394E-35T	593	110	15,400	1.28
394E-36T	593	117	15,400	1.59
394E-39T	593	124	11,200	1.78
394E-37T	677	27.6	13,000	0.57
394E-38T	677	41.4	13,000	2.78

DISTRIBUTION

1–8. ARGONNE NATIONAL LABORATORY, 9700 South Cass Avenue, Argonne, IL 60439

A. R. Brunsvold, Manager, Steam Generators and IHXs, LCDM
O. K. Chopra, Metallurgist, Corrosion Group
D. R. Ferguson, Director, FRSTMC
T. F. Kassner, Leader Corrosion Group
W. J. Shack, Leader, Metals Property Group
W. R. Simmons, Manager, LCDM
R. W. Weeks, Associate Director Materials Science Division
R. S. Zeno, Director, Components Technology Division

9–10. BABCOCK AND WILCOX COMPANY, Research and Development Center, 91 Stirling Avenue, Barberton, OH 44203

D. D. Mokris, Project Manager, Nuclear Equipment Division
C. C. Schultz, Research Specialist

11. BABCOCK AND WILCOX COMPANY, Box 1260, Lynchburg, VA 20545

D. W. Montgomery, Project Manager, LMFBR-LDP

12. BATTELLE-COLUMBUS LABORATORIES, 505 King Avenue, Columbus, OH 43201

C. E. Jaske, Senior Research Specialist

13. BECHTEL POWER CORPORATION, P. O. Box 3965, San Francisco, CA 94119

S. Golan, LDP Project Manager, Research and Engineering Division

14. BOEING ENGINEERING AND CONSTRUCTION COMPANY, P. O. Box 3707, Seattle, WA 98124

D. D. Cox, Director, Energy Systems Development

15. BURNS AND ROE, INC., 700 Kinderkamack Road, Oradell, NJ 07469

C. S. Ehrman, Project Manager, Advanced Breeder Reactor Projects

16–19. COMBUSTION ENGINEERING, INC., 911 W. Main Street, Chattanooga, TN 37402

G. C. Bodine, Consulting Engineering, Metallurgical and Materials Laboratory
D. A. Canonico, Director of Research
J. R. Ray, Section Manager, Miscellaneous Vessels, Nuclear Design Engineering
E. W. Pickering, Jr.

20–22. COMBUSTION ENGINEERING, INC., 1000 Prospect Hill Road, Windsor, CT 06095

P.E.C. Bryant, Director, Materials and Chemistry Development
A. L. Gaines, LDP Project Manager
G. H. Rowe, Advanced Development Department

23–32. DEPARTMENT OF ENERGY, Washington, DC 20545

Office of Nuclear Powers Systems

High-Temperature Reactor Division

J. E. Fox

Office of Fossil Energy

Technical Coordination Staff

S. J. Dapkunas

Office of Fusion Energy

T. C. Reuther, Materials and Radiation Effects Branch

Office of Breeder Technology Projects, NE-53

W. A. Nelson, Jr., Director

Breeder Mechanical Component Development Division, NE-53

F. X. Gavigan, Director
C. M. Purdy, Assistant Director, Materials and Structures
C. C. Beals, Manager, Materials Technology
C. C. Bigelow, Manager, Structures Technology

Fuels Division

D. K. Magnus, Director

23–32. DEPARTMENT OF ENERGY, Washington, DC 20545 (cont.)

Office of Clinch River Breeder Reactor Plant, NE-52

J. R. Longenecker, Director

33. DOE, CHICAGO OPERATIONS OFFICE, 9700 South Cass Avenue, Argonne, IL 60439

J. M. Borg, Technology Management Division

34–35. DOE, CLINCH RIVER BREEDER REACTOR PROJECT OFFICE, P. O. Box U, Oak Ridge, TN 37830

C. H. Fox, Assistant Director for Engineering
E. A. Wright, Chief, Reactor and Plant Components Branch

36. DOE, OAK RIDGE OPERATIONS OFFICE, P. O. Box E, Oak Ridge, TN 37830

Office of Nuclear Research and Development

E. E. Hoffman, Manager, National Materials Programs

37–38. DOE, TECHNICAL INFORMATION CENTER, P. O. Box 62, Oak Ridge, TN 37830 (2)

39. FOSTER-WHEELER DEVELOPMENT CORPORATION, 110 S. Orange Avenue, Livingston, NJ 07039

W. R. Apblett, Jr., Senior Vice President

40–41. GENERAL ATOMIC COMPANY, P. O. Box 81608, San Diego, CA 92138

J. E. Chafey, Project Engineer, HTGR Generic Technology Program
D. I. Roberts, Department Manager, Structural Materials

42–43. GENERAL ELECTRIC COMPANY, Advanced Reactor Systems Department, 175 Curtner Avenue, San Jose, CA 95125

D. Dutina, Manager, Plant Materials Engineering
P. Roy, Manager, Plant Materials and Process Development

44–45. GENERAL ELECTRIC COMPANY, Advanced Reactor Systems Department, P. O. Box 508, Sunnyvale, CA 94086

A. W. Dalcher, Manager, Component Structural Analysis
S. M. Davies, LDP Project Manager

46–55. HANFORD ENGINEERING DEVELOPMENT LABORATORY, P. O. Box 1970, Richland, WA 99352

M. J. Anderson, Manager, Reactor and Systems Stress Analysis Section
T. K. Bierlein, Manager, Materials Properties
L. D. Blackburn, Structural Engineering
D. S. Gelles, Senior Scientist
J. J. Holmes, Manager, Mechanical Metallurgy
L. A. James, Structural Engineering
R. L. Knecht, Manager, Structural Engineering
D. E. Mahagin, Manager, RF&MTMC
L. K. Severud, Manager, Plant Analysis Subdivision
W. F. Sheely, Manager, Materials Technology

56–57. IDAHO NATIONAL ENGINEERING LABORATORY, P. O. Box 1625, Idaho Falls, ID 83401

D. D. Keiser, Manager, Materials Technology Division
G. E. Korth, Program Manager, Fuels and Materials Division

58. LAWRENCE LIVERMORE LABORATORY, P. O. Box 808, Mail Code L-332, Livermore, CA 94550

E.N.C. Dalder, Metallurgist

59. NAVAL RESEARCH LABORATORY, 4555 Overlook Avenue, SW, Washington, DC 20375

D. J. Michel, Manager, High-Temperature Metals Section

60–88. OAK RIDGE NATIONAL LABORATORY, P. O. Box X, Oak Ridge, TN 37830

J. J. Blass, Manager, Structural Design Technology, MSTMC, 9204-1, MS-11
E. E. Bloom, Section Head, Materials Science, 4500S, MS-276
R. A. Bradley, Manager, Fossil Energy Materials Program, 4500S, MS-160

60–88. OAK RIDGE NATIONAL LABORATORY, P. O. Box X, Oak Ridge, TN 37830 (cont.)

C. R. Brinkman, Group Leader, Mechanical Properties, 4500S, MS-T22
J. M. Corum, Head, Structural Mechanics, 9204-1, MS-11
J. R. DiStefano, Manager, Materials Technology, MSTMC, 4500S, MS-T34 (2)
G. M. Goodwin, Group Leader, Welding and Brazing Group, 4508, MS-207
J. C. Griess, Jr., Materials Compatibility Group, 4500S, MS-T30
W. O. Harms, Director, MSTMC, 4500N, I205H
R. L. Heestand, Group Leader, Metals Processing Group, 4508, MS-135
J. A. Horak, MSTMC, 4508, MS-230
R. L. Huddleston, Group Leader, Material Behavior Modeling, 9204-1, MS-11
C. R. Hudson, Manager, Program Analysis and Control, MSTMC, 4500N, I205B
J. F. King, Welding and Brazing Group, 4508, MS-226
R. K. Nanstad, Group Leader, Pressure Vessel Technology, 4500S, MS-D61
P. Patriarca, Manager, Breeder Reactor Materials, 4508, MS-115
C. E. Pugh, Group Leader, Heavy Section Steel Technology Program, 9204-1, MS-6
D. N. Robinson, Engineering Technology Division, 9204-1, MS-11
V. K. Sikka, Metals and Ceramics Division, 4500S, MS-C51 (5)
G. M. Slaughter, Section Head, Engineering Materials, 4500S, MS-C46
R. W. Swindeman, Metals and Ceramics Division, 4500S, MS-B54
G. T. Yahr, Engineering Technology Division, 9204-1, MS-11
Laboratory Records Department - RC (2)

89–95. ROCKWELL INTERNATIONAL, Energy Systems Group, 8900 DeSoto Avenue, Canoga Park, CA 91304

R. A. Johnson, Project Manager, Large Breeder Reactor Programs
C. C. Connors, Manager, Engineering Design Group
K. R. Jaquay, Manager, Piping System Facility
R. I. Jetter, Manager, Structural and Materials Engineering Design Group
H. M. Minami, Project Manager, Refueling and Structural Integration
J. P. Page, Engineer, Steam Generator Projects
H. C. Wieseneck, Vice President and General Manager

96. STONE AND WEBSTER ENGINEERING CORPORATION, Box 2325, Boston, MA 02107

G. Garabedian, Project Manager, LMFBR-LDP

97–103. WESTINGHOUSE ELECTRIC CORPORATION, Advanced Reactors Division, P. O. Box 158, Madison, PA 15663

C. A. Anderson, Manager, Large Plant Projects
E. C. Bishop, Manager, Sodium Components Technology
D. N. Elliott, Manager, Structural Technology and Component Test
D. S. Griffin, Manager, Computer Systems and Structural Mechanics
W. E. Ray, Manager, Materials and Processes
A. L. Snow, Structural Mechanics
K. C. Thomas, Manager, Materials Engineering and Mechanical Testing

104–105. WESTINGHOUSE ELECTRIC CORPORATION, Nuclear Components Division, P. O. Box 12831, Pendacola, FL 32576

C. R. Adkins, Project Manager, BRCP
P. J. Langford, Manager, Structural Analysis, BRCP

☆ U.S. GOVERNMENT PRINTING OFFICE: 1983-646-055/278